ORIGINAL ARTICLES

ALUMINUM PHTHALOCYANINE NANOPARTICLES ACTIVATION FOR LOCAL FLUORESCENCE SPECTROSCOPY IN DENTISTRY

Zolotareva J.O.[1], **Farrakhova D.S.**[1, 2, 3], **Kupriyanova E.N.**[4], **Loschenov V.B.**[1, 2, 3]
[1]National Research Nuclear University MEPhI, Moscow, Russia
[2]Prokhorov General Physics Institute of the Russian Academy of Sciences, Moscow, Russia
[3]Dentospek LLC, Troitsk, Moscow, Russia
[4]SAHI «Dental Clinic No. 11 of the Moscow City Health Department», Moscow, Russia

Abstract

Early diagnosis of caries and tooth enamel microcracks is of great importance for preventing the destruction of healthy tooth enamel. In order to detect microcracks in the enamel and pathogenic microflora foci that can cause caries, nanoform of aluminum phthalocyanine (AlPc) can be used as a marker. In a colloidal solution, the nanoparticles do not fluoresce, unlike their molecular form. To convert the particle into its molecular form, it is necessary to have a solvent or specific environment (bacteria, macrophages, etc.). That is why the hydrophobic nanoparticles of aluminum phthalocyanine (nAlPc) can act as markers for detecting hidden pathogenic microflora during fluorescent diagnostics. Further reduction of the diagnosis time and increase the efficiency can be achieved by using biologically compatible surfactants as additional activators of nAlPc.

In order to carry out local fluorescence spectroscopy of enamel microcracks and pathogenic microflora foci on the enamel surface, a model compound containing surfactants, auxiliary components and nAlPc colloid at a concentration of 10 mg/l was prepared.

Studies on the interaction of the model compound with nAlPc and Protelan MST-35 with tooth enamel ex vivo have shown this surfactant to be a promising auxiliary activator of the nanoparticles, allowing conducting local fluorescence spectroscopy of the tooth enamel surface 3 min after application. In addition, statistical processing of the results showed the effectiveness of using the model compound for local fluorescence spectroscopy of the enamel surface in order to detect the enamel microcracks and the pathogenic microflora accumulation foci that can lead to the development of a cariogenic process.

Keywords: local fluorescence spectroscopy, nanoparticles, aluminum phthalocyanine, fluorescence, enamel microcracks, caries.

For citations: Zolotareva J.O., Farrakhova D.S., Kupriyanova E.N., Loschenov V.B. Aluminium phthalocyanine nanoparticles activation for local fluorescence spectroscopy in dentistry, *Biomedical Photonics*, 2018, T. 7, No. 3, pp. 4-20. (in Russian). doi: 10.24931/2413–9432–2018–7–3–4–20.

Contacts: Zolotareva J.O., e-mail: JOKuznetsova@mail.ru

АКТИВАЦИЯ НАНОЧАСТИЦ ФТАЛОЦИАНИНА АЛЮМИНИЯ ДЛЯ ЛОКАЛЬНОЙ ФЛУОРЕСЦЕНТНОЙ СПЕКТРОСКОПИИ В СТОМАТОЛОГИИ

Ю.О. Золотарева[1], **Д.С. Фаррахова**[1, 2, 3], **Е.Н. Куприянова**[4], **В.Б. Лощенов**[1, 2, 3]
[1]Национальный исследовательский ядерный университет МИФИ, Москва, Россия
[2]Институт общей физики им. А.М. Прохорова Российской Академии Наук, Москва, Россия
[3]ООО «Дентоспек», Троицк, Москва, Россия
[4]АУЗ «Стоматологическая поликлиника №11 ДЗМ», Москва, Россия

Резюме

Ранняя диагностика кариеса и микротрещин эмали имеет большое значение для предотвращения разрушения здоровой эмали зубов. Для выявления микротрещин эмали и очагов скопления патогенной микрофлоры, которые могут стать причиной развития кариеса, в качестве маркера используется фталоцианин алюминия (AlPc) в виде наночастиц. В коллоидном растворе наночастицы не обладают собственной флуоресценцией, в отличие от молекулярной формы. Для перевода частицы в молекулярную форму необходимо присутствие растворителя или специфического окружения (бактерии, макрофаги и др.). Поэтому гидрофобные наночастицы фталоцианина алюминия (nAlPc) могут выступать в качестве маркера для обнаружения скрытых очагов скопления патогенной микрофлоры во время проведения флуоресцентной диагностики. Для сокращения времени диагностики и увеличения эффективности в качестве дополнительных активаторов nAlPc могут быть использованы биологически совместимые поверхностно-активные вещества (ПАВ).

Для проведения локальной флуоресцентной спектроскопии микротрещин эмали и очагов скопления патогенной микрофлоры на поверхности эмали была приготовлена модельная смесь, содержащая ПАВ, вспомогательные компоненты и коллоида nAlPc в концентрации 10 мг/л.
Исследования по взаимодействию модельной смеси с nAlPc и протеланом с эмалью зубов *ex vivo* показали перспективность использования этого ПАВ для дополнительной активации наночастиц, что позволяет проводить локальную флуоресцентную спектроскопию поверхности эмали зубов через 3 мин после нанесения. Также статистическая обработка результатов показала эффективность использования модельной смеси для локальной флуоресцентной спектроскопии поверхности эмали для выявления микротрещин эмали и очагов скопления патогенной микрофлоры, которая может привести к развитию кариесогенного процесса.

Ключевые слова: локальная флуоресцентная спектроскопия, наночастицы, фталоцианин алюминия, флуоресценция, микротрещины эмали, кариес.

Для цитирования: Золотарева Ю.О., Фаррахова Д.С., Куприянова Е.Н., Лощенов В.Б. Активация наночастиц фталоцианина алюминия для локальной флуоресцентной спектроскопии в стоматологии // Biomedical Photonics. – 2018. – Т. 7, № 3. – С. 4-20. doi: 10.24931/2413–9432– 2018–7–3–4–20.

Контакты: Золотарева Ю.О., e-mail: JOKuznetsova@mail.ru

Introduction

According to the World Health Organization, dental caries affects approximately 60–90% of schoolchildren and almost 100% of adults worldwide [1]. Early diagnosis of the disease and its timely treatment will not only preserve dental health for many years, but also improve the quality of life.

Currently, the methods used for early diagnosis of caries and various types of tooth enamel damage include visual inspection and probing, X-ray and a number of optical methods. The most common optical methods include the use of Raman scattering, optical coherence tomography, light scattering spectroscopy and local fluorescence spectroscopy.

Raman scattering is used to diagnose periodontitis by saliva analysis [2, 3], as well as to detect caries on the basis of a change in the composition and structure of enamel [4-6]. The disadvantages of this method are its use mainly in *ex vivo* conditions, and in the presence of an already formed damage of tooth enamel. This method may not be used to diagnose enamel microcracks and hidden foci of accumulation of pathogenic microflora. Optical coherence tomography makes it possible to detect qualitative and quantitative morphological changes in hard dental tissues *in vivo*. Due to its good spatial resolution, the method is suitable for the early diagnosis of dental diseases, such as caries, as well as periodontal tissue diseases, including oral cancer. Three-dimensional imaging is another advantage that optical coherence tomography provides in dentistry applications. However, the application of this method is limited by the depth of penetration of optical radiation into biological tissue and the relatively high cost of the procedure [7]. Local fluorescence spectroscopy, which uses ultraviolet radiation for diagnostics, makes it possible to identify the extent and boundaries of enamel caries damage, but it does not solve the problem of diagnosis in the early stages of caries development, when the waste products of bacteria are present in small quantities [8].

Local fluorescence spectroscopy using laser radiation with a wavelength in the red region of the spectrum is a more advanced diagnostic tool. This method can be used to diagnose dental calculus [9, 10], caries [11–15] and inflammatory processes of periodontal tissues [16]. To conduct local fluorescence spectroscopy of enamel in the visible range of the spectrum, a sufficient amount of endogenous porphyrins is necessary, which are the product of the vital activity of bacteria accumulating in enamel areas damaged by caries, in microcracks or on the surface of dental calculus [8, 17]. But in the early stages of caries development, autofluorescence of pathogenic microflora is weakly expressed, which makes it difficult to conduct local fluorescence spectroscopy.

In 2007, it was proposed to use aluminum phthalocyanine nanoparticles (nAlPc) to detect pathogenic microflora localized in microdamage areas of tooth enamel [18]. Nanoparticles are used as a marker due to the fact that nAlPc are not fluorescent and photoactive in an aqueous medium [19], but when interacting with a specific biological environment, they begin to fluoresce and exhibit photodynamic activity. For fluorescence to occur, it is necessary that the phthalocyanine molecules separate from the particle surface or are in a partially bound state [20], which usually occurs in the presence of a solvent or a specific environment (bacteria, macrophages, etc.) [19-23]. The mechanism of the occurrence of fluorescence can presumably be described with a model involving the transition of molecules on the surface of a nanoparticle from the para position to the ortho position [19, 20, 22–24].

A number of authors [25, 26] indicate the possibility of fluorescence diagnostics of enamel microdamages 15 minutes after the application of colloid of nanoparticles to the enamel surface.

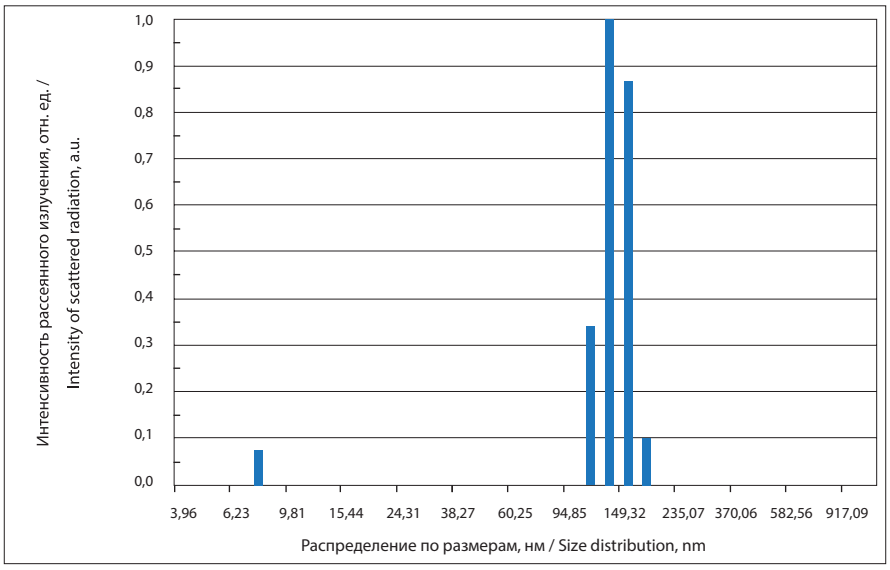

Рис. 1. Распределение nAlPc по гидродинамическому радиусу
Fig. 1. Distribution of nAlPc hydrodynamic radius

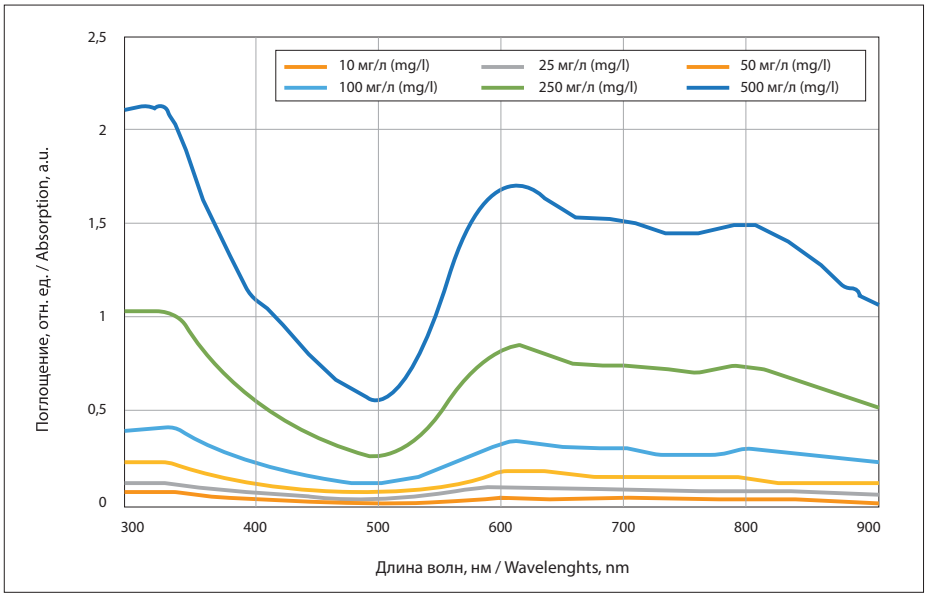

Рис. 2. Спектры поглощения коллоидных растворов nAlPc в концентрациях 10, 25, 50, 100, 250 и 500 мг/л
Fig. 2. Absorption spectra of nAlPc colloidal solutions at concentrations of 10, 25, 50, 100, 250 and 500 mg/l

It is also known from the literature that, due to the photodynamic effect, water-soluble forms of aluminum phthalocyanine have an inhibitory effect on the growth of a number of bacteria that cause various types of damage of tooth enamel and periodontal tissues. In particular, photodynamic therapy with desulfurized aluminum phthalocyanine leads to the death *Streptococcus sanguis, Porphyomonas gingivalis, Escherichia coli, Streptococcus mutans, Candida albicans Actinobacillus actinotnycetetttcotnitans Streptococcus sobrinus, Lactobacillus casei* and *Actinomyces viscosus* [27–31], with chlorinated aluminum phthalocyanine, to the death of *Candida albicans* [32, 33], and with the use of a nanoemulsion, *Staphylococcus aureus* [34].

To reduce the waiting time for fluorescence enhancement, it was proposed to use a surfactant as an additional nAlPc activator, which would transfer a part of the surface molecules of nanoparticles to a more mobile

state. These molecules, without detaching themselves from the nanoparticle, can interact with the microenvironment and exhibit their fluorescence and photodynamic properties, which are close to their characteristics in molecular form.

The goal of this research is to study the interaction of laser radiation with nAlPc on the enamel surface for phototheranostics of initial caries. To achieve this goal, it is necessary to develop a method for controlling the concentration and size of particles in a colloid, and select the optimal surfactant in terms of health safety and fluorescence characteristics for additional activation of nAlPc.

To conduct local fluorescence spectroscopy of the enamel surface in order to detect enamel microcracks and foci of accumulation of pathogenic microflora, model mixtures were prepared containing different surfactants, nAlPc colloid and auxiliary components, and the spectro-fluorescence characteristics of *in vitro* mixtures and *ex vivo* tooth enamel were analyzed.

Materials and methods

Preparation of colloid of aluminum phthalocyanine nanoparticles

The colloidal solution of nAlPc was made with coarse-grained AlPc crystals produced by FSUE SSC NIOPIK (Russia) and distilled water. The crystals were dispersed with the use of Bandelin SONOPLUS HD2070 ultrasonic homogenizer with a KE76 tip (20 kHz, amplitude 165 μm) (Germany). The duration of dispersion was 30 minutes. The colloidal solution was then centrifuged in Centrifuge ELMI CM-6M unit for 10 minutes at a speed of 35,000 rpm. After centrifugation, large particles precipitated. Small particles in the upper layer were collected with the use of an automatic pipette dispenser. To control the particle size in the colloid, a static and dynamic light scattering spectrometer Photocor Complex (Russia) was used. A cuvette with a colloidal solution was irradiated with a low-intensity laser with an excitation wavelength of 635 nm to detect scattered light on the particles.

Fig. 1 shows the results of measuring the hydrodynamic radius of nAlPc in an aqueous medium at a concentration of 10 mg/l. nAlPc particles with a hydrodynamic radius of 140±36 nm and 9±2 nm scatter light in 97% and 3% of cases, respectively.

It is essential that an aqueous suspension of nanoparticles does not fluoresce. To study the interaction of nAlPc with enamel surface microflora, the colloid nAlPc at a concentration of 10 mg/L was used.

Monitoring the concentration of colloidal solution of aluminum phthalocyanine nanoparticles

To control the concentration of nAlPc in the colloid, a normalization curve was constructed based on experimental data. The absorption spectra (Fig. 2) of colloidal nAlPc solutions with known concentrations were measured with a Hitachi U-3400 spectrophotometer (Japan). The values of the optical density of colloids at an absorption wavelength of 538 nm which were plotted on a graph and were found to have a linear relationship were selected (Fig. 3). The concentration of the prepared nAlPc colloid was controlled with a normalization curve.

Preparation of experimental samples for studying the interaction of aluminum phthalocyanine nanoparticles with various surfactants

In order to study the possibility of using various surfactants as additional activators of nAlPc, experimental samples containing 0.5–2% surfactant and a colloidal solution of nAlPc at a concentration of 10 mg/L were prepared. The following were used as additional activators of nanoparticles: Tween 80, Propyleneglycol, Protelan MST-35, Plantacare 1200 UP, Lauryl Glucoside and sodium laurylethoxysulfate. Tween 80 is a hydrophilic non-ionic surfactant commonly used to increase bioavailability and targeted drug delivery in preclinical *in vivo* studies [35–37]. Propyleneglycol is used in the food industry as a food additive E1520. Plantacare, Protelan and sodium lauryl ethoxysulfate are approved as ingredients for toothpastes [38]. The control sample was an aqueous colloidal solution of nAlPc at a concentration of 10 mg/L without additives.

The creation of a model mixture with aluminum phthalocyanine nanoparticles and surfactants for local enamel fluorescence spectroscopy

To conduct *ex vivo* PD of tooth enamel, a model mixture was prepared containing nAlPc (10 mg / L), protelan (1%) and some additional components. The additional components were substances which are usually used in the production of toothpaste in accordance with GOST 7983–99 "Toothpastes. General specifications." Protelan is a surfactant that is produced from 100% of natural ingredients and does not harm living organisms or the environment where people live.

Before preparing the model compound, we optimized the structure and concentration of the components. A sample of the model mixture was studied immediately after preparation and after it had been held in a special thermostat (42°C, 1 month), which is equivalent to exposure at room temperature for 12 months.

To study the spectral properties of nAlPc, additional samples were used in the model mixture with Protelan: the basis of the model mixture without nAlPc and Protelan and the model mixture containing only nAlPc Additional samples of the model mixture were prepared to test the hypothesis stating that a surfactant can activate surface nanoparticle molecules like a solvent. The

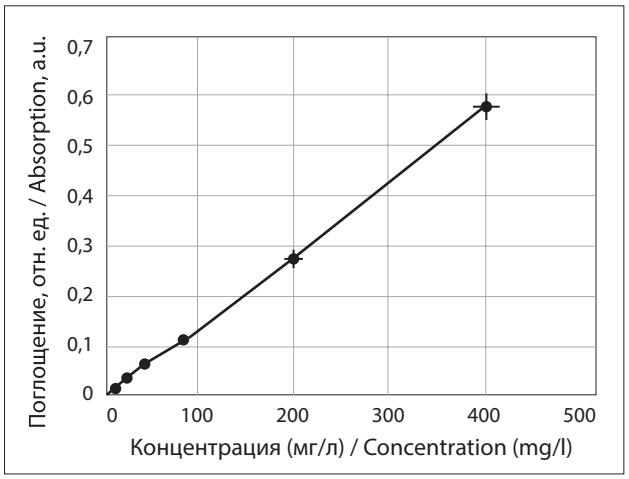

Рис. 3. График нормировочной кривой зависимости поглощения от концентрации коллоида nAlPc, применявшийся для контроля концентрации коллоидного раствора nAlPc
Fig. 3. The graph of the normalized curve used to control nAlPc colloid concentration: the dependence of the absorption on the concentration of the nAlPc colloid

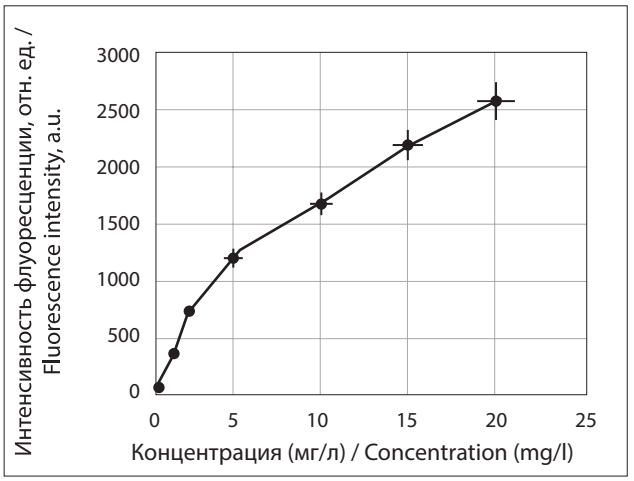

Рис. 4. Зависимость интенсивности флуоресценции nAlPc, перешедших в молекулярную форму, от концентрации при растворении в ДМСО
Fig. 4. The dependence of the fluorescence intensity of nAlPc, transformed into a molecular form, on the concentration at dissolution in DMSO

difference between the solvent of nanoparticles and the surfactant is that the solvent transfers surface molecules to a free state, while the surfactant makes them more mobile and capable of interacting with microflora without separating them from the surface of nanoparticles [38–40].

The control of the fraction of activated aluminum phthalocyanine nanoparticles in an aqueous solution and a model mixture

To quantify the fraction of activated nAlPc in the sample (converted to molecular form) depending on the concentration of surfactants and the interaction time, a calibration curve was produced. To construct, we used the experimental data obtained by the interaction of an organic solvent, dimethyl sulfoxide (DMSO) [41] with various concentrations of nAlPc (LESA-01-BIOSPEC spectrometer (Russia)). The findings are represented in Fig. 4. From the data obtained, it can be seen that for a concentration of nanoparticles of 10 mg/L at 100% solubility (complete transition to molecular form) in DMSO, the fluorescence intensity is 1700 relative units. Thus, knowing the concentration of nAlPc in the experimental sample and using the calibration curve, we can determine the fraction of activated nAlPc (converted to molecular form) as the ratio of the fluorescence intensity of nAlPc in the solution to the fluorescence intensity of nAlPc in DMSO.

To quantify the percentage of activated nanoparticles in the composition of the ready model mixture, a sample was prepared containing the model mixture and DMSO. The concentration of nanoparticles in the experimental sample was 2.5 mg/L. To achieve uniform composition, the sample was subjected to ultrasonic treatment. After that, the maxima of the fluorescence intensities of the model mixture and the experimental sample with DMSO were obtained where complete dissolution of nAlPc was observed, which signals the transition to the molecular form. The ratio between the fluorescence maxima was used to determine the fraction of activated nAlPc in the ready model mixture.

The biological samples for experimental research

To study the interaction of nAlPc with tooth enamel and pathogenic microflora contained on the surface and in microdamages of tooth enamel, human teeth were used (a total of 41 samples), which had been removed for various clinical indications. from the time of their removal to the time of the experiment, samples of extracted teeth were contained in an aqueous 0.9% sodium chloride solution for maximum preservation of microflora contained on the enamel surface.

During the experiment, an nAlPc colloid or model mixture was applied to the surface of the tooth enamel and washed off with water after 3 minutes.

An experimental unit for studying the interaction of a colloid of aluminum phthalocyanine nanoparticles with surfactants, a colloid of aluminum phthalocyanine nanoparticles and a model mixture of aluminum phthalocyanine nanoparticles and Protelan with tooth enamel surface microflora

An experimental unit was assembled for the research, consisting of a laser source for exciting fluorescence and a miniature universal spectrometer for recording and analyzing fluorescent signals.

A laser (632.8 nm) was used as a radiation source exciting fluorescence. The signal was detected with a LESA-01-BIOSPEC laser spectrometer (Russia) [42]. The measurement unit scheme is shown in Fig. 5.

Fluorescence measurement in samples containing nAlPc and surfactant was carried out at the following time intervals: 0–180 minutes, 1–6 days. For measurements, the cuvette with the sample was placed in a specially designed chamber (Fig. 4) with a sufficient level of protection against the impact of alien sources. The fiber optic probe (FOP) is in contact with the sample at an angle of 15° to prevent reflected light from the opposite wall of the Eppendorf device from entering the receiving fibers. The FOP consists of one light fiber and six receiving fibers. The distal end diameter is 1.8 mm.

During the studies on the interaction of the colloid nAlPc and the model mixture (with nAlPc and Protelan) with the surface microflora of tooth enamel, the FOP was placed in contact with the sample.

To visually assess the fluorescence image of the enamel surface before and after applying the model mixture to the tooth enamel, a video fluorescent system was used, which consists of a laser radiation source (635 nm), a light filter with a transmission range of 650–1500 nm, and a sensitive black-and-white camera.

Results processing

When studying the interaction of nAlPc with various surfactants, the processing of the results obtained in the form of spectra on LESA-01 Biospec unit was carried out in several stages. At the first stage, the spectra were averaged for each time point (with Uno Momento software supported in the MS Windows environment). The next step was normalization to the laser peak in order to be able to compare several spectra obtained at different time intervals and to take into account the influence of various factors (measurement geometry, laser power). Then, for each experimental sample, a chart was produced for the temporal dependence of the nAlPc fluorescence intensity upon interaction with various surfactants at various concentrations. The results were processed in a similar manner when studying the spectroscopic properties of a model mixture with nAlPc and Protelan.

The experimental results with biological samples included two groups. The first group consisted of a collagen solution of nAlPc and biological samples of human teeth, and the second group included a model mixture with nAlPc and Protelan and biological samples.

For each sample from both groups, a series of enamel autofluorescence spectra before and AlPc fluorescence spectra after applying a colloid of nanoparticles or a model mixture on tooth enamel were obtained. Each series of spectra was a set of data obtained for various areas on the surface of tooth enamel. The data obtained in the study of the interaction of the colloid nAlPc and the model mixture with tooth enamel *ex vivo* were normalized by the exposure time. Based on the series of

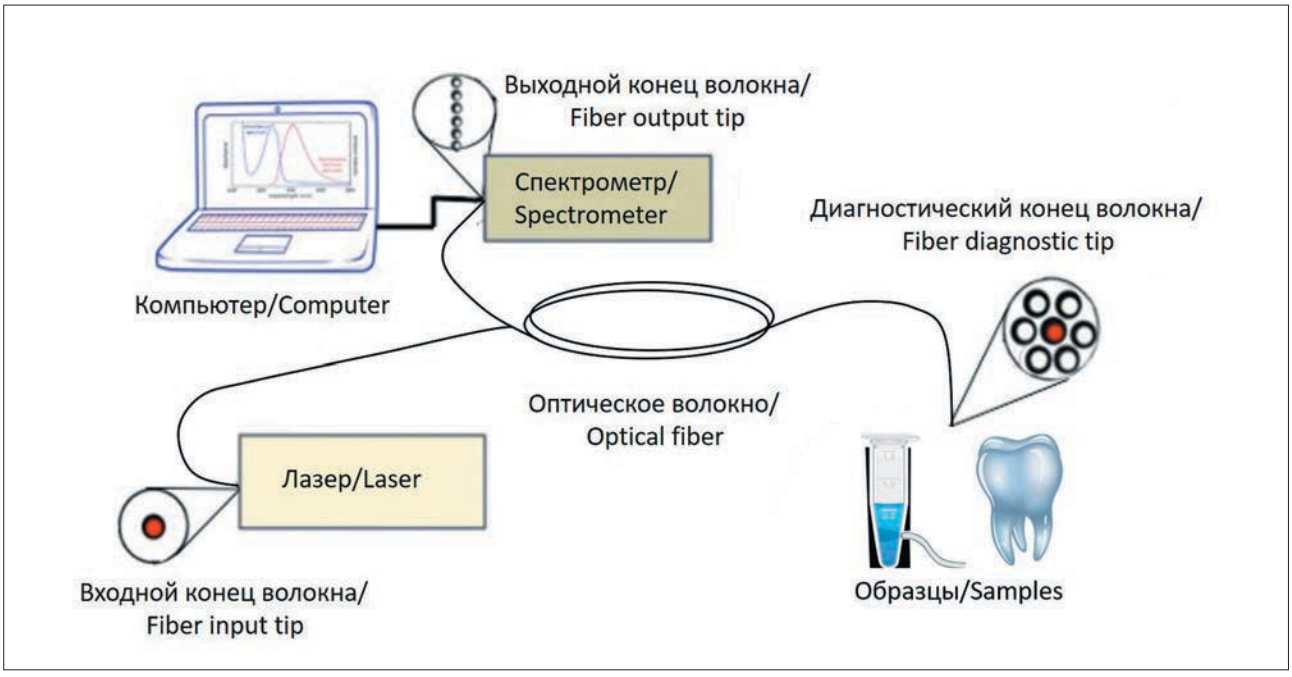

Рис. 5. Схематическое представление измерительной установки
Fig. 5. Experimental setup

spectra for each biological sample, the average value of the autofluorescence spectrum up to and AlPc fluorescence after applying a colloid of nanoparticles or a model mixture on tooth enamel was calculated.

Then, using the average spectrum value, for each sample, the enamel autofluorescence coefficient k_{af} was calculated as the ratio of the areas under the enamel autofluorescence spectrum to the area under the laser peak. Similar actions were performed to calculate the fluorescence coefficient k_{fl} of nAlPc after applying the colloid to the enamel, for a single sample.

Thus, for each experimental group of samples, an array of data was obtained with the enamel autofluorescence coefficients before and nAlPc fluorescence coefficients after applying a colloid of nanoparticles or a model mixture to the tooth enamel surface. To assess the difference in fluorescence from the enamel surface before and after application of experimental compositions with nAlPc, the fluorescence enhancement coefficient was calculated for each sample, which is the ratio of k_{fl} to k_{af}, and the area chosen for the calculation of k_{af} was the area under the autofluorescence spectrum which corresponded to the boundaries of the nAlPc fluorescence signal:

$$k_{DK} = \frac{k_{fl}}{k_{af}}$$

The fluorescence enhancement coefficients for each sample were used for statistical processing of experimental results, which was performed with the use of Statistics SPSS v23.0 computer program. The two groups of teeth (with the use of a colloidal solution of nAlPc or a model compound with nAlPc) were compared with Student's t-test.

Results and discussion

The results of the study of the interaction of aluminum phthalocyanine nanoparticles with various surfactants

It is known that surfactants affect the photophysical and photochemical properties of organic molecules. In the presence of surfactants, the acid-base properties of the molecules in the basic state and excited state change. The spectral and luminescent characteristics and the state of aggregation of the dyes change. A large number of chemical reactions in the presence of surfactants proceed differently from the way they occur in solutions [43].

Ethanol and surfactants act on the state of the medium in approximately the same way [40]. Since ethanol is a solvent of nAlPc nanoparticles [41], surfactants interacting with nanoparticles can activate them the way a solvent does [38, 39].

The study of the dynamics of interaction of aluminum phthalocyanine nanoparticles with propylene glycol

During the experiment, the dependence of the fluorescence index of nanoparticles upon interaction with propylene glycol (concentration 0.5–2%) over a time interval from 0 min to 7 days was investigated. It was found that propylene glycol does not interact with nanoparticles and does not cause nAlPc fluorescence.

The study of the dynamics of the interaction between aluminum phthalocyanine nanoparticles and Tween 80

The surface-active substance Tween 80 (polysorbate-80) is an emulsifier that is used in the food and cosmetic industries [39]. In [44], Tween 80 was used to prepare an emulsion to improve targeted delivery of chlorinated AlPc and to enhance the biodistribution of nanoparticles by coating the surface of AlPc particles [41]. Biologically compatible surfactants (Tweens) can be used to reduce the molecular aggregation that is observed for hydrophobic phthalocyanines, such as AlPc, in an aqueous medium. It is known that aggregation leads to deterioration of the effectiveness of photodynamic therapy and reduces the intensity of fluorescence [45].

Figure 6 shows a graph of the temporal dependence of nAlPc fluorescence intensity during interaction with Tween 80 at various concentrations. The graphs show that a strong increase in nAlPc fluorescence is observed at almost all time intervals when interacting with Tween 80. An increase in nAlPc fluorescence continues for up to 4 days. Then there is a decline followed by subsequent growth.

It was also noted that after 4 days, the nanoparticles in the experimental samples begin to precipitate. Shaking results in the formation of flakes, which do not dissolve. The maximum fraction of activated molecules located on the nAlPc surface varies in the range of 6–8% of their total calculated amount at Tween 80 concentrations of 0.5–2%.

The study of the dynamics of interaction between aluminum phthalocyanine nanoparticles and sodium lauryl ethoxysulfate

Sodium lauryl ethoxysulfate is an extremely hydrophilic surfactant [38]. At concentrations of 1% and 2% in the sample, it causes an increase in nAlPc fluorescence for up to 3-4 days, then the nanoparticles begin to precipitate, and the fluorescence decreases (Fig. 7).

The relatively low fluorescence of nAlPc is caused by the presence of 0.5% sodium lauryl ethoxysulfate in the sample. The fraction of activated molecules varies in the range of 0.5–3% when sodium lauryl ethoxysulfate has concentrations of 0.5–2%.

Investigation of the interaction of aluminum phthalocyanine nanoparticles as a function of time of interaction with Protelan

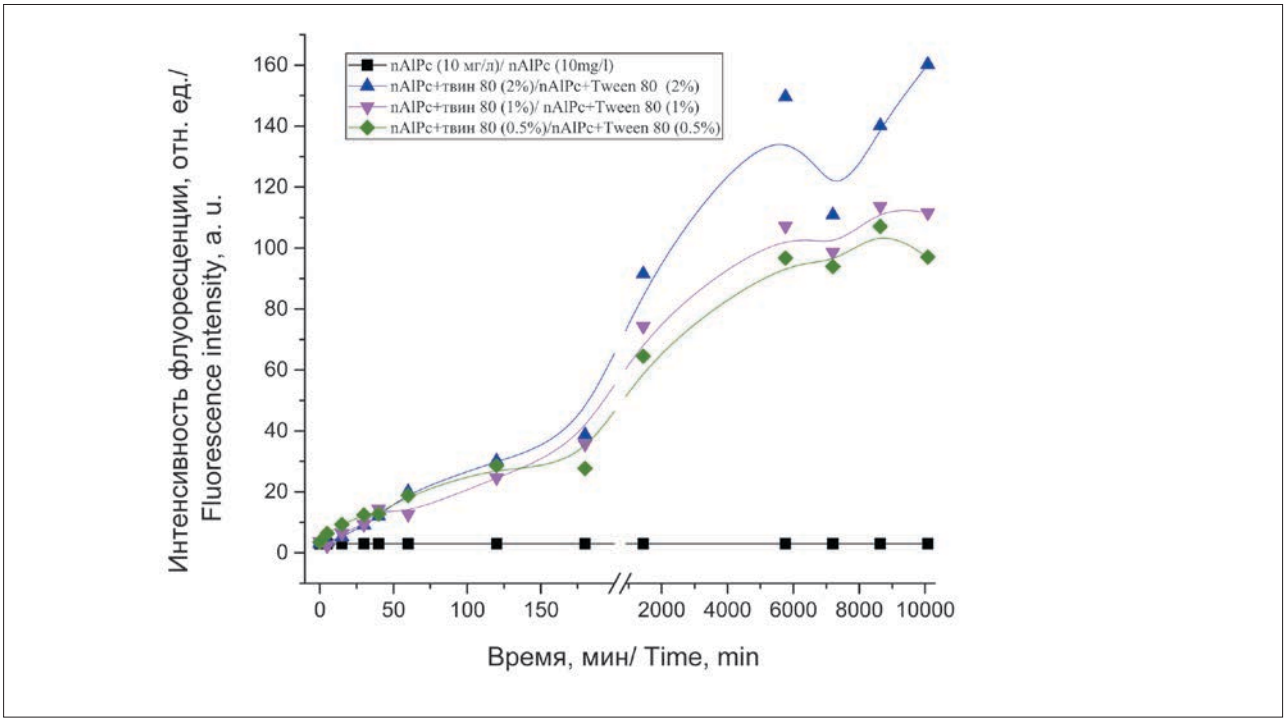

Рис. 6. Динамика интенсивности флуоресценции nAlPc при взаимодействии с твин 80 в концентрациях 0,5–2%
Fig. 6. The dependence of the fluorescence intensity on time in interaction with Tween 80 in concentrations of 0.5–2%

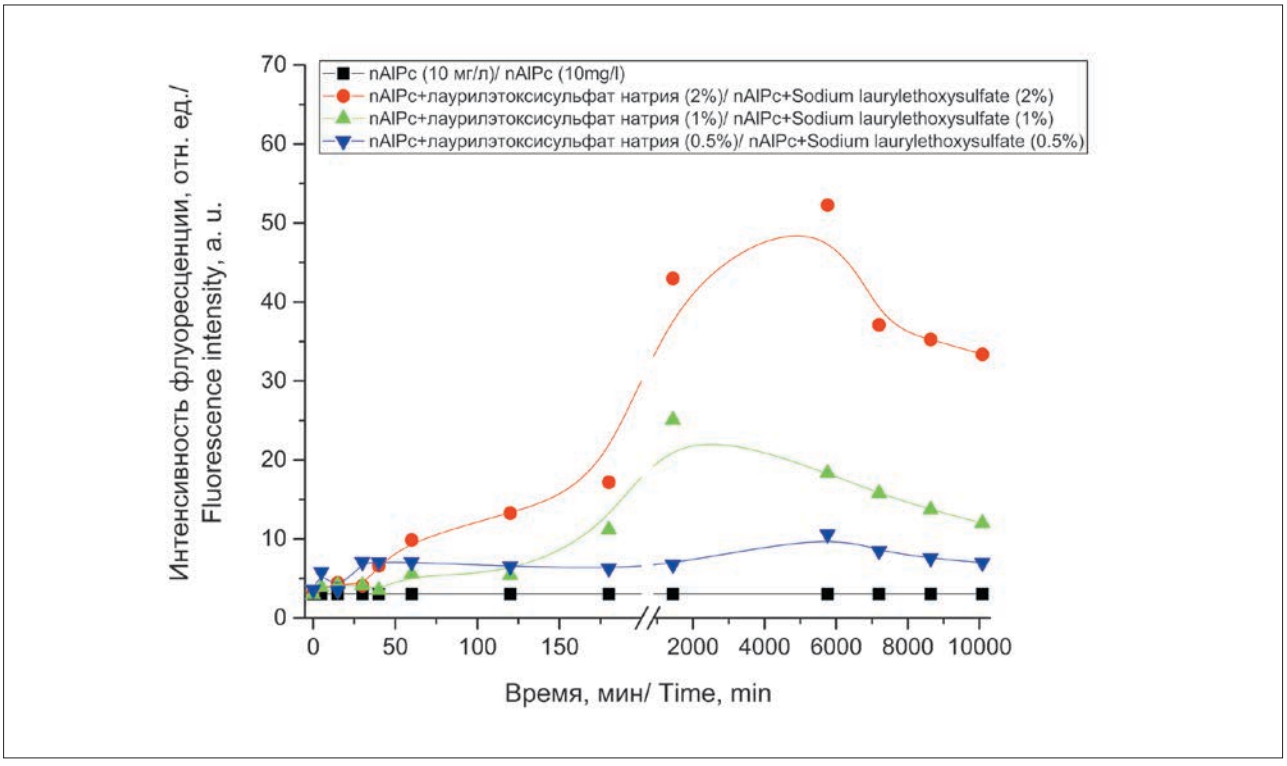

Рис. 7. Динамика интенсивности флуоресценции nAlPc при взаимодействии с лаурилэтоксисульфатом натрия в концентрациях 0,5–2%
Fig. 7. The dependence of the fluorescence intensity of nAlPc on time at interaction with sodium laurylethoxysulfate in concentrations of 0.5–2%

Protelan is obtained from 100% natural, renewable plant materials and does not contain sulfates, preservatives, EO groups and 1,4-dioxane. As a chemical substance, Protelan is characterized by high foaming ability and is used in the production of oral care products. This surfactant is also used in space, does not harm the body or the environment. It is easily biodegradable and approved by Cosmos standard [46]. In the interaction of nanoparticles with Protelan at concentrations of 0.5% and 1%, there is a strong increase in the maximum fluorescence intensity at 6 days after sample preparation, and at a concentration of 2% at 4 days (Fig. 8).

The decrease in fluorescence of nanoparticles is associated with their aggregation and precipitation. The fraction of activated nanoparticles varies in the range of 2–4.5% at surfactant concentrations of 0.5–2%.

The study of the dynamics of the interaction between aluminum phthalocyanine nanoparticles and Plantacare

Plantacare (Lauryl Glucoside) is synthesized from natural raw materials during the rectification of vegetable fats (coconut oil and glucose). In cosmetics, it acts as an emulsifier, dispersant, natural foaming agent, increases the viscosity; it is completely non-toxic and easily biodegradable. When interacting with nAlPc, it causes their fluorescence, the increase of which lasts up to 3–6 days, depending on the concentration. The decrease in fluorescence of nanoparticles is associated with their aggregation and subsequent precipitation. The fraction of activated nAlPc varies in the range of 0.6–2% at surfactant concentrations of 0.5–2% (Fig. 9).

Fluorescence spectra of aluminum phthalocyanine nanoparticles when interacting with various surfactants

During the experiment, it was revealed that there is a definite shift in the nAlPc fluorescence wavelength upon interaction with sodium lauryl sulfate compared to other surfactants by 15 nm, regardless of the concentration of substances and the time after the start of interaction. Figure 10 shows the fluorescence spectrum of nAlPc 40 min after the interaction with various types of surfactants (in 2% concentration).

It was hypothesized that the shift in the fluorescence wavelength may be due to the difference in the pH of the surfactant solution with nanoparticles or the absorbing characteristics of the surfactant.

For each surfactant, the pH values were: for Propyleneglycol, 5.5–8; for Tween, 80 - 5.5–7.5; for sodium lauryl ethoxysulfate, 7–9; for Protelane, 9–10; for Plantacare, 11.5–12.5. As can be seen from the data presented, there is no relationship between the pH of the samples and the shift in the wavelength of the nAlPc fluorescence upon interaction with sodium lauryl sulfate compared to other surfactants. It is also important to note that none of the experimental samples possessed a critical concentration of surfactant micellization, and the type of hydrophilic surfactant group does not affect the fluorescence of nanoparticles [39].

Plots of absorption spectra of various surfactants were obtained at a concentration of 1% by volume with the use of a Hitachi U-3400 spectrophotometer (Japan).

The measurement results showed that all surfactants do not absorb in the spectral range from 350 nm to 850 nm and do not strongly affect the nAlPc fluorescence spectra. Therefore, the reason for the change in the fluorescence wavelengths of the nanoparticles upon interaction with sodium lauryl ethoxysulfate relative to other spectra is not completely clear.

The spectroscopic properties of a model mixture with aluminum phthalocyanine nanoparticles and Protelan for local fluorescence enamel surface spectroscopy

The experiment for the study of the spectroscopic properties of nAlPc in the composition of the model mixture for the PD enamel state included the use of various samples: the basis of the model mixture without nAlPc and Protelan; model mix with nAlPc; model mix with nAlPc and Protelan. The main objective of the experiment was to test the hypothesis that surfactants interacting with nAlPc is capable of activating surface molecules like a solvent, the only difference being that a solvent transfers the molecules to the free state and a surfactant makes them more mobile and reactive without detaching them from the nanoparticle [38–40].

Samples of the model mixture were studied immediately after preparation and after exposure to a special thermostat at 42°C for 1 month, which is equivalent to being at room temperature for 12 months. The findings of the research are represented in Fig. 11. The peak at a wavelength of 632.8 nm corresponds to laser radiation scattered back from the sample surface, which was used to normalize the fluorescence spectra (670 nm) and to numerically estimate the concentration of fluorescent components.

As can be seen from the obtained experimental data, the spectroscopic properties of the model mixture immediately after preparation and after exposure which simulates 12-month storage, changed in the form of a two-fold fluorescence growth. Calculations show that fluorescent molecules are bound to nanoparticles. The pH of the model mixture was 6.27. The composition also did not contain any microflora: *Enterobacteriaceae, Pseudomonas aeruginosa, Staphylococcus aureus*, mold fungi and yeast. The model mixture is microbiologically pure and homogeneous, and its thickness is suitable for the use in a clinical setting.

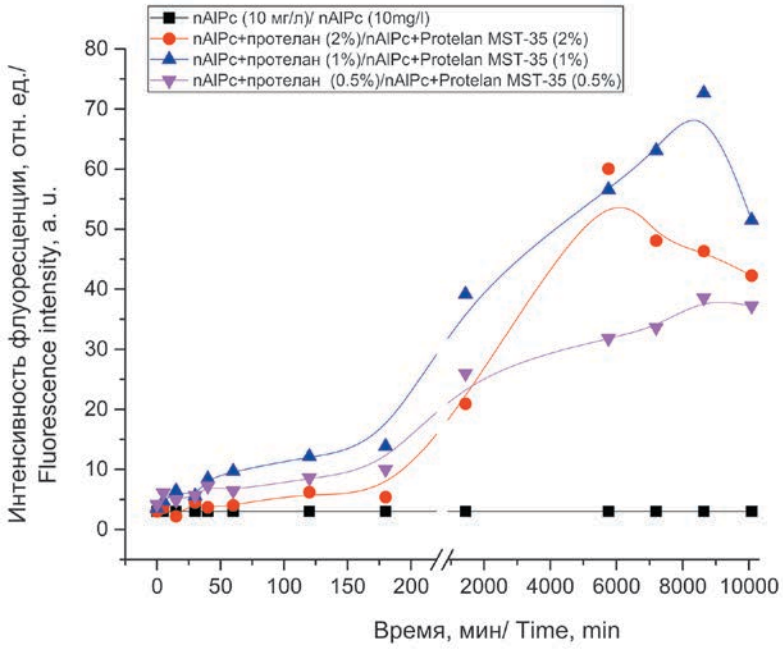

Рис. 8. Динамика интенсивности флуоресценции nAlPc при взаимодействии с протеланом в концентрациях 0,5–2%.
Fig. 8. The dependence of the fluorescence intensity of nAlPc on time at interaction with Protelan MST-35 in concentrations of 0.5–2%

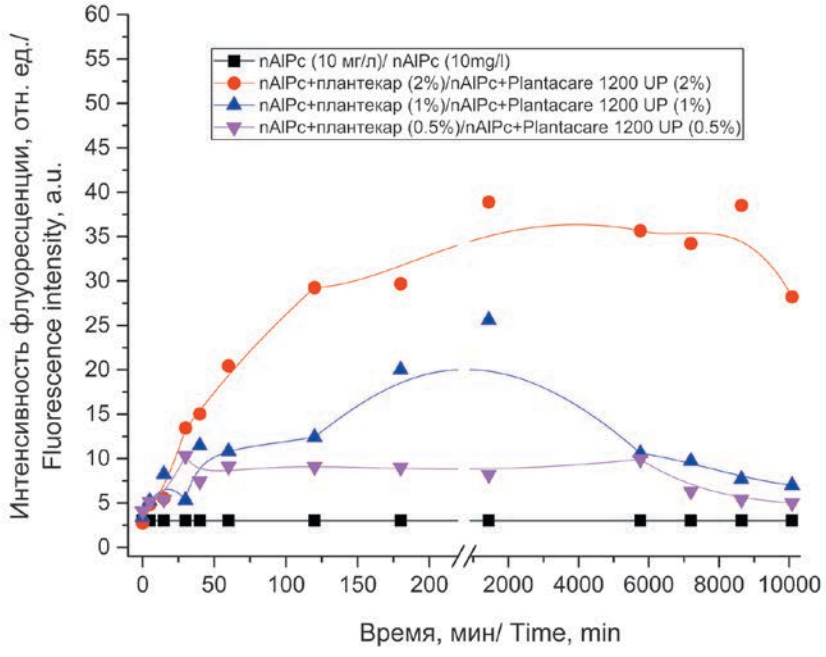

Рис. 9. Динамика интенсивности флуоресценции nAlPc при взаимодействии с плантекаром в концентрациях 0,5–2%.
Fig. 9. The dependence of the fluorescence intensity of nAlPc on time at interaction with Plantacare 1200 UP in concentrations of 0.5–2%

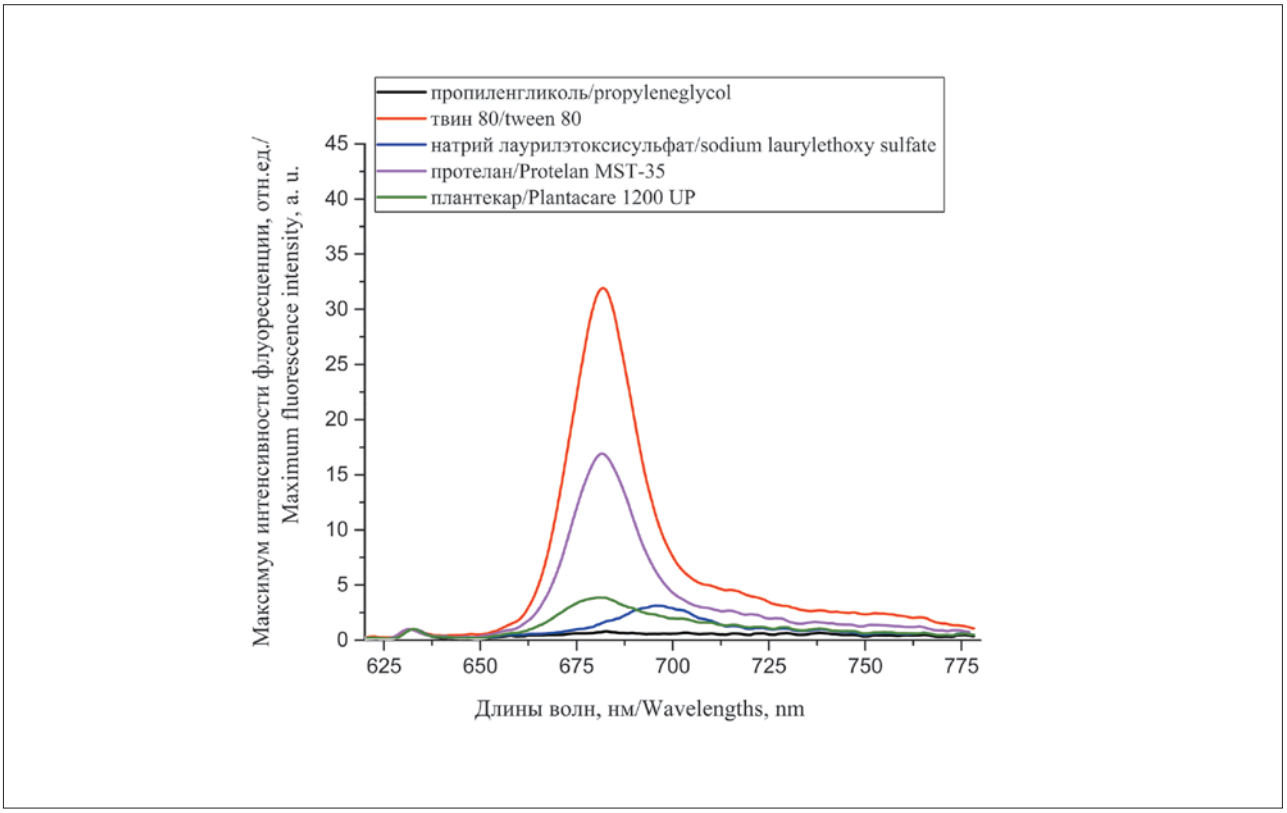

Рис. 10. Спектры флуоресценции nAlPc при взаимодействии с различными ПАВ через 120 мин после приготовления образцов
Fig. 10. Fluorescence spectra of nAlPc interacting with various surfactants 120 min after sample preparation

The preliminary shelf life of the model mixture is at least 12 months.

To quantify the percentage of activated molecules in the composition of the finished model mixture with nAlPc and Protelan, a sample was prepared containing the model mixture and DMSO, which is a solvent of nanoparticles. The concentration of nanoparticles in the experimental sample was 2.5 mg/L. The results of measuring the fluorescence of nanoparticles in the sample, as well as in the model mixture, are presented in Fig. 12.

The fluorescence intensity of all molecules upon dissolution of nAlPc in DMSO is about 100 relative units, at a concentration of nAlPc in the sample of 2.5 mg/L. At the stated concentration in the model mixture of 10 mg/l, the fluorescence intensity of the phthalocyanine molecules has to be 400 relative units. As can be seen from fig. 10 and 11, the fluorescence intensity in the composition of the model mixture is approximately 4–8 relative units. Thus, it can be concluded that about 1–5% of molecules in the activated model are in the activated state. Such a small number of molecules in a free state will allow not only to increase the efficiency and reduce the time of PD, but also to distinguish between the fluorescence of nanoparticles in the presence and in the absence of pathogenic microflora in the area under examination.

The results of a study of the interaction of colloid nanoparticles of aluminum phthalocyanine with enamel ex vivo

The results of studies to identify the nature of the interaction of the colloidal solution of nAlPc with enamel *ex vivo* tooth samples showed that after 3 min there is a low fluorescence due to autofluorescence of microflora and slight activation of surface nanoparticle molecules. A marked increase in the fluorescence of nAlPc occurs 1 h after the application of the colloidal solution. This suggests that it takes some time for the activation of surface nanoparticle molecules by pathogenic microflora located on the surface of the tooth enamel.

To conduct fluorescence diagnostics in a clinical setting, one hour required for fluorescence enhancement is too long an interval for the procedure. This problem is solved by introducing an additional nAlPc activator into

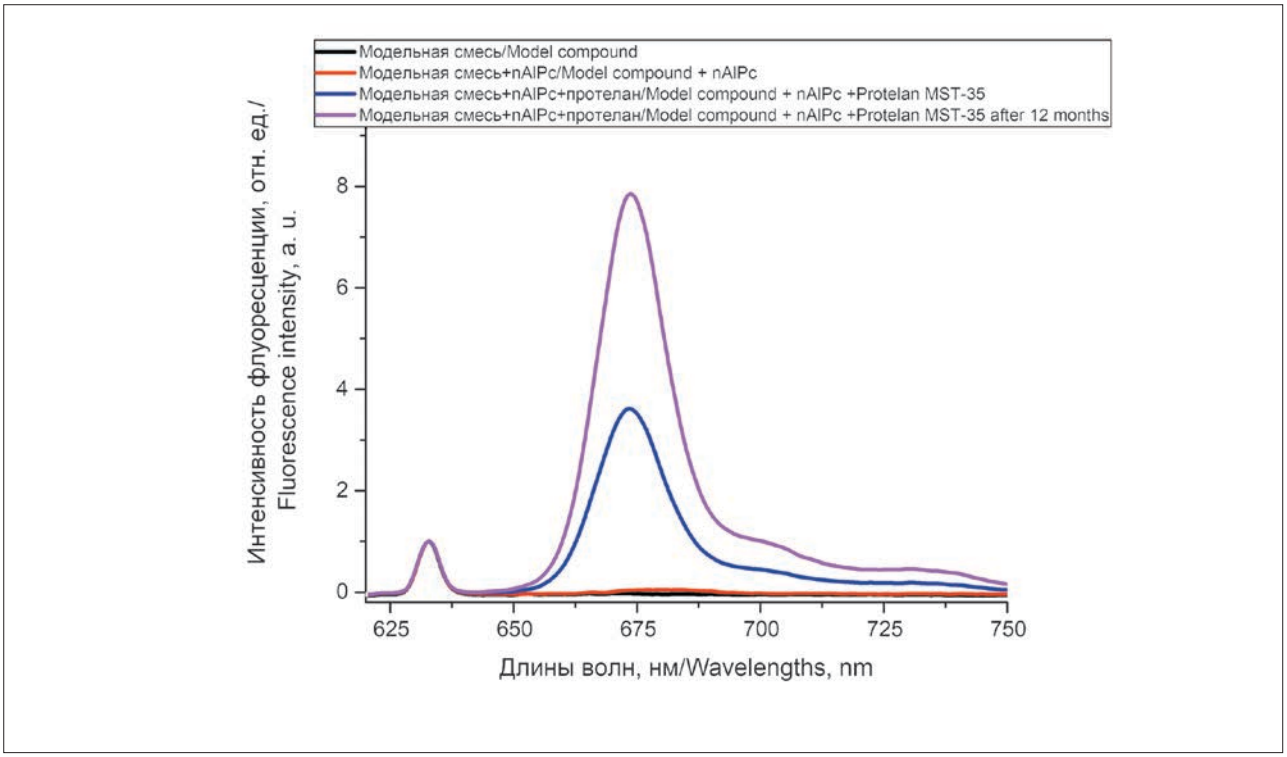

Рис. 11. Спектры флуоресценции модельной смеси, модельной смеси с nAlPc и модельной смеси с nAlPc и протеланом, полученные сразу после приготовления и через 12 мес
Fig. 11. Fluorescence spectra of the model compound, the model compound with nAlPc and the model compound with nAlPc and Protelan MST-35 measured immediately after preparation and 12 months later

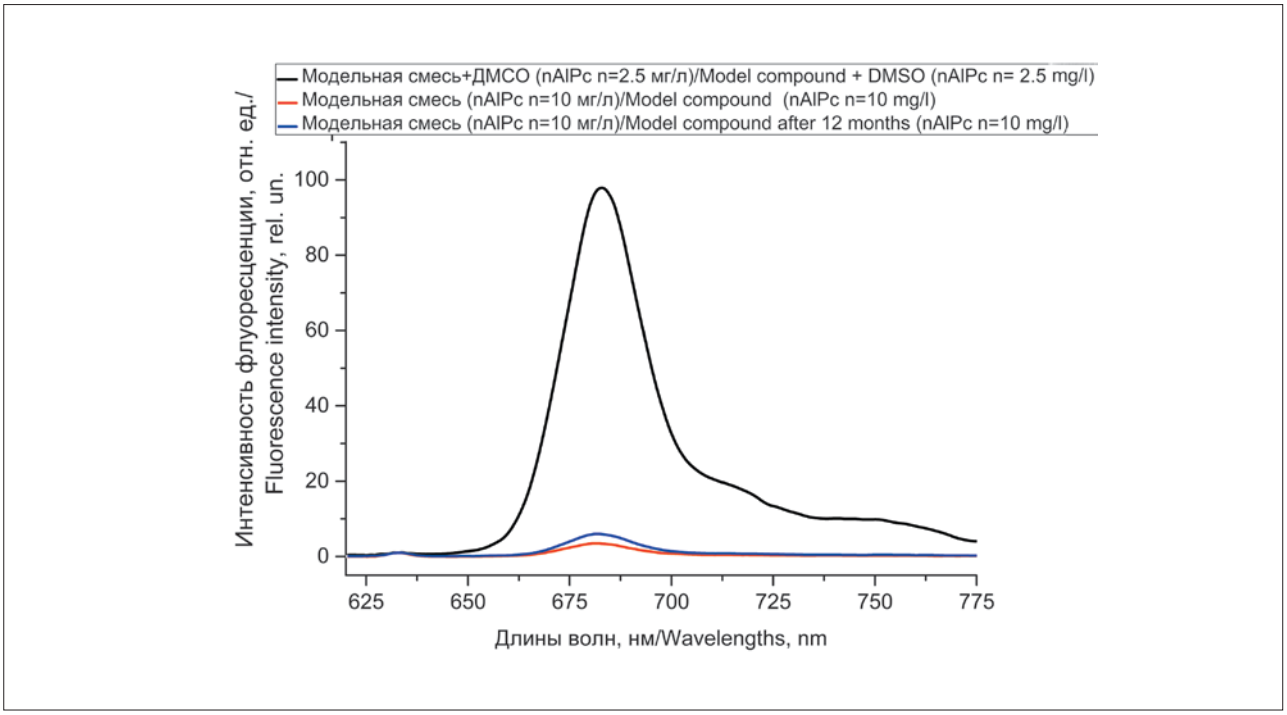

Рис. 12. Спектры флуоресценции модельной смеси с nAlPc (2,5 мг/л) и ДМСО и модельной смеси с nAlPc (10 мг/л) сразу после приготовления и спустя 12 мес
Fig. 12. Fluorescence spectra of the model compound (nAlPc 2.5 mg/l) with DMSO, and model compound (nAlPc 10 mg/l) immediately after preparation and 12 months later

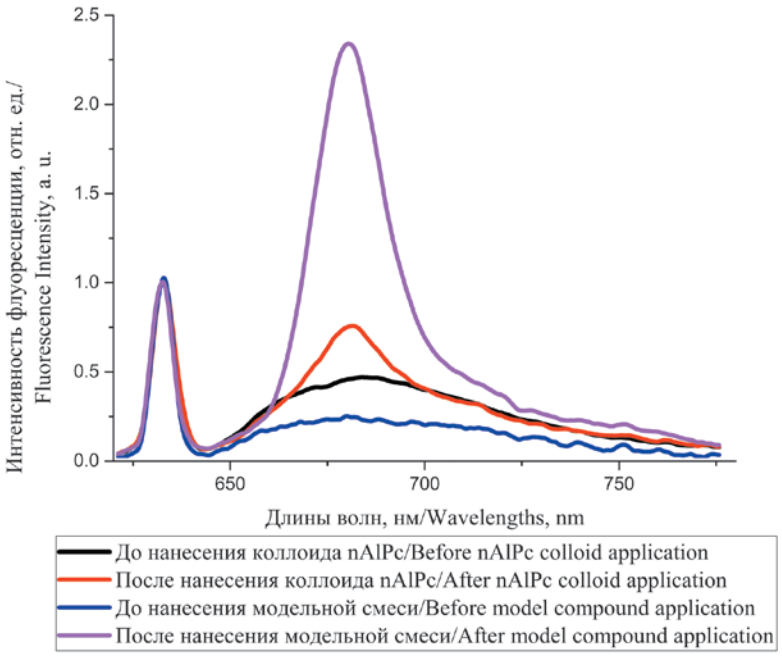

Рис. 13. Спектры флуоресценции nAlPc до и после нанесения модельной смеси с ПАВ и коллоида nAlPc на поверхность эмали зубов (экспозиция 3 мин)
Fig. 13. nAlPc fluorescence spectra before and after the application of the model compound with surfactant and nAlPc colloid on the tooth enamel surface (3 min exposition)

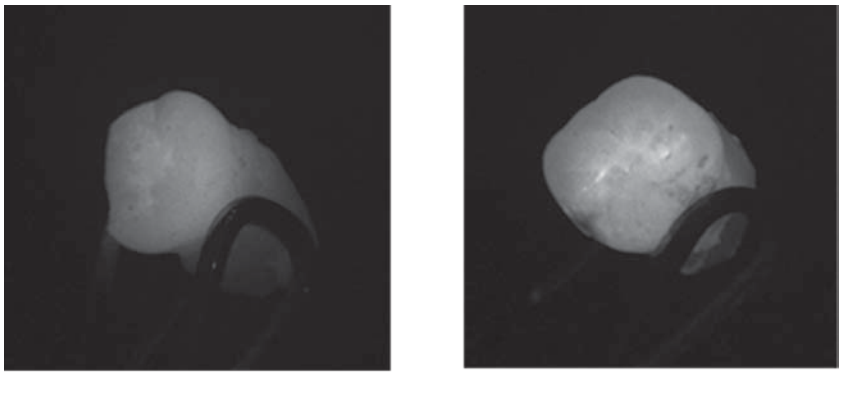

a b

Рис. 14. Видео-флуоресцентные изображения поверхности эмали зубов:
а – до нанесения модельной смеси;
б – через 3 мин после нанесения модельной смеси
Fig. 14. Video-fluorescent images of the tooth enamel surface:
a – before the model compound application;
b – 3 min after the model compound application

the colloid, which will reduce the time of the diagnostic process.

For this experimental group, fluorescence amplification factors were calculated for each sample (3 minutes after colloid application), which were used in the further statistical calculations.

The results of a study of the interaction of the model mixture and the surface microflora of tooth enamel

The study examined the interaction of the model mixture (with nAlPc and Protelan) with the surface microflora of tooth enamel. For each sample, the fluorescence enhancement coefficient was calculated as described in the Materials and Methods section. Figure 13 shows an example of enamel autofluorescence spectra before application and fluorescence of nAlPc after application of the model mixture.

Figure 14 shows video fluorescence images of the surface of the tooth enamel before applying the model mixture (*a*) and after 3 minutes (*b*).

Statistical processing of two groups of measurements on human teeth *ex vivo* (with a colloidal solution of nAlPc and a model mixture with nAlPc) using Student's t-test of reliability showed that the calculation results are statistically significant ($p < 0.05$), and the use of Protelan for additional activation of nAlPc is justified.

Conclusions

Experimental studies have shown reliable effectiveness of use of nAlPc in the composition of the model mixture for local fluorescence spectroscopy of the enamel surface to identify microcracks of enamel and potential foci of pathogenic microflora accumulation.

Based on the analysis of the results of studying the interaction of the nAlPc colloid with various surfactants, we can conclude that in the initial time period, it is the smallest particles and molecules in the colloid that interact with the surfactant, and after the lapse of time, molecules related to larger particles contribute to the fluorescence intensity.

Spectroscopic studies of the model mixture with nAlPc and Protelan showed the effectiveness of the use of this surfactant for additional activation of nanoparticles, which makes it possible to perform PD on the enamel surface of teeth 3 minutes after application. The addition of Protelane to the model mixture for conducting PD of dental enamel activates no more than 1–5% of nAlPc molecules.

In the future, the combined use of nAlPc with surfactants will increase not only the sensitivity and efficiency of PD of hard tooth tissues, but also the effectiveness of PDT of periodontal tissues.

A part of the experimental work related to the production of the model mixture was performed with the financial support of OOO Dentospek company (Troitsk, Moscow, Russia).

REFERENCES

1. Thomas S.S., Mohanty S., Jayanthi J.L., Varughese J.M., Balan A., Subhash N. Clinical trial for detection of dental caries using laser-induced fluorescence ratio reference standard, *J. Biomed. Opt.*, 2013, Vol. 15, No. 2, pp. 1–8.
2. Gonchukov S.A., Sukhinina A.A., Bakhmutov D.N., Biryukova T.B., Tsvetkov M.C., Bagratashvily V.C. Periodontitis diagnostics using resonance Raman spectroscopy on saliva, *Laser Phys. Lett.*, 2013, Vol. 10, No. 7, 075610.
3. Gonchukov S., Sukhinina A., Bakhmutov D., Minaeva S. Raman spectroscopy of saliva as a perspective method for periodontitis diagnostics, *Laser Phys. Lett.*, 2012, Vol. 9, No. 1, pp. 73–77.
4. Ramakrishnaiah R., Rehman G., Basavarajappa S., Alkhuraif A., Durgesh B.H., Khan A.S., Rehman I. Applications of Raman Spectroscopy in Dentistry: Analysis of Tooth Structure, *Appl. Spectrosc. Rev.*, 2014, Vol. 50, No. 4, pp. 332–350.
5. Tsuda H., Arends J. Raman Spectroscopy in Dental Research: A Short Review of Recent Studies, *Adv. Dent. Res.*, 1997,Vol. 11, No. 4, pp. 539–547.
6. Buchwald T., Okulus Z., Szybowicz M. Raman spectroscopy as a tool of early dental caries detection–new insights, *J. Raman Spectrosc.*, 2017, Vol. 48, No. 8, pp. 1094–1102.
7. Hsieh Y.-S., Ho Y.C., Lee S.Y., Chuang C.C., Tsai J.C., Lin K.F., Sun C.W. Dental Optical Coherence Tomography, *Sensors (Basel)*, 2013, Vol. 13, No. 7, pp. 8928–8949.
8. Chen Q.G., Zhu H.H., Xu Y., Lin B., Chen H. Quantitative method to assess caries via fluorescence imaging from the perspective of autofluorescence spectral analysis, *Laser Phys.*, 2015, Vol. 25, No. 8, pp. 1–9.

ЛИТЕРАТУРА

1. Thomas S.S., Mohanty S., Jayanthi J.L., et al. Clinical trial for detection of dental caries using laser-induced fluorescence ratio reference standard // J. Biomed. Opt. – 2013. – Vol. 15, No. 2. – P. 1–8.
2. Gonchukov S.A., Sukhinina A.A., Bakhmutov D.N., et al. Periodontitis diagnostics using resonance Raman spectroscopy on saliva // Laser Phys. Lett. – 2013. – Vol. 10, No. 7. – 075610.
3. Gonchukov S., Sukhinina A., Bakhmutov D., Minaeva S. Raman spectroscopy of saliva as a perspective method for periodontitis diagnostics // Laser Phys. Lett. – 2012. – Vol. 9, No. 1. – P. 73–77.
4. Ramakrishnaiah R., Rehman G., Basavarajappa S., et al. Applications of Raman Spectroscopy in Dentistry: Analysis of Tooth Structure // Appl. Spectrosc. Rev. – 2014. – Vol. 50, No. 4. – P. 332–350.
5. Tsuda H., Arends J. Raman Spectroscopy in Dental Research: A Short Review of Recent Studies // Adv. Dent. Res. – 1997. – Vol. 11, No. 4. – P. 539–547.
6. Buchwald T., Okulus Z., Szybowicz M. Raman spectroscopy as a tool of early dental caries detection–new insights // J. Raman Spectrosc. – 2017. – Vol. 48, No. 8. – P. 1094–1102.
7. Hsieh Y.-S., Ho Y.C., Lee S.Y., et al. Dental Optical Coherence Tomography // Sensors (Basel). – 2013. – Vol. 13, No. 7. – P. 8928–8949.
8. Chen Q.G., Zhu H.H., Xu Y., et al. Quantitative method to assess caries via fluorescence imaging from the perspective of autofluorescence spectral analysis // Laser Phys. – 2015. – Vol. 25, No. 8. – P. 1–9.

9. Buchalla W., Lennon A.M., Attin T. Fluorescence spectroscopy of dental calculus, *J. Periodontal Res*., 2004, Vol. 39, No. 5, pp. 327–332.
10. Bakhmutov D., Gonchukov S., Sukhinina A. Fluorescence spectroscopy of dental calculus, *Laser Phys. Lett*., 2010, Vol. 7, No. 5, pp. 384–387.
11. Bakhmutov D.N., Gonchukov S.A., Kharchenko O., Nikiforova O., Vdovin Yu. Early Dental Caries Detection by Fluorescence Spectroscopy, *Laser Phys. Lett*., 2004, Vol. 1, No. 11, pp. 565–569.
12. Bakhmutov D.N., Gonchukov S.A., Kharchenko O. Early caries naked-eyed examination, *Laser Phys. Lett*., 2008, Vol. 5, No. 5, pp. 375–378.
13. Borisova E.G., Uzunov T.T., Avramov L.A. Early Differentiation between Caries and Tooth Demineralization Using Laser-Induced Autofluorescence Spectroscopy, *Lasers Surg. Med*., 2004, Vol. 34, No. 3, pp. 249–253.
14. Drakaki E., Makropoulou M., Khabbaz M., Serafetinideset A.A. Reflectance, scattering and laser induced fluorescence for the detection of dental caries, *Proc. SPIE*, 2003, 5141_348.
15. Drakaki E.A., Makropoulou M.I., Khabbaz M., Serafetinides A.A. Laser Induced Fluorescence in diagnosis of dental caries, *Proc. SPIE*, 2003, Vol. 5149, pp. 45–52.
16. Sinyaeva M.L., Mamedov A.A., Vasilchenko S.Y., Volkova A.I., Loschenov V.B. Fluorescence Diagnostics in Dentistry, *Laser Phys*., 2004,Vol. 14, No. 8, pp. 1132–1140.
17. Schoenly J.E., Seka W., Featherstone J.D., Rechmann P. Near-UV laser treatment of extrinsic dental enamel stains, *Lasers Surg. Med*., 2012, Vol. 44, No. 4, pp. 339–345.
18. Sinyaeva M.L., Vasil'chenko S.Yu., Volkova A.I., Korovin S.B., Mamedov Ad.A., Kuz'min S.G., Luk'yanets E.A., Loshchenov V.B., Konov V.I. Use of aluminum phthalocyanine nanoparticles for tooth enamel microdamage detection, Rossiyskie nanotekhnologii, 2007, Vol. 2, No. 11–12. pp. 58–63. (in Russian)
19. Steiner R., Breymayer J., Rueck A., Loschenov V.B., Ryabova A.V. Crystalline organic nanoparticles for diagnosis and PDT, *Proc. SPIE*, 2015, Vol. 9308, pp. 1–7.
20. Breymayer J., Rück A., Ryabova A.V., Loschenov V.B., Steiner R.W..Fluorescence investigation of the detachment of aluminum phthalocyanine molecules from aluminum phthalocyanine nanoparticles in monocytes/macrophages and skin cells and their localization in monocytes/macrophages, *Photodiagnosis Photodyn. Ther*., 2014,Vol. 11, No. 3, pp. 380–390.
21. Vasilchenko S.Y. Volkova A.I., Ryabova A.V., Loschenov V.B., Konov V.I., Mamedov A.A., Kuzmin S.G., Lukyanets E.A. Application of aluminum phthalocyanine nanoparticles for fluorescent diagnostics in dentistry and skin autotransplantology, *J. Biophotonics*, 2010, Vol. 3, No. 5–6, pp. 336–346.
22. Kuznetsova J.O., Makarov V.I. Application of nanophotosensitizers (aluminum phthalocyanine nanoparticles) for early diagnosis and prevention of inflammatory diseases, *J. Phys. Conf. Ser*., 2016, Vol. 737, No. 1, pp. 1–3.
23. Kuznetsova J.O., Farrakhova D.S., Yassin M.G. Aluminum phthalocyanine nanoparticles as a contrast agent for the detection of tooth enamel microcracks, *Photon Lasers Med*., 2016, Vol. 5, No. 4, pp. 267–322.
24. Bystrov F.G., Makarov V.I., Pominova D.V., Ryabova A.V., Loshchenov V.B. Analysis of photoluminescence decay kinetics of aluminum phthalocyanine nanoparticles interacting with immune cells, *Biomedical Photonics*, 2016, Vol. 5, No. 1, pp. 3–8. (in Russian)
25. Sinyaeva M.L., Panchenko V.Y., Sabotinov N.V., Mamedov A.A., Lervkin V.V., Kharnas S.S., Volkova A.I., Loschenov V.B., Berezin A.N., Kiselev G.L. Optimization of parodontium tissue irradiation method for fluorescent diagnostic (FD) and photodynamic therapy (PDT), *Proc. SPIE*, 2004, Vol. 5449, pp. 462–465.

9. Buchalla W., Lennon A.M., Attin T. Fluorescence spectroscopy of dental calculus // J. Periodontal Res. – 2004. – Vol. 39, No. 5. – P. 327–332.
10. Bakhmutov D., Gonchukov S., Sukhinina A. Fluorescence spectroscopy of dental calculus // Laser Phys. Lett. – 2010. – Vol. 7, No. 5. – P. 384–387.
11. Bakhmutov D.N., Gonchukov S.A., Kharchenko O., et al. Early Dental Caries Detection by Fluorescence Spectroscopy // Laser Phys. Lett. – 2004. – Vol. 1, No. 11. – P. 565–569.
12. Bakhmutov D.N., Gonchukov S.A., Kharchenko O. Early caries naked-eyed examination // Laser Phys. Lett. – 2008. – Vol. 5, No. 5. – P. 375–378.
13. Borisova E.G., Uzunov T.T., Avramov L.A. Early Differentiation between Caries and Tooth Demineralization Using Laser-Induced Autofluorescence Spectroscopy // Lasers Surg. Med. – 2004. – Vol. 34, No. 3. – P. 249–253.
14. Drakaki E., Makropoulou M., Khabbaz M., Serafetinideset A.A. Reflectance, scattering and laser induced fluorescence for the detection of dental caries // Proc. SPIE. – 2003. – 5141_348.
15. Drakaki E.A., Makropoulou M.I., Khabbaz M., Serafetinides A.A. Laser Induced Fluorescence in diagnosis of dental caries // Proc. SPIE. – 2003. – Vol. 5149. – P. 45–52.
16. Sinyaeva M.L., Mamedov A.A., Vasilchenko S.Y., et al. Fluorescence Diagnostics in Dentistry // Laser Phys. – 2004. – Vol. 14, No. 8. – P. 1132–1140.
17. Schoenly J.E., Seka W., Featherstone J.D., Rechmann P. Near-UV laser treatment of extrinsic dental enamel stains // Lasers Surg. Med. – 2012. – Vol. 44, No. 4. – P. 339–345.
18. Синяева М.Л., Васильченко С.Ю., Волкова А.И. и др. Использование наночастиц фталоцианина алюминия для детектирования микроповреждений эмали зубов // Российские нанотехнологии. – 2007. – Т. 2, № 11–12. – С. 58–63.
19. Steiner R., Breymayer J., Rueck A., et al. Crystalline organic nanoparticles for diagnosis and PDT // Proc. SPIE. – 2015. – Vol. 9308. – P. 1–7.
20. Breymayer J., Rück A., Ryabova A.V., et al. Fluorescence investigation of the detachment of aluminum phthalocyanine molecules from aluminum phthalocyanine nanoparticles in monocytes/macrophages and skin cells and their localization in monocytes/macrophages // Photodiagnosis Photodyn. Ther. – 2014. – Vol. 11, No. 3. – P. 380–390.
21. Vasilchenko S.Y. Volkova A.I., Ryabova A.V., et al. Application of aluminum phthalocyanine nanoparticles for fluorescent diagnostics in dentistry and skin autotransplantology // J. Biophotonics. – 2010. – Vol. 3, No. 5–6. – P. 336–346.
22. Kuznetsova J.O., Makarov V.I. Application of nanophotosensitizers (aluminum phthalocyanine nanoparticles) for early diagnosis and prevention of inflammatory diseases // J. Phys. Conf. Ser. – 2016. – Vol. 737, No. 1. – P. 1–3.
23. Kuznetsova J.O., Farrakhova D.S., Yassin M.G. Aluminum phthalocyanine nanoparticles as a contrast agent for the detection of tooth enamel microcracks // Photon Lasers Med. – 2016. – Vol. 5, No. 4. – P. 267–322.
24. Быстров Ф.Г., Макаров В.И., Поминова Д.В. и др. Исследование кинетики затухания фотолюминесценции молекулярных нанокристаллов фталоцианина алюминия при взаимодействии с иммунокомпетентными клетками // Biomed. Photonics. – 2016. – Т. 5, № 1. – P. 3–8.
25. Sinyaeva M.L., Panchenko V.Y., Sabotinov N.V., et al. Optimization of parodontium tissue irradiation method for fluorescent diagnostic (FD) and photodynamic therapy (PDT) // Proc. SPIE. – 2004. – Vol. 5449. – P. 462–465.
26. Васильченко С.Ю., Волкова А.И., Коровин С.Б. и др. Исследование флюоресцентных свойств наночастиц фталоцианина алюминия в микроповреждениях эмали зуба // Рос. биотер. журн. – 2006. – Т. 5, № 2. – С. 77–80.

26. Vasil'chenko S.Yu., Volkova A.I., Korovin S.B., Loshchenov V.B., Sinyaeva M.L., Mamedov Ad.A., Luk'yanets E.A., Kuz'min S.G. Investigation of aluminum phthalocyanine nanoparticles fluorescent properties in tooth enamel microdamage, *Ros. bioter. zhurn.*, 2006, Vol. 5, No. 2, pp. 77–80. (in Russian)
27. Dobson J., Wilson M. Sensitization of oral bacteria in biofilms to killing by light from a low-power laser, *Arch. Oral Biol.*, 1992, Vol. 37, No. 11, pp. 883–887.
28. Lacey J.A., Phillips D. The photobleaching of disulfonated aluminium phthalocyanine in microbial systems, *Photochem. Photobiol. Sci.*, 2002, Vol. 1, No. 2, pp. 120–125.
29. Lacey J.A., Phillips D. Fluorescence lifetime measurements of disulfonated aluminium phthalocyanine in the presence of microbial cells, *Photochem. Photobiol. Sci.*, 2002, Vol. 1, No. 6, pp. 378–383.
30. Wilson M., Dobson J., Sarkar S. Sensitization of periodontopathogenic bacteria to killing by light from a low-power laser, *Oral Microbiol. Immunology*, 1993, No. 8, pp. 182–187.
31. Carrera E.T., Dias H.B., Corbi S.C.T., Marcantonio R.A.C., Bernardi A.C.A., Bagnato V.S., Hamblin M.R., Rastelli A.N.S. The application of antimicrobial photodynamic therapy (aPDT) in dentistry: a critical review, *Laser Phys.*, 2016, Vol. 26, No. 12. doi: 10.1088/1054–660X/26/12/123001
32. Yin R., Hamblin M.R. Antimicrobial Photosensitizers: Drug Discovery Under the Spotlight, *Curr. Med. Chem.*, 2015, Vol. 22, No. 18, pp. 2159–2185.
33. Carmello J.C., Alves F., Ribeiro A., Basso F.G., de Souza Costa C.A., Tedesco A.C., Primo F.L., Mima E.G., Pavarina A.C. In vivo photodynamic inactivation of Candida albicans using chloro-aluminum phthalocyanine, *Oral Dis.*, 2016, Vol. 22, No. 5, pp. 415–422.
34. Ribeiro A.P., Andrade M.C., Bagnato V.S., Vergani C.E., Primo F.L., Tedesco A.C., Pavarina A.C. Antimicrobial photodynamic therapy against pathogenic bacterial suspensions and biofilms using chloro-aluminum phthalocyanine encapsulated in nanoemulsions, *Lasers Med. Sci.*, 2015, Vol. 30, No. 2, pp. 549–559.
35. Ragelle H., Crauste-Manciet S., Seguin J., Brossard D., Scherman D., Arnaud P., Chabot G.G. Nanoemulsion formulation of fisetin improves bioavailability and antitumour activity in mice, *Int. J. Pharm.*, 2012, Vol. 427, No. 2, pp. 452–459.
36. Zhang H., Yao M., Morrison R.A., Chong S. Commonly used surfactant, Tween 80, improves absorption of P-glycoprotein substrate, digoxin, in rats, *Arch Pharm Res*, 2015, Vol. 26, No. 9, pp. 768–772.
37. Natarajan J., Baskaran M., Humtsoe L.C., Vadivelan R., Justin A. Enhanced brain targeting efficacy of Olanzapine through solid lipid nanoparticles, *Artif. Cells. Nanomedicine. Biotechnol.*, 2016, Vol. 45, No. 2, pp. 364–371.
38. Salaguer J.-L. *Surfactants Types and Uses*. Venezuela, Laboratorio FIRP, 2002. 49 p.
39. Kholmberg K., Yensson B., Kronberg B., Lindman B. *Poverkhnostno-aktivnye veshchestva i polimery v vodnykh rastvorakh* [Surfactants and polymers in aqueous solutions]. Moscow, BINOM, Laboratoriya znaniy Publ., 2013. 513 p.
40. Savvin S.B. *Poverkhnostno-aktivnye veshchestva* [Surfactants]. Moscow, Nauka Publ., 1991. 251 p.
41. Asem H., El-Fattah A.A., Nafee N., Zhao Y., Khalil L., Muhammed M., Hassan M., Kandil S. Development and biodistribution of a theranostic aluminum phthalocyanine nanophotosensitizer, *Photodiagnosis Photodyn. Ther.*, 2016, Vol. 13, pp. 48–57.
42. Loschenov V., Konov V., Prokhorov A. Photodynamic therapy and fluorescence diagnostics, *Laser Phys.*, 2000, Vol. 10, No. 6, pp. 1188–1207.
43. Ivanov V.L., Lyashkevich S.Yu. Influence of surfactants on the chain reaction of halogen photosubstitution by a sulfonyl hydroxide group in halogenhydroxynaphthalenes, *Khimiya*
27. Dobson J., Wilson M. Sensitization of oral bacteria in biofilms to killing by light from a low-power laser // Arch. Oral Biol. – 1992. – Vol. 37, No. 11. – P. 883–887.
28. Lacey J.A., Phillips D. The photobleaching of disulfonated aluminium phthalocyanine in microbial systems // Photochem. Photobiol. Sci. – 2002. – Vol. 1, No. 2. – P. 120–125.
29. Lacey J.A., Phillips D. Fluorescence lifetime measurements of disulfonated aluminium phthalocyanine in the presence of microbial cells // Photochem. Photobiol. Sci. 2002. – Vol. 1, No. 6. – P. 378–383.
30. Wilson M., Dobson J., Sarkar S. Sensitization of periodontopathogenic bacteria to killing by light from a low-power laser // Oral Microbiol. Immunology. – 1993. – No. 8. – P. 182–187.
31. Carrera E.T., Dias H.B., Corbi S.C.T., et al. The application of antimicrobial photodynamic therapy (aPDT) in dentistry: a critical review // Laser Phys. – 2016. – Vol. 26, No. 12. doi: 10.1088/1054–660X/26/12/123001
32. Yin R., Hamblin M.R. Antimicrobial Photosensitizers: Drug Discovery Under the Spotlight // Curr. Med. Chem. – 2015. – Vol. 22, No. 18. – P. 2159–2185.
33. Carmello J.C., Alves F., Ribeiro A., et al. In vivo photodynamic inactivation of Candida albicans using chloro-aluminum phthalocyanine // Oral Dis. – 2016. – Vol. 22, No. 5. – P. 415–422.
34. Ribeiro A.P., Andrade M.C., Bagnato V.S., et al. Antimicrobial photodynamic therapy against pathogenic bacterial suspensions and biofilms using chloro-aluminum phthalocyanine encapsulated in nanoemulsions // Lasers Med. Sci. – 2015. – Vol. 30, No. 2. – P. 549–559.
35. Ragelle H., Crauste-Manciet S., Seguin J., et al. Nanoemulsion formulation of fisetin improves bioavailability and antitumour activity in mice // Int. J. Pharm. – 2012. – Vol. 427, No. 2. – P. 452–459.
36. Zhang H., Yao M., Morrison R.A., Chong S. Commonly used surfactant, Tween 80, improves absorption of P-glycoprotein substrate, digoxin, in rats // Arch Pharm Res. – 2015. – Vol. 26, No. 9. – P. 768–772.
37. Natarajan J., Baskaran M., Humtsoe L.C., et al. Enhanced brain targeting efficacy of Olanzapine through solid lipid nanoparticles // Artif. Cells. Nanomedicine. Biotechnol. – 2016. – Vol. 45, No. 2. – P. 364–371.
38. Salaguer J.-L. Surfactants Types and Uses. – Venezuela: Laboratorio FIRP, 2002. – 49 p.
39. Холмберг К., Йёнссон Б., Кронберг Б., Линдман Б. Поверхностно-активные вещества и полимеры в водных растворах. – Москва: БИНОМ. Лаборатория знаний, 2013. – 513 с.
40. Саввин С.Б. Поверхностно-активные вещества. – М.: Наука, 1991. – 251 с.
41. Asem H., El-Fattah A.A., Nafee N., et al. Development and biodistribution of a theranostic aluminum phthalocyanine nanophotosensitizer // Photodiagnosis Photodyn. Ther. – 2016. – Vol. 13. – P. 48–57.
42. Loschenov V., Konov V., Prokhorov A. Photodynamic therapy and fluorescence diagnostics // Laser Phys. – 2000. – Vol. 10, No. 6. – P. 1188–1207.
43. Иванов В.Л., Ляшкевич С.Ю. Влияние поверхностно-активных веществ на цепную реакцию фотозамещения галогена сульфогруппой в галогенгидроксинафталинах // Химия высоких энергий. – 2013. – Т. 47, No. 4. – С. 293–297.
44. Silva E.P.O., Franchi L.P., Tedescoa A.C. Chloro-aluminium phthalocyanine loaded in ultradeformable liposome for photobiology studies on human glioblastoma // RSC Adv. – 2016. – Vol. 83. – P. 1–10.
45. Muehlmann L.A., Ma B.C., Longo J.P., et al. Aluminum-phthalocyanine chloride associated to poly(methyl vinyl ether-

vysokikh energiy, 2013, Vol. 47, No. 4, pp. 293–297. (in Russian)
44. Silva E.P.O., Franchi L.P., Tedescoa A.C. Chloro-aluminium phthalocyanine loaded in ultradeformable liposome for photobiology studies on human glioblastoma, *RSC Adv.*, 2016, Vol. 83, pp. 1–10.
45. Muehlmann L.A., Ma B.C., Longo J.P., Almeida Santos Mde F., Azevedo R.B. Aluminum-phthalocyanine chloride associated to poly(methyl vinyl ether-co-maleic anhydride) nanoparticles as a new third-generation photosensitizer for anticancer photodynamic therapy, *Int. J. Nanomedicine*, 2014, Vol. 9, pp. 1199–1213.
46. Cath T.Y., Adams D., Childress A.E. Membrane contactor processes for wastewater reclamation in space: II. Combined direct osmosis, osmotic distillation, and membrane distillation for treatment of metabolic wastewater, *J. Memb. Sci.*, 2005, Vol. 257, No. 1–2, pp. 111–119.

co-maleic anhydride) nanoparticles as a new third-generation photosensitizer for anticancer photodynamic therapy // Int. J. Nanomedicine. – 2014. – Vol. 9. – P. 1199–1213.
46. Cath T.Y., Adams D., Childress A.E. Membrane contactor processes for wastewater reclamation in space: II. Combined direct osmosis, osmotic distillation, and membrane distillation for treatment of metabolic wastewater // J. Memb. Sci. – 2005. – Vol. 257, No. 1–2. – P. 111–119.

INTRAOPERATIVE FLUORESCENT SPECTROSCOPY AND PHOTODYNAMIC THERAPY OF RECURRENT PELVIS MINOR TUMORS WITH LOCAL RADIATION DAMAGE

Vasilev L.A.[1], Panov N.S.[1], Kapinus V.N.[1], Kaplan M.A.[1], Kostyuk I.P.[1], Kaprin A.D.[2]
[1]A.Tsyb Medical Radiological Research Center – branch of the National Medical Research Radiological Center, Moscow, Russia
[2]P.Herzen Moscow Oncology Research Institute – branch of the National Medical Research Radiological Center of the Ministry of Health of the Russian Federation, Moscow, Russia

Abstract

This work presents the results of performing intraoperative photodynamic therapy (IOPDT) on 22 patients with recurrent pelvic tumors (cervical cancer – in 18 patients, cancer of the corpus uteri – in 3 patients, cancer of the anal canal – in 1 patient). Prior to the PDT procedure, the patients were injected with photolon photosensitizer (PS) at a dose of 1.0–1.1 mg/kg. After the injection of PS, local fluorescence spectroscopy of tumor lesions was performed to determine the accumulation of drug in various areas of tumors and healthy tissue. Intraoperative laser irradiation was carried out 3–5 hours after the photolon injection with light at 662 nm wavelength using "Latus-2" laser device with a power density of 140 mW/cm^2 and the density of light energy of 40–60 J/cm^2, the number of irradiation fields was 3–5 depending on the anatomical features.

The follow-up period after surgical treatment combined with PDT was from 6 to 24 months. Analyzing the immediate results of the treatment, there were no undesirable events or increase in the number of postoperative complications compared to patients treated without IOPDT. Were registered: transient increase in ALT and AST levels – in 5 patients (13.6%), reduction of oxygenation during anesthesia – in 20 (90.9%), transient fevers in the postoperative period – in 7 (31.8%).

It was noted that IOPDT with photolon drug, while slightly extending the time of the operation, is well tolerated by patients and does not lead to an increase in the number of early postoperative complications or the length of hospitalization.

Key words: evisceration, locally spread tumors of pelvis minor, radiation therapy, radiation damage, tumor recurrence, intraoperative photodynamic therapy, cytoreductive surgery.

For citations: Vasilev L.A., Panov N.S., Kapinus V.N., Kaplan M.A., Kostyuk I.P., Kaprin A.D. Intraoperative fluorescent spectroscopy and photodynamic therapy of recurrent pelvis minor tumors with local radiation damage, *Biomedical photonics*, 2018, Vol. 7, No. 3, pp. 21-28 (in Russian). doi: 10.24931/2413–9432–2018–7–3–21–28.

Contacts: Kapinus V.N., e-mail: kapinus70@mail.ru

ИНТРАОПЕРАЦИОННАЯ ФЛУОРЕСЦЕНТНАЯ СПЕКТРОСКОПИЯ И ФОТОДИНАМИЧЕСКАЯ ТЕРАПИЯ ПРИ РЕЦИДИВНЫХ ОПУХОЛЯХ МАЛОГО ТАЗА НА ФОНЕ МЕСТНЫХ ЛУЧЕВЫХ ПОВРЕЖДЕНИЙ

Л.А. Васильев[1], Н.С. Панов[1], В.Н. Капинус[1], М.А. Каплан[1], И.П. Костюк[1], А.Д. Каприн[2]
[1]МРНЦ им. А.Ф. Цыба – филиал ФГБУ «НМИЦ радиологии» Минздрава России, Обнинск, Россия
[2]МНИОИ им П.А.Герцена – филиал ФГБУ «НМИЦ радиологии» Минздрава России, Москва, Россия

Резюме

В статье представлены результаты применения интраоперационной фотодинамической терапии (ИОФДТ) у 22 пациентов с рецидивными опухолями органов малого таза (рецидив рака шейки матки – 18 больных, рецидив рака тела матки – 3, рецидив рака анального канала – 1). Для проведения ФДТ пациентам вводили фотосенсибилизатор (ФС) фотолон в дозе 1,0–1,1 мг/кг. После введения ФС выполнялась локальная флуоресцентная спектроскопия опухолевых поражений для определения накопления ФС в различных участках опухоли и в здоровой ткани. Интраоперационное лазерное облучение проводили через 3–5 ч после введения

фотолона светом с длиной волны 662 нм на лазерном аппарате «Латус-2» с плотностью мощности 140 мВт/см^2 и плотностью световой энергии 40–60 Дж/см^2, количество полей облучения составило 3–5 в зависимости от анатомических особенностей.
Период наблюдения за больными после выполнения им хирургического вмешательства в сочетании с ФДТ составил от 6 до 24 мес. При анализе непосредственных результатов лечения не было отмечено нежелательных явлений и увеличения количества послеоперационных осложнений по сравнению с группой больных, которым хирургическое лечение выполнено без ИОФДТ. Зарегистрированы: транзиторное повышение уровня АЛТ и АСТ у 5 пациентов (13,6%), падение оксигенации при введении в наркоз – у 20 (90,9%), транзиторная лихорадка в послеоперационном периоде – у 7 (31,8%).
Отмечено, что исследуемая методика ИОФДТ с препаратом фотолон при незначительном увеличении времени операции хорошо переносится пациентами и не приводит к увеличению количества ранних послеоперационных осложнений и сроков госпитализации.

Ключевые слова: эвисцерация, местно-распространенные опухоли малого таза, лучевая терапия; лучевые повреждения, рецидивы опухолей, интраоперационная фотодинамическая терапия, циторедуктивные операции.

Для цитирования: Васильев Л.А., Панов Н.С., Капинус В.Н., Каплан М.А., Костюк И.П., Каприн А.Д. Интраоперационная флуоресцентная спектроскопия и фотодинамическая терапия рецидивов опухолей малого таза на фоне местных лучевых повреждений // Biomedical photonics. – 2018. – Т. 7, № 3. – С. 21-28. doi: 10.24931/2413–9432–2018–7–3–21–28.

Контакты: Капинус В.Н., e-mail: kapinus70@mail.ru

Introduction

Malignant tumors of the pelvic organs account for more than 25% in the general structure of cancer in the Russian Federation, and the number of patients with this pathology is growing (Fig. 1) [1].

The growth of a pelvic tumor often involves the muscular aponeurotic and bone structures, so radical surgical removal becomes an impossible task and radiation therapy remains the main treatment method. Given this fact, as well as the biological characteristics of malignant neoplasms of this localization, oncologists often have to deal with the relapse of the tumor after radiation exposure. According to some authors, the frequency of such relapses ranges from 14% to 58%, depending on the stage of the disease at the beginning [2, 3]. Radiation therapy is known to affect not only tumor cells, but also neighboring healthy structures. In this connection, such disorders as intra-pelvic radiation fibrosis, radiation-related inflammatory changes, interorgan fistulas, etc. emerge.

The experience gained by oncological institutions in recent years has significantly changed the understanding of the possibilities of surgical treatment for patients with relapses of pelvic tumor after a radical course of radiation therapy. This is due to the fact that in 85–92% of cases relapses after radiotherapy are locally preva-

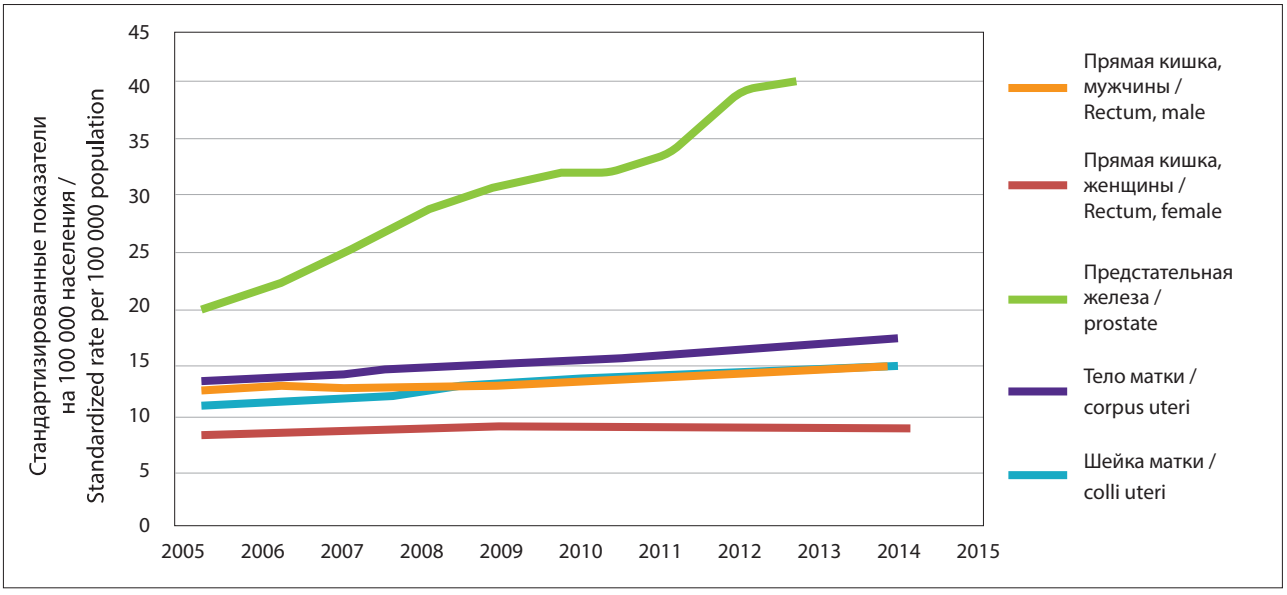

Рис. 1. Ежегодный рост онкологической заболеваемости в Российской Федерации с 2005 по 2015 гг.
Fig. 1. Annual growth of cancer morbidity in Russian Federation from 2005 to 2015

lent, and the main type of care for patients is pelvic evisceration [4]. However, extended and combined surgery, accompanied by extensive intervention on the lymphatic tract and resection of neighboring organs, vascular and nervous structures, does not always lead to a permanent recovery due to the high frequency of progression of the tumor process expressed in subclinical metastases.

To increase the level of ablasticity and reduce the risk of developing repeated local relapse and metastasis in locally advanced pelvic tumors, a search is underway for new methods of specific therapy on the surgical field which can improve oncological treatment results with minimal side effects.

The introduction of intraoperative photodynamic therapy (IOPDT) methods seems to be one of the most promising areas of research in this sphere due to their low invasiveness, low rate of complications and a fairly high degree of reproducibility.

Photodynamic therapy (PDT) is a method of local exposure aimed at a tumor, which is performed in several stages. At the first stage, the patient is administered a photosensitizer (PS). Systemic administration of most photosensitizers leads to the binding of the drug in the blood with lipoproteins (mainly those with low density), globulins and albumins. A longer delay of PS in tumor tissue, compared with healthy tissue, is explained by a large number of lipoprotein receptors in actively proliferating cells, which leads to the selective accumulation of lipoprotein complexes with PS in tumor cells.

At the second stage, the PS molecule is activated by laser radiation. When light is absorbed by a photosensitizer molecule, photochemical reactions start with the formation of singlet oxygen and free radicals, which completely destroy tumor cells over a short period.

It was found that PDT can rapidly induce apoptosis of tumor cells, which allowed a deeper understanding of the nature of their photochemical death and attracted significantly more interest in this method in practical oncology. A specific property of apoptosis after PDT is the high rate of its initiation (less than 30 min) after photodamage. PDT can initiate an apoptotic response directly, bypassing the intermediate transmission pathways of intracellular signals, which may be absent in a number of multidrug-resistant tumors. Studies have shown that lower light doses contribute to the development of apoptosis, while higher ones lead to necrosis. It was determined that the mechanism of triggering apoptosis after PDT is the release of cytochrome C and other mitochondrial factors from the damaged mitochondria into the cytoplasm. Apparently, PDT can initiate other apoptosis development pathways, including modulation of regulatory events of the cell cycle through cyclin-dependent kinases [5–7].

An important feature of the photodynamic effect is the possibility of simultaneous medical and diagnostic procedures, such as fluorescence diagnostics (PD) [8]. FD is based on the ability of tumor cells to accumulate elevated concentrations of endogenous porphyrins and their derivatives, the amount of which increases with the development of pathological processes, as well as other exogenous (administered externally, for example, intravenously) photoactive substances (photosensitizers [9]) and the resulting fluorescence upon irradiation with a certain light wavelengths, and special instruments (spectrum analyzers) determine and record the level of fluorescence at specific points. This method makes it possible to assess the level of PS accumulation in tissues and the prevalence of the tumor process.

Starting from the 1980s, experimental studies were conducted on the effectiveness of peritoneum IOPDT in rabbits [10] and mice [11] with the use of hematoporphyrin derivative as a photosensitizer. In the treatment of CC531 intestinal carcinoma implanted in rat intraperitoneal fatty tissue, in PDT with the use of a photofrin photosensitizer, administered at 5 mg/kg (exposure parameters: wavelength: 628 nm, radiation density: 25–75 J/cm^2), an increase in disease-free survival was observed in all animals of the main group [12].

In parallel, preclinical studies were conducted to determine the indications and potential benefits of IOPDT, assess the toxicity of this type of treatment, and the degree of exposure to PDT on blood flow in the intestinal wall. Research by S. Suzuki et al. did not determine a significant damage to blood vessels or the development of any significant ischemia after IOPDT. In this case, there were no cases of intestinal wall perforation after IOPDT, and no toxicity of the studied method was observed, with the exception of a slight transient decrease in the number of lymphocytes and a moderate increase in the level of transaminases [13].

Several studies examined the effect of IOPDT with various photosensitizers on the inter-intestinal anastomosis, where anastomotic insolvency was not detected [14–17].

Clinical studies have been conducted in the United States to study the distribution of the photosensitizer photofrin, administered at a dose of 2.5 mg/kg, in healthy and tumor tissue and the effectiveness of IOPDT in combination with cytoreductive surgery in patients with disseminated malignant neoplasms of the abdominal cavity, pelvis and retroperitoneal space. Researchers noted significant individual and group variability in the accumulation of the photosensitizer in the tumor and in healthy tissue. Complications that occurred in the early postoperative period, such as a significant amount of discharge by drainage in the early days, as well as cases of thrombocytopenia and pathological values of the liver tests, are described [18–19].

The results of the first phase of clinical studies on the use of IOPDT on the bed of a remote tumor with photofrin (dose: 2.0 mg / kg) in patients with primary or recurring squamous cell carcinoma of the head and neck were published. In the dose range of laser light (30–75 J/cm^2), no dose-limiting toxic effects were observed in patients; the highest used dose of laser light (75 J/cm^2) was considered safe, the follow-up period for patients ranged from 66 to 97 months, while only 6 of them showed progression of the disease [20].

In our country, the use of IOPDT was developed and justified in respect of photosensitizers alasens and photosens in patients with breast cancer [21], photohem and photosens in patients with gastric cancer with peritoneal dissemination, as well as with primary and metastatic lesions of the peritoneum [22, 23]. IOPDT of the peritoneum was tolerated well and did not result in an increase of the frequency, nature and severity of postoperative complications. The use of IOPDT after surgery in patients with conditionally definitive treatment (R0), with less than 15 affected lymph nodes, made it possible to increase the median survival of patients from 29.3 to 43.6 months, and annual survival from 80.0 ± 5.7% to 93.7±4.2%, three-year survival, from 45.5 ± 7.6% to 82.1 ± 7.1% [24].

Thus, literature data indicate a fairly safe use of IOPDT in patients with malignant neoplasms in combination with cytoreductive and palliative treatment. It is advisable to continue the research into the methods of local-regional exposure with the use of IOPDT to improve the results of surgical treatment of pelvic tumors on the background of radiation injuries.

Materials and methods

The aim of this study was to improve the results of treatment of patients with recurrent malignant tumors of the pelvic organs on the background of local radiation injuries by the development and use of IOPDT.

The study group consisted of 22 patients with recurrent tumors of the pelvic organs. The vast majority of patients were women, and the average age was 52.4 years (46.2 ± 16.8 years). The nosological forms of the disease were as follows: cervical cancer, in 18 patients (81.8%), cancer of the uterus, in 3 patients (13.6%), anal cancer, in 1 patient (4.5%).

All patients at the first stage of treatment received radiation therapy according to a radical plan. The progression of the disease after radiation therapy was diagnosed at follow-up within 3 (continued growth) to 60 (recurrence of the disease) months. Relapse distribution with the breakdown by localization was as follows: central relapse was diagnosed in 18 patients (81.8%), and lateral in 4 (18.2%). In this case, the central relapse is the local tumor process that occurred in the primary tumor zone after a radical course of treatment, while the lateral relapse is a regional relapse in the lymph nodes along the main vascular trunk of the pelvis (iliac vessels).

In connection with the treatment of the patients, surgical removal of the tumor was performed in various scopes: anterior evisceration of the pelvis was performed in 6 cases (27.3%), total supralevator evisceration in 8 (36.4%), posterior evisceration in 3 (13.6%), and in 4 patients (18.2%), extended pelvic lymphadenectomy due to lateral recurrence, and in one patient, complete pelvic infralevator evisceration was performed (4.5%). According to pathomorphological data, it was found that R0 resection was performed in 19 cases (86.4%), and R1 in 3 cases (13.6%).

After the resection stage, all patients underwent intraoperative photodynamic exposure of the tumor bed and the regional metastasis pathways. In lateral recurrence, PDT was performed only on the bed of the lateral tumor recurrence.

For IOPDT performed as a part of the combined treatment of recurrent and residual tumors of the small pelvis, patients were first administered PS photolon (a complex of sodium chloride Chlorin e6 and low molecular weight medical polyvinylpyrrolidone developed by RUE Belmedpreparaty, the Republic of Belarus, registration certificate P N015948/01 of 11/30/2012) in a dose of 1.0-1.1 mg/kg, dissolved in 100 ml of 0.9% sodium chloride.

All patients gave informed consent for PDT with intravenous administration of photolon in a hospital setting.

As mentioned earlier, the advantage of PDT is its ability to produce local fluorescence spectroscopy of tumor lesions after administration of photosensitizers. This procedure makes it possible to determine the accumulation of the photosensitizer in various parts of the tumor and healthy tissue in the area of the surgical field. Local fluorescence spectroscopy was performed with the use of LESA-6 complex (ZAO "BIOSPEC", Russia). The radiation of a He-Ne laser with a wavelength of 633 nm was used as a source of radiation exciting the fluorescence of the photosensitizer in biological tissues. The average laser radiation power was 2 mW, and the energy density of local laser radiation on the surface of tissues during one examination was no more than 1 J/cm^2 (Fig. 2).

The spectra of tissues obtained by local measurements were analyzed in terms of the shape, magnitude, and amplitude of the signal. The indicators measured included the area of intensity of the fluorescence (S2) and the area of laser radiation reflected from tissues (S1), as well as their ratio (S2/S1). The ratio of S2/S1 indicators (diagnostic parameter) was used to determine the accumulation of the photosensitizer in the tissues (Fig. 3). Based on the results of each spectral study, a protocol was compiled automatically.

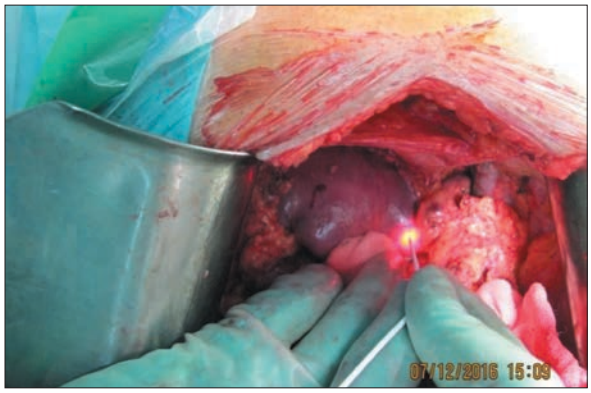

a b

Рис. 2. Проведение интраоперационной флуоресцентной спектроскопии на здоровых и поражённых тканях:
а – опухолевая ткань;
б – здоровый участок кишки
Fig. 2. Intraoperative fluorescence spectroscopy of healthy and diseased tissues:
a – tumor tissue;
b – healthy part of colon

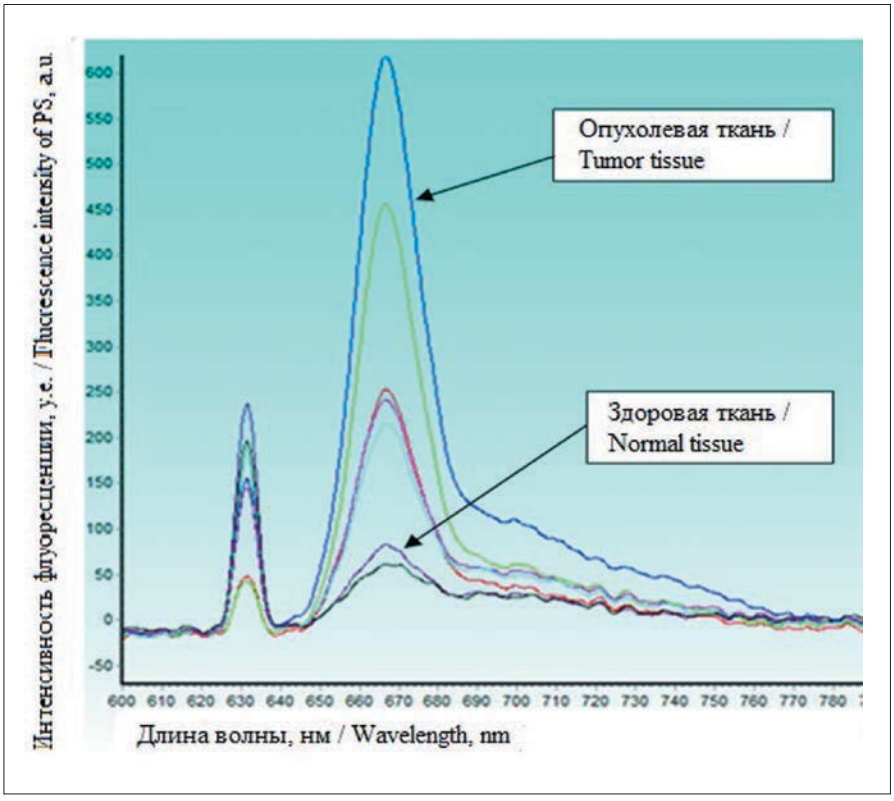

Рис. 3. Спектры флуоресценции, регистрируемые у пациентов
Fig. 3. Fluorescence spectra registered in patients

Intraoperative laser irradiation of the bed of the removed tumor and the area of regional metastasis under conditions of good hemostasis was performed in 3-5 hours after photolon was administered, with light wavelength of 662 nm produced by Latus-2 laser device (ZAO Poluprovodnikovyie Pribory, St. Petersburg, registration

Рис. 4. Сеанс интраоперационной фотодинамической терапии:
а – на ложе удалённой опухоли;
б – на пути регионарного метастазирования
Fig. 4. Intraoperative photodynamic therapy:
a – at the bed of the removed tumor;
b – on the path of regional metastasis

certificate No. FS 022a2006/3307-06 dated 05.16.2006) with a power density of 140 mW/cm^2 and the use of flexible monofilament quartz optical fibers, the light energy density was 40-60 J/cm^2, and the number of irradiation fields was 3–5 depending on the anatomical features (Fig. 4). Additionally, shielding of the loops of the small and large intestine with the sterile material, and, if necessary, other anatomical structures in the operating area, was performed.

The patients were recommended to observe the light regime for 2-3 days after the treatment. No cases of skin phototoxicity have been reported.

Results and discussion

The study found that after the administration of photolon in a dose of 1.0-1.1 mg/kg, an increase in the level of fluorescence in the tumor and unchanged tissues in the area of surgical intervention was recorded in all patients. Fluorescence contrast ranged from 1.4:1–5.0:1 and averaged 2.9 ± 0.4. The data obtained indicate that when using a photosensitizer in the indicated dose, sufficient selectivity of drug accumulation in pathological foci is observed compared to healthy tissues, which can be used for selective intraoperative exposure to PDT with chlorine preparations in order to increase the ablasticity of the operation.

The period of observation of patients after surgical treatment combined with photodynamic therapy ranged from 6 to 24 months. The analyzis of the immediate results of treatment showed no undesirable phenomena and no increase in the number of postoperative complications, with the exception of a transient increase in ALT and AST levels in 5 patients (13.6%), a drop in oxygenation upon introduction to general anesthesia, in 20 (90.9%), transient postoperative fever, in 7 (31.8%). These complications did not require special correction and resolved independently after 10-14 days. The use of the studied IOPDT technique did not lead to an increase in hospitalization, however, in 5 patients (22.7%), inflammation of the laparotomy wound was noted, which required its surgical treatment. However, it is currently not possible to associate this complication with IOPDT due to the small number of patients in the group and the presence of this complication in patients who did not receive IOPDT. Obviously, this zone fell into the field of previous radiation therapy and there were radiation injuries of the anterior abdominal wall, including skin and subcutaneous fat.

To formulate the final conclusions on the benefits of the antitumor effect of PDT, it is planned to recruit a representative group of patients with recurrent pelvic tumors against the background of local radiation injuries, the treatment of which will include IOPDT with photolone, and to further evaluate such criteria as relapse-free survival (in the case of radical surgery, R0), overall survival and quality of life.

Conclusion

According to clinical and experimental studies, PDT can affect tumor cells and, as a result, increase the overall survival of cancer patients.

Intraoperative photodynamic therapy represents a fundamentally new approach in the combined treatment of patients with locally advanced pelvic tumors

after a radical course of radiation therapy. According to preliminary data, IOPDT with chlorine preparations does not increase the number of early postoperative complications and is well tolerated by patients, while the increase to the surgery duration caused by it is insignificant.

The method is promising in terms of further research, and the accumulation of clinical material and the development of exposure modes will make it possible to evaluate its effectiveness and impact on the frequency of tumor relapses in the pelvic organs in the presence of local radiation injuries.

REFERENCES

1. *Zlokachestvennye novoobrazovaniya v Rossii v 2015 godu* [Malignant neoplasms in Russia in 2015], by eds Kaprin A.D., Starinskii V.V., Petrova G.V. Moscow, MNIOI im. P.A. Gertsena – filial FGBU NMITS radiologii Minzdrava Rossii Publ., 2017. pp. 18–19.
2. Datta N.R., Stutz E., Liu M., Rogers S., Klingbiel D., Siebenhüner A., Singh S., Bodis S. Concurrent chemoradiotherapy vs. radiotherapy alone in locally advanced cervix cancer: A systematic review and meta-analysis, *Gyn. Oncology*, 2017, Vol. 145(2), pp. 374–385.
3. Monk B.J., Tewari K.S., Koh W.-J. Multimodality therapy for locally advanced cervical carcinoma: state of the art and future directions, *J. Clin. Oncol.*, 2007, Vol. 25, pp. 2952–2965.
4. Kostyuk I.P., Vasil'ev L.A., Krest'yaninov S.S. Classification of locally spread neoplasms of pelvis minor and secondary tumor lesions of the bladder, *Onkourologiya*, 2014, No. 1, pp. 39–43. (in Russian)
5. Buytaert E., Dewaele M., Agostinis P. Molecular effectors of multiple cell death pathways initiated by photodynamic therapy, *Biochim. Biophys. Acta.*, 2007, Vol. 1776(1), pp. 86–107.
6. Mroz P., Yaroslavsky A., Kharkwal G.B., Michael R. Cell Death Pathways in Photodynamic Therapy of Cancer, *Hamblin Cancers*, 2011, Vol. 3, pp. 2516–2539.
7. Ahmad N., Feyes D.K., Agarwal R., Mukhtar H. Photodynamic therapy results in induction of WAF1/CIP1/P21 leading to cell cycle arrest and apoptosis, *Proc. Natl. Acad. Sci. USA*, 1998, Vol. 95, No. 12, pp. 6977–6982.
8. Rogatkin D., Shumskiy V., Tereshenko S., Polyakov P. Laser-based noninvasive spectrophotometry – an overview of possible medical application, *Photonics & Laser in Medicine*, 2013, Vol. 2, No. 3, pp. 225–240.
9. Mycek M.-A., Pogue B.W. *Handbook of biomedical fluorescence*. New-York, Marcel Dekker Inc., 2003. 665 p.
10. Douglass H.O. Jr., Nava H.R., Weishaupt K.R., Boyle D., Sugerman M.G., Halpern E., Dougherty T.J. Intra-abdominal applications of hematoporphyrin photoradiation therapy, *Exp. Med. Biol.*, 1983, Vol. 160, pp. 15–21.
11. Tochner Z., Mitchell J.B., Harrington F.S., Smith P., Russo D.T., Russo A. Treatment of murine intraperitoneal ovarian ascitic tumor with hematoporphyrin derivative and laser light, *Cancer Res.*, 1985, Vol. 45(7), pp. 2983–2987.
12. Veenhuizen R.B., Marijnissen J.P., Kenemans P., Ruevekamp-Helmers M.C., 't Mannetje L.W., Helmerhorst T.J., Stewart F.A. Intraperitoneal photodynamic therapy of the rat CC531 adenocarcinoma, *Br. J. Cancer*, 1996, Vol. 73(11), pp. 1387–1392.
13. Suzuki S.S., Nakamura S., Sakaguchi S. Experimental study of intra-abdominal photodynamic therapy, *Lasers Med. Sci.*, 1987, Vol. 2, pp. 195–203.
14. DeLaney T.F., Sindelar W.F., Tomas G.F., DeLuca A.M., Taubenberger J.K. Tolerance of small bowel anastomoses in rabbits to photodynamic therapy with dihematoporphyrin ethers and 630 nm red light, *Lasers Surg. Med.*, 1993, Vol. 13(6), pp. 664–671.
15. Major A.L., Rose G.S., Svaasand L.O., Lüdicke F., Campana A., van Gemert M.J. Intraperitoneal photodynamic therapy in the fischer 344 rat using 5-aminolevulinic acid and violet laser light: a toxicity study, *J. Photochem. Photobiol.*, 2002, Vol. 66, pp. 107–114.

ЛИТЕРАТУРА

1. Злокачественные новообразования в России в 2015 году / Под ред. Каприна А.Д., Старинского В.В., Петровой Г.В. – М.: МНИОИ им. П.А. Герцена – филиал ФГБУ «НМИЦ радиологии» Минздрава России, 2017. – С. 18–19.
2. Datta N.R., Stutz E., Liu M., et al. Concurrent chemoradiotherapy vs. radiotherapy alone in locally advanced cervix cancer: A systematic review and meta-analysis // Gyn. Oncology. – 2017. – Vol. 145(2). – P. 374–385.
3. Monk B.J., Tewari K.S., Koh W.-J. Multimodality therapy for locally advanced cervical carcinoma: state of the art and future directions // J. Clin. Oncol. – 2007. – Vol. 25. – P. 2952–2965.
4. Костюк И.П., Васильев Л.А., Крестьянинов С.С. Классификация местно-распространенных новообразований малого таза и вторичного опухолевого поражения мочевого пузыря // Онкоурология. – 2014. – № 1. – С. 39–43.
5. Buytaert E., Dewaele M., Agostinis P. Molecular effectors of multiple cell death pathways initiated by photodynamic therapy // Biochim. Biophys. Acta. – 2007. – Vol. 1776(1). – P. 86–107.
6. Mroz P., Yaroslavsky A., Kharkwal G.B., Michael R. Cell Death Pathways in Photodynamic Therapy of Cancer // Hamblin Cancers. – 2011. – Vol. 3. – P. 2516–2539.
7. Ahmad N., Feyes D.K., Agarwal R., Mukhtar H. Photodynamic therapy results in induction of WAF1/CIP1/P21 leading to cell cycle arrest and apoptosis // Proc. Natl. Acad. Sci. USA. – 1998. – Vol. 95, No. 12. – P. 6977–6982.
8. Rogatkin D., Shumskiy V., Tereshenko S., Polyakov P. Laser-based non-invasive spectrophotometry – an overview of possible medical application // Photonics & Laser in Medicine. – 2013. – Vol. 2, No. 3. – P. 225–240.
9. Mycek M.-A., Pogue B.W. Handbook of biomedical fluorescence. – N.Y.: Marcel Dekker Inc., 2003. – 665 p.
10. Douglass H.O. Jr., Nava H.R., Weishaupt K.R., et al. Intra-abdominal applications of hematoporphyrin photoradiation therapy // Exp. Med. Biol. – 1983. – Vol. 160. – P. 15–21.
11. Tochner Z., Mitchell J.B., Harrington F.S., et al. Treatment of murine intraperitoneal ovarian ascitic tumor with hematoporphyrin derivative and laser light // Cancer Res. – 1985. – Vol. 45(7). – P. 2983–2987.
12. Veenhuizen R.B., Marijnissen J.P., Kenemans P., et al. Intraperitoneal photodynamic therapy of the rat CC531 adenocarcinoma // Br. J. Cancer. – 1996. – Vol. 73(11). – P. 1387–1392.
13. Suzuki S.S., Nakamura S., Sakaguchi S. Experimental study of intra-abdominal photodynamic therapy // Lasers Med. Sci. – 1987. – Vol. 2. – P. 195–203.
14. DeLaney T.F., Sindelar W.F., Tomas G.F., et al. Tolerance of small bowel anastomoses in rabbits to photodynamic therapy with dihematoporphyrin ethers and 630 nm red light // Lasers Surg. Med. – 1993. – Vol. 13(6). – P. 664–671.
15. Major A.L., Rose G.S., Svaasand L.O., et al. Intraperitoneal photodynamic therapy in the fischer 344 rat using 5-aminolevulinic acid and violet laser light: a toxicity study // J. Photochem. Photobiol. – 2002. – Vol. 66. – P. 107–114.

16. Griffin G.M., Zhu T., Solonenko M., Del Piero F., Kapakin A., Busch T.M., Yodh A., Polin G., Bauer T., Fraker D., Hahn S.M. Preclinical evaluation of motexafin lutetium-mediated intraperitoneal photodynamic therapy in a canine model, *Clin. Cancer Res.*, 2001, Vol. 7(2), pp. 374–381.
17. Ross H.M., Smelstoys J.A., Davis G.J., Kapatkin A.S., Del Piero F., Reineke E., Wang H., Zhu T.C., Busch T.M., Yodh A.G., Hahn S.M. Photodynamic therapy with motexafin lutetium for rectal cancer: a preclinical model in the dog, *Surg. Res.*, 2006, Vol. 135(2), pp. 323–330.
18. DeLaney T.F., Sindelar W.F., Tochner Z., Smith P.D., Friauf W.S., Thomas G., Dachowski L., Cole J.W., Steinberg S.M., Glatstein E. Phase I study of debulking surgery and photodynamic therapy for disseminated intraperitoneal tumors, *Int. J. Radiat. Oncol. Biol. Phys.*, 1993, Vol. 25(3), pp. 445–457.
19. Hahn S.M., Fraker D.L., Mick R., Metz J., Busch T.M., Smith D., Zhu T., Rodriguez C., Dimofte A., Spitz F., Putt M., Rubin S.C., Menon C., Wang H.W., Shin D., Yodh A., Glatstein E. A Phase II trial of intraperitoneal photodynamic therapy for patients with peritoneal carcinomatosis and sarcomatosis, *Clin. Cancer Res.*, 2006, Vol. 12(8), pp. 2517–2525.
20. Rigual N.R., Shafirstein G., Frustino J., Seshadri M., Cooper M., Wilding R.N.G., Sullivan M.A., Henderson B. Adjuvant intraoperative photodynamic therapy in head and neck cancer, *JAMA Otolaryngol Head Neck Surg*, 2013, Vol. 139(7), pp. 706–711.
21. Filonenko E.V., Saribekyan E.K., Ivanova-Radkevich V.I. Capabilities of intraoperative photodynamic therapy for treatment of locally advanced breast cancer, *Biomedical Photonics*, 2016, Vol. 5, No. 1, pp. 9–14. (in Russian)
22. Pankratov A.A., Suleymanov E.A., Lukyanets E.A., Venediktova Y.B., Plyutinskaya A.D. Experimental confirmation for selection of irradiation regimens for intraperitoneal photodynamic therapy with porphyrin and phthalocyanine photosensitizers, *Biomedical Photonics*, 2017, Vol. 6, No. 2, pp. 12–20. (in Russian)
23. Suleymanov E.A., Kaprin A.D., Filonenko E.V., Homyakov V.M., Grishin N.A., Moskvicheva L.I., Urlova A.N. Intraoperative fluorescence diagnosis of peritoneal dissemination in patients with gastric cancer, *Biomedical Photonics*, 2016, Vol. 5, No. 3, pp. 9–18. (in Russian)
24. Vashakmadze L.A., Filonenko E.V., Butenko A.V., Kirillov N.V., Khomyakov V.M. Long-term outcomes for surgical treatment in patients with locally advanced and disseminated gastric cancer combined with intraoperative photodynamic therapy, *Biomedical Photonics*, 2013, Vol. 2, No. 1, pp. 3–10. (in Russian)

16. Griffin G.M., Zhu T., Solonenko M., et al. Preclinical evaluation of motexafin lutetium-mediated intraperitoneal photodynamic therapy in a canine model // Clin. Cancer Res. – 2001. –Vol. 7(2). – P. 374–381.
17. Ross H.M., Smelstoys J.A., Davis G.J., et al. Photodynamic therapy with motexafin lutetium for rectal cancer: a preclinical model in the dog // Surg. Res. – 2006. – Vol. 135(2). – P. 323–330.
18. DeLaney T.F., Sindelar W.F., Tochner Z., et al. Phase I study of debulking surgery and photodynamic therapy for disseminated intraperitoneal tumors // Int. J. Radiat. Oncol. Biol. Phys. – 1993. – Vol. 25(3). – P. 445–457.
19. Hahn S.M., Fraker D.L., Mick R., et al. A Phase II trial of intraperitoneal photodynamic therapy for patients with peritoneal carcinomatosis and sarcomatosis // Clin. Cancer Res. – 2006. – Vol. 12(8). – P. 2517–2525.
20. Rigual N.R., Shafirstein G., Frustino J., et al. Adjuvant intraoperative photodynamic therapy in head and neck cancer // JAMA Otolaryngol Head Neck Surg. – 2013. – Vol. 139(7). – P. 706–711.
21. Филоненко Е.В., Сарибекян Э.К., Иванова-Радкевич В.И. Возможности интраоперационной фотодинамической терапии в лечении местнораспространенного рака молочной железы // Biomedical Photonics. – 2016. – Т. 5, № 1. – С. 9–14.
22. Панкратов А.А., Сулейманов Э.А., Лукьянец Е.А. и др. Экспериментальное обоснование выбора режимов облучения для интраперитонеальной фотодинамической терапии на основе порфиринов и фталоцианинов // Biomedical Photonics. – 2017. – Т. 6, № 2. – С. 12–20.
23. Сулейманов Э.А., Каприн А.Д., Филоненко Е.В. и др. Интраоперационная флуоресцентная диагностика перитонеальной диссеминации у больных раком желудка // Biomedical Photonics. – 2016. – Т. 5, № 3. – С. 9–18.
24. Вашакмадзе Л.А., Филоненко Е.В., Бутенко А.В. и др. Отдаленные результаты хирургического лечения больных местнораспространенным и диссеминированным раком желудка в сочетании с интраоперационной фотодинамической терапией // Biomedical Photonics. – 2013. – Т. 2, № 1. – С. 3–10.

BIOLOGICAL MATERIALS IN BREAST CANCER RECONSTRUCTIVE SURGERY

Zikiryahodjaev A.D. [1,2,3], **Ermoshchenkova M.V.** [1,2], **Chissov V.I.** [1,2], **Shirokih I.M.** [3]
[1]P.Herzen Moscow Oncology Research Institute – branch of the National Medical Research Radiological Center of the Ministry of Health of the Russian Federation, Moscow, Russia
[2]The First Sechenov Moscow State Medical University under Ministry of Health of the Russian Federation, Moscow, Russia
[3]Peoples Friendship University of Russia, Moscow, Russia

Abstract

Currently, reconstructive-plastic surgery is becoming the standard for surgical and combined treatment of breast cancer (BC) patients. With a one-stage reconstruction of the breast, the use of biological implants that can replace muscle autografts and, consequently, reduce trauma, blood loss and operation time, and also to avoid defects in the donor zones is becoming topical. From 2014 to 2017, 151 reconstructive operations on 121 patients with BC (average age 41.5 years) using synthetic and biological materials were carried out in P.Herzen Moscow Oncology Research Institute. 0 stage of BC TisN0M0 was diagnosed in 11 (9.1%) patients, I stage – in 52 (42.9%), IIA – in 41 (33.9%), IIB – in 9 (7.4%), IIIA – in 4 (3.3%), IIIB – in 2 (1.7%), IIIC – in 2 (1.7%). To strengthen the lower slope, a biological implant – Permacol acellular dermal matrix, was used in 34 cases. Cosmetic result was rated as excellent in 20 (58.9%) cases, good in 11 (32.3%), unsatisfactory in 3 (8,8%). Biological materials are an important addition to various options for breast reconstruction. The criterion for selecting the material for strengthening the lower slope of the breast with subcutaneous or cutaneous mastectomy for cancer with a one-stage reconstruction using a silicone endoprosthesis is the pinch-test value.

Keywords: breast cancer, breast cancer reconstructive surgery, acellular dermal matrix, biological implant, biological implant.

For citations: Zikiryahodjaev A.D., Ermoshchenkova M.V., Chissov V.I., Shirokih I.M. Biological materials in breast cancer reconstructive surgery, *Biomedical Photonics*, 2018, T. 7, No. 3, pp. 29–35. (in Russian). doi: 10.24931/2413–9432–2018–7– 3–29–35.

Contacts: Ermoshchenkova M.V., e-mail: maryerm@mail.ru

БИОЛОГИЧЕСКИЕ МАТЕРИАЛЫ В РЕКОНСТРУКТИВНОЙ ХИРУРГИИ РАКА МОЛОЧНОЙ ЖЕЛЕЗЫ

А.Д. Зикиряходжаев [1, 2, 3], **М.В. Ермощенкова** [1, 2], **В.И. Чиссов** [1, 2], **И.М. Широких** [3]
[1]МНИОИ им. П.А. Герцена – филиал Национального медицинского исследовательского центра радиологии МЗ РФ, Москва, Россия
[2] Первый Московский государственный медицинский университет им. И.М. Сеченова МЗ РФ, Москва, Россия
[3]Российский университет дружбы народов, Москва, Россия

Резюме

В настоящее время реконструктивно-пластические операции становятся стандартным вариантом при хирургическом и комбинированном лечении больных раком молочной железы (РМЖ). При одномоментной реконструкции молочной железы актуальным становится применение биологических имплантатов, способных заменить мышечные аутотрансплантаты и, следовательно, сократить травматичность, кровопотерю и время операции, а также избежать дефектов донорских зон. С 2014 по 2017 гг. в МНИОИ им. П.А. Герцена выполнена 151 реконструктивная операция у 121 больной РМЖ (средний возраст 41,5 лет) с применением синтетических и биологических материалов. 0 стадия РМЖ TisN0M0 была диагностирована у 11 (9,1%) больных, I стадия – у 52 (42,9%), IIA– у 41 (33,9%), IIB – у 9 (7,4%), IIIA – у 4 (3,3%), IIIB – у 2 (1,7%), IIIC – у 2 (1,7%). С целью укрепления нижнего склона в 34 случаях был использован биологический имплантат – ацеллюлярный дермальный матрикс Permacol. Отличные косметические результаты отмечены в 20 (58,9%) случаях, хорошие – в 11 (32,3%), неудовлетворительные – в 3 (8,8%). Биологические материалы являются важным дополнением к различным вариантам реконструкции молочной железы. Критерием выбора материала для укрепления нижнего склона молочной железы при подкожной или кожесохранной мастэктомии по поводу рака с одномоментной реконструкцией силиконовым эндопротезом является величина pinch-теста.

Ключевые слова: рак молочной железы, реконструктивные операции при раке молочной железы, ацеллюлярный дермальный матрикс, биологический имплантат.

Для цитирования: Зикиряходжаев А.Д, Ермощенкова М.В., Чиссов В.И., Широких И.М. Биологические материалы в реконструктивной хирургии рака молочной железы // Biomedical Photonics. – 2018. – Т. 7, № 3. – С. 29–35. doi: 10.24931/2413–9432–2018–7–3–29–35.

Контакты: Ермощенкова М.В., e-mail: maryerm@mail.ru

Introduction

Currently, reconstructive plastic surgery is becoming a standard option in the surgical and combined treatment of patients with breast cancer and is seen as an etiotropic treatment of mental disorders associated with the loss of femininity and the integrity of one's own body [1–5].

About 50% of patients after mastectomy want to have the mammary gland reconstructed [6]. In recent years, the need for single-step organ reconstruction has increased, as it prevents psychological collapse and depression associated with the loss of femininity [7, 8].

Breast reconstruction methods can be divided into three groups: reconstruction with the use of synthetic or biological materials (expanders and various implants), own tissues and the combination of these methods [9–12].

Radical subcutaneous/skin-sparing mastectomies, subject to proper patient selection, provide an alternative to radical mastectomy and allow primary breast plasty to be performed. Various muscle autografts are used in the process of reconstruction with silicone prosthesis in order to protect the lower slope of the mammary gland; however, their use is associated with some difficulties and complications. Among them, increased trauma, the need to isolate a vascular pedicle, long-lasting lymphorrhea lymphorrhea in the donor area upon flap separatiuon from latissimus dorsi, a scar in the donor area, as well as the risk of marginal necrosis, liposclerosis, liponecrosis, thrombosis of microvascular anastomoses when free autologous flaps are used. Therefore, the use of artificial materials is relevant because they can replace muscle autografts, which helps to reduce trauma, blood loss, operation time and prevent defects of donor areas, while maintaining surgery effectiveness.

In 1970, V. Cumberland and J. Scales first formulated the criteria for an ideal implant. In particular, the implant material should not be physically softened by tissue discharge, cause an inflammation or rejection reaction, shrink during healing, cause allergies or sensitization, be carcinogenic, or trigger local complications [13–15].

Plastic and reconstructive surgery has been continuously developing, and a promising area in the reconstructive breast surgery is the use of biological implant: acellular dermal matrix (ADM). ADM was originally created to correct the shape of the breast after augmentation, however, several cases of using this material in a two-stage reconstruction with a tissue expander were later described. The use of ADM gained popularity in 2005. Its use made it possible to made it possible to create a pocket for prosthesis/tissue expander without using anterior serratus muscle or rectus abdominis [16, 17]. The advantages of ADM include a decrease in the intensity of postoperative pain syndrome, the absence of damage in the donor area, as well as improved aesthetic results [16–21]. However, several authors noted an increase in the number of postoperative infectious complications, seromas, and explantations with the use of ADM [17, 19, 22-24].

The main methodological goal of using biological implants in breast reconstruction is to increase the subpectoral space for the installation of a silicone endoprosthesis, to reduce its pressure on the skin, and to ensure good coverage of the endoprosthesis.

Currently, the majority of dermal matrices used for breast reconstruction are human, porcine, or bovine matrices. Human matrix brands are Alloderm (LifeCell, USA), Flex HD (Ethicon, USA), Neoform (Mentor, USA), DermaMatrix (Synthes, USA). The porcine matrix includes Strattice (LifeCell, USA) and Permacol (Covidien, USA). Only one type of bovine matrix is represented on the market in the form of Surgimend (TEI Biosciences, USA). ADM can be used in both immediate and delayed breast reconstruction. Immediate reconstruction has certain advantages, which are preservation of skin case and favorable conditions for the formation of a pocket for a prosthesis [25].

The use of ADM in implantation became popular after K. H. Breuing et al. published the results of the use of ADM for covering the inferolateral slope of the mammary gland [26, 27]. The effectiveness and success of single-step reconstruction with the use of ADM were proved by the analysis of the results of several random-

ized clinical trials. The safety of the method is evidenced by the low rate of adverse events [18, 21, 26–28]. For instance, K. H. Breuing reported complications in 6.9% (2/30) of patients, Zienowicz's et al. [19, 21, 23, 25] in 25% (6/24), with the development of skin flaps necrosis which was treated locally. The largest sample of single-step reconstructions with the use of endoprosthesis and ADM is presented by A.S. Colwellet al. [22]: the complication rate was 14.8% (49/331), including 9.1% (30/331) of cases of skin grafts necrosis resulting in the removal of the endoprosthesis in 1.5% (5/331) of the patients. These results provide evidence of the successful ADM use in single-step breast reconstruction.

A proper selection of patients is required to achieve the bestpossible results. Excellent condition of skin flaps is necessary, and the patients have to be willing to have a natural or smaller breast size [27].

One of the advantages of ADM is the reduction of pain syndrome due to lower pectoralis major muscle tension [16, 29].

Despite the fact that ADM was first described in connection with capsular contracture treatment, there is currently no long-term evidence of capsular contracture prevention due to the use of ADM [16, 21, 30–32].

Many authors point out that ADM provides the best aesthetic results, but there are only 2 studies that support this assertion. S. L. Spear et al., who used a five-point scale for evaluation, obtained identical results for breast reconstructed with endoprosthesis and ADM and the contralateral unreconstructed breast, 3.68 versus 3.98 ($p = 0.3$) [33, 34]. Also, A. J. Vardanian et al. showed that the overall aesthetic result, estimated by independent observers on a scale of 1to 4, was statistically significantly greater in the group where ADM was used (3.26), compared with the group without ADM (2.87). It was also noted that the submammary fold was in better position in the group of patients with ADM (3.35) compared with the group without ADM (2.94) [29].

Complications of ADM use are similar to complications in breast reconstruction with implants and can be divided into early (hematoma, seroma, infectious complications, skin flap necrosis, endoprosthesis rejection) and late complications (asymmetry, implant wrinkling, incorrect position, capsular contracture, and late infectious complications). Hematoma occurs in less than 5% of cases; its treatment is standard for all reconstructions. Seroma, unlike hematoma, involves many contradictions, since ADM is associated with an increased risk of seroma development, as shown by the results of two studies [16, 20]. For instance, Y. S. Chun states seroma development in 14.1% of patients in the group with ADM versus 2.7% in the group without ADM [16]. Similar, J. R. Parks reports 29.9% seromas in the group with ADM and 15.7% in the group without ADM [28]. However, there have been many studies which did not discover a statistically significant difference in the development of seromas associated with ADM [17, 21, 24, 31, 33, 35]. For instance, according to A. S. Liu et al. [35], the frequency of seromas was 7.1% in the group with ADM versus 3.9% in the group without ADM, and according to S.T. Lanier et al. [17], 13.4% against 6.7%, respectively. Taking into account the findings of these studies, it is important to take measures to minimize the risk of seroma development by the installation of vacuum drainage, which must not be removed prematurely.

Infectious complications when using ADM are observed in a high percentage of patients (35.4%), which may be explained by the presence of the second foreign material in addition to the implant. There are many reports showing an increase in the number of infectious complications in patients with ADM; therefore, the authors note the importance of timely antibiotic therapy [16, 17, 23, 24, 36–38].

Contraindications against the use of ADM are similar to those against endoprosthetics. Selection factors include an assessment of the need for unilateral or bilateral reconstruction, body type, body mass index, width of the chest, comorbidities, and the psychological profile of the patient. Ideal candidates for reconstruction by endoprosthesis and ADM are slim patients undergoing bilateral reconstruction who have adequate skin flaps after mastectomy, and thin patients without breast ptosis who are to have a unilateral reconstruction. Larger size and increased ptosis of the breast make it more difficult to achieve symmetry, and, therefore, it becomes necessary to perform contralateral mastopexy or reduction mammoplasty.

At present, there are no absolute contraindications for ADM use, but obesity, smoking and breast size of more than 600 grams are associated with an increased risk of postoperative complications. For better results, a combination of ablasticity and reconstructive techniques of the surgeon is required. All incisions must be pre-marked, submammary fold must be marked and, if possible, preserved during the mastectomy, skin flaps should be thick enough to preserve adequate circulation and to prevent possible loss of the skin graft [17, 23, 24].

In our opinion, the selection criterion for strengthening the lower slope of the breast in subcutaneous or skin-saving mastectomy with silicone implant in the cancer treatment with single-step reconstruction is the value of pinch-test. With a pinch test greater than 0.5 cm, either a synthetic implant and an ADM can be used. When the value of the pinch-test is less than 0.5 cm, the preference should be given to ADM.

Materials and methods

From 2014 to 2017, P. A. Hertsen Moscow Oncology Research Center performed 151 reconstructive

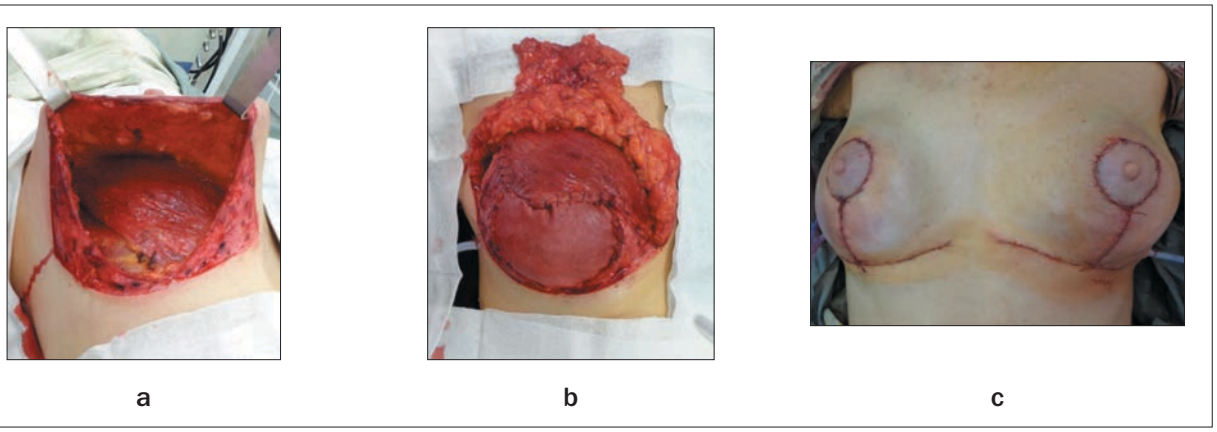

Рис. 1. Реконструктивный этап с применением силиконового эндопротеза и ацеллюлярного дермального матрикса:
а – вид полости раны после завершения этапа подкожной мастэктомии;
б – окончательный вид сформированного кармана с помещенным эндопротезом;
в – вид послеоперационных ран
Fig. 1. Reconstructive stage with the use of silicone endoprosthesis and acellular dermal matrix:
a – view of the wound cavity after the completion of subcutaneous mastectomy stage;
b – final view of the formed pocket with the placed endoprosthesis;
c – view of the postoperative wounds

operations with the use of synthetic and biological materials in 121 breast cancer patients, their mean age being 41.5. 0 TisN0M0 stage breast cancer was diagnosed in 11 (9.1%) patients, stage I – in 52 (42.9%), IIA – in 41 (33.9%), IIB – in 9 (7.4%), IIIA – in 4 (3.3%), IIIB – in 2 (1.7%), IIIC – in 2 (1.7%). The volume of the silicone endoprosthesis varied from 160 to 585 cm^3; its size depended on the individual anatomical characteristics of the patient. Permacol acellular dermal matrix was used as biological material in 34 cases.

The following is a description of the technique of mammary gland reconstruction with the use of biological implant. After mastectomy and careful hemostasis pockets of skin were formed (Fig. 1*a*). Inferolateral part of the pectoralis major muscle was separated from the anterior chest wall. Electrodissection was used to form a subpectoral pocket reaching the marked levels along the perimeter of the breast to be formed. After the successful creation of a subpectoral pocket, the ADM sheet was prepared in accordance with the manufacturer's instructions. ADM was then sutured to the chest wall with the reconstruction of the lateral and lower submammary folds (Fig. 1*c*). Most surgeons prefer using absorbable seam materials, in particular, Polydioxanone 2/0 or Vicryl 2/0. After the ADM was reliably attached to the submammary fold, the pocket width was measured for the selection of an implant. After careful hemostasis in the pocket and a prosthesis placement, the edge of ADM was hemmed to the inferior and lateral edges of the pectoralis major muscle. For a reliable silicone prosthesis cover, serratus anterior was isolated and ADM was fixed to the latter in the lateral section. In all cases, a closed space was formed to create a tight fit on the prosthesis, but without creating pressure on the skin flaps (Fig. 1*b*). The wound was sutured in layers, while two vacuum drains were retained (Fig. 1*c*).

Results

In the group of patients in which ADM was used, 1 patient developed necrosis of skin flaps. In 1 patient, the development of a long-existing seroma of small volume was observed in the central area of the postoperative scar. In 1 case, during adjuvant multiagent chemotherapy 4 months after surgery with the use of an endoprosthesis and ADM, the development of a skin reaction in the form of severe hyperemia was revealed, which required conservative treatment. In 2 (1.7%) cases, ADM and endoprosthesis were removed due to suppuration of the postoperative wound. In the group with ADM, excellent cosmetic results were noted in 20 (58.9%) cases, good in 11 (32.3%), and unsatisfactory in 3 (8.8%). The view of a patient (clinical diagnosis: left side breast cancer ypT2N0M0G2L0V0PR. stage IIA, Her2/neu-positive subtype,the state after a 8 courses of neoadjuvant drug therapy) before and after surgery with ADM is shown in Fig. 2.

Conclusion

Biological materials are an important element of various breast reconstruction options. Their advantages are to reduce the invasiveness of surgery by eliminating the need to use autologous muscle trans-

Рис. 2. Вид пациентки до (рис. 2а) и 1 мес после (рис. 2б) радикальной подкожной мастэктомии слева с одномоментной реконструкцией силиконовым эндопротезом и ацеллюлярным дермальным матриксом, аугментации правой молочной железы
Fig. 2. View of the patient before (Fig. 2a) and 1 month after (Fig. 2b) of radical subcutaneous mastectomy on the left side with one-stage reconstruction using a silicone endoprosthesis and acellular dermal matrix, augmentation of the right breast

plants, shortening the time of surgery, the possibility of expanding the pocket for the endoprosthesis and reducing pain.

The selection criterion for strengthening the lower slope of the breast in subcutaneous or skin-saving mastectomy with silicone implant in the cancer treatment with single-step reconstruction is the value of pinch-test. With a pinch test of more than 0.5 cm, both synthetic implant and ADM are suitable. If the pinch test value is less than 0.5 cm, ADM is preferable.

REFERENCES

1. Aseev A.V. Psychological problems associated with breast cancer, *Klinicheskaya meditsina*, 1993, No. 3, pp. 30–34. (in Russian)
2. Awan B.A., Samargandi O.A., Alghamdi H.A., Sayegh A.A., Hakeem Y.J., Merdad L., Merdad A.A. The desire to utilize post-mastectomy breast reconstruction in Saudi Arabian women. Predictors and barriers, *Saudi Med J.*, 2015, Vol. 36(3), pp. 304–309.
3. Morrow M., Li Y., Alderman A.K., Jagsi R., Hamilton A.S., Graff J.J., Hawley S.T., Katz S.J. Access to breast reconstruction after mastectomy and patient perspectives on reconstruction decision making, *JAMA Surg.*, 2014, Vol. 149(10), pp. 1015–1021.
4. Reshetov I.V., Chissov V.I. *Plasticheskaya i rekonstruktivnaya mikrokhirurgiya v onkologii* [Plastic surgery in oncology]. Moscow, OOO RIF Publ., 2001. 200 p.

ЛИТЕРАТУРА

1. Асеев А.В. Психологические проблемы, связанные с раком молочной железы // Клиническая медицина. – 1993. – № 3. – С. 30–34.
2. Awan B.A., Samargandi O.A., Alghamdi H.A., Sayegh A.A., Hakeem Y.J., Merdad L., Merdad A.A. The desire to utilize postmastectomy breast reconstruction in Saudi Arabian women. Predictors and barriers // Saudi Med J. – 2015. – Vol. 36(3). – P. 304–309.
3. Morrow M., Li Y., Alderman A.K., Jagsi R., Hamilton A.S., Graff J.J., Hawley S.T., Katz S.J. Access to breast reconstruction after mastectomy and patient perspectives on reconstruction decision making // JAMA Surg. – 2014. – Vol. 149(10). – P. 1015–1021.
4. Решетов И.В., Чиссов В.И. Пластическая и реконструктивная микрохирургия в онкологии. – М.: ООО РИФ, 2001. – 200 с.

5. Filonenko E.V., Saribekyan E.K., Ivanova-Radkevich V.I. Capabilities of intraoperative photodynamic therapy for treatment of locally advanced breast cancer, *Biomedical Photonics*, 2016, Vol. 5, No. 1, pp. 9–14. (in Russian)
6. Chalnot P., Michon J. Le dedoublement du sein restant, *Ann Chir Plast*, 1958, Vol. 3, p. 35.
7. Semiglazov V.F. *Minimal'nyj rak molochnoj zhelezy* [Minimal breast cancer]. Leningrad, Meditsina Publ., 1992. 276 p.
8. Sharova O.N., Vasil'ev S.A., Bujkov V.A., Vazhenin A.V. Reconstruction of the breast as the most constructive mechanism of psychological protection for women after radical treatment of breast cancer, *Annaly plasticheskoj, rekonstruktivnoj i ehstheticheskoj khirurgii*, 2001, No. 1, pp. 43–49. (in Russian)
9. Burlakov A.S. Reconstructive surgery in the treatment of patients with breast cancer, *Vestnik Moskovskogo onkologicheskogo obshhestva*, 2002, No. 9, pp. 1–8. (in Russian)
10. Omranipour R., Bobin J.Y., Esouyeh M. Skin Sparing Mastectomy and Immediate Breast Reconstruction (SSMIR) for early breast cancer: eight years single institution experience, *World J Surg Oncol*, 2008, Vol. 6, p. 43.
11. Pacifico M.D., See M.S., Cavale N., Collyer J., Francis I., Jones M.E., Hazari A., Boorman J.G., Smith R.W. Preoperative planning for DIEP breast reconstruction: early experience of the use of computerised tomography angiography with VoNavix 3D software for perforator navigation, *J Plast Reconstr Aesthet Surg*, 2009, Vol. 62(11), pp. 1464–1469.
12. Rietjens M., De Lorenzi F., Venturino M., Petit J.Y. The suspension technique to avoid the use of tissue expanders in breast reconstruction, *Ann Plast Surg*, 2005, Vol. 54(5), pp. 467–470.
13. Cumberland V.H. A preliminars report on the use of prefabricated nylon weave in the repair of ventral hernia, *Med J Aust*, 1952, Vol. 1(5), pp. 143–144.
14. Scales J.T. Discussion on metals and synthetic materials in relation to soft tissues: tissue reaction to synthetic materials, *Proc R Soc Med*, 1953, Vol. 46, p. 647.
15. Razumovskij A.Yu., Smirnova S.V. Use of implant materials for diaphragm plastic surgery in newborns, *Khirurgiya*, 2012, No. 11, pp. 90–95. (in Russian)
16. Chun Y.S., Verma K., Rosen H., Lipsitz S., Morris D., Kenney P., Eriksson E. Implant-based breast reconstruction using acellular dermal matrix and the risk of postoperative complications, *Plast Reconstr Surg*, 2010, Vol. 125(2), pp. 429–436.
17. Lanier S.T., Wang E.D., Chen J.J., Arora B.P., Katz S.M., Gelfand M.A., Khan S.U., Dagum A.B., Bui D.T. The effect of acellular dermal matrix use on complication rates in tissue expander/implant breast reconstruction, *Ann Plast Surg*, 2018, Vol. 64(5), pp. 674–678.
18. Glasberg S.B., Light D. AlloDerm and Strattice in breast reconstruction: a comparison and techniques for optimizing outcomes, *Plast Reconstr Surg*, 2012, Vol. 129(6), pp. 1223–1233.
19. Hoppe I.C., Yueh J.H., Wei C.H., Ahuja N.K., Patel P.P., Datiashvili R.O. Complications Following Expander/Implant Breast Reconstruction Utilizing Acellular Dermal Matrix: A Systematic Review and Meta-Analysis, *Open Access Journal of Plastic Surgery*, 2013, Vol. 11, pp. 417–428.
20. Salzberg C.A. Nonexpansive immediate breast reconstruction using human acellular tissue matrix graft (AlloDerm), *Ann Plast Surg*, 2006, Vol. 57(1), pp. 1–5.
21. Seth A.K., Hirsch E.M., Fine N.A., Kim J.Y. Breast Reconstruction – Current Perspectives and State of the Art Techniques. Utility of acellular dermis-assisted breast reconstruction in the setting of radiation: a comparative analysis, *Plast Reconstr Surg*, 2012, Vol. 130(4), pp. 750–758.
22. Colwell A.S., Damjanovic B., Zahedi B., Medford-Davis L., Hertl C., Austen W.G.Jr. Retrospective review of 331 consecutive immediate single-stage implant reconstructions with acellular dermal matrix: indications, complications, trends, and costs, *Plast Reconstr Surg*, 2011, Vol. 128(6), pp. 1170–1178.

5. Филоненко Е.В., Сарибекян Э.К., Иванова-Радкевич В.И. Возможности интраоперационной фотодинамической терапии в лечении местнораспространенного рака молочной железы // Biomedical Photonics. – 2016. – Т. 5, № 1. – С. 9–14.
6. Chalnot P., Michon J. Le dedoublement du sein restant // Ann Chir Plast. – 1958. – Vol. 3. – P. 35.
7. Семиглазов В.Ф. Минимальный рак молочной железы. – Ленинград: Медицина, 1992. – 276 с.
8. Шарова О.Н., Васильев С.А., Буйков В.А., Важенин А.В. Реконструкция молочной железы как наиболее конструктивный механизм психологической защиты у женщин после радикального лечения рака молочной железы // Анналы пластической, реконструктивной и эстетической хирургии. – 2001. – № 1. – С. 43–49.
9. Бурлаков А.С. Восстановительная хирургия в лечении больных раком молочной железы // Вестник Московского онкологического общества. – 2002. – № 9. – С. 1–8.
10. Omranipour R., Bobin J.Y., Esouyeh M. Skin Sparing Mastectomy and Immediate Breast Reconstruction (SSMIR) for early breast cancer: eight years single institution experience // World J Surg Oncol. – 2008. – Vol. 6. – P. 43.
11. Pacifico M.D., See M.S., Cavale N., Collyer J., Francis I., Jones M.E., Hazari A., Boorman J.G., Smith R.W. Preoperative planning for DIEP breast reconstruction: early experience of the use of computerised tomography angiography with VoNavix 3D software for perforator navigation // J Plast Reconstr Aesthet Surg. – 2009. – Vol. 62(11). – P. 1464–1469.
12. Rietjens M., De Lorenzi F., Venturino M., Petit J.Y. The suspension technique to avoid the use of tissue expanders in breast reconstruction // Ann Plast Surg. – 2005. – Vol. 54(5). — P. 467–470.
13. Cumberland V.H. A preliminars report on the use of prefabricated nylon weave in the repair of ventral hernia // Med J Aust. – 1952. — Vol. 1(5). – P. 143–144.
14. Scales J.T. Discussion on metals and synthetic materials in relation to soft tissues: tissue reaction to synthetic materials // Proc R Soc Med. – 1953. – Vol. 46. – P. 647.
15. Разумовский А.Ю., Смирнова С.В. Использование имплантационных материалов для пластики диафрагмы у новорожденных // Хирургия. – 2012. – № 11. – С. 90–95.
16. Chun Y.S., Verma K., Rosen H., Lipsitz S., Morris D., Kenney P., Eriksson E. Implant-based breast reconstruction using acellular dermal matrix and the risk of postoperative complications // Plast Reconstr Surg. – 2010. – Vol. 125(2). – P. 429–436.
17. Lanier S.T., Wang E.D., Chen J.J., Arora B.P., Katz S.M., Gelfand M.A., Khan S.U., Dagum A.B., Bui D.T. The effect of acellular dermal matrix use on complication rates in tissue expander/implant breast reconstruction // Ann Plast Surg. – 2018. – Vol. 64(5). – P. 674–678.
18. Glasberg S.B., Light D. AlloDerm and Strattice in breast reconstruction: a comparison and techniques for optimizing outcomes // Plast Reconstr Surg. – 2012. – Vol. 129(6). – P. 1223–1233.
19. Hoppe I.C., Yueh J.H., Wei C.H., Ahuja N.K., Patel P.P., Datiashvili R.O. Complications Following Expander/Implant Breast Reconstruction Utilizing Acellular Dermal Matrix: A Systematic Review and Meta-Analysis // Open Access Journal of Plastic Surgery. – 2013. – Vol. 11. – P. 417–428.
20. Salzberg C.A. Nonexpansive immediate breast reconstruction using human acellular tissue matrix graft (AlloDerm) // Ann Plast Surg. – 2006. – Vol. 57(1). – P. 1–5.
21. Seth A.K., Hirsch E.M., Fine N.A., Kim J.Y. Breast Reconstruction – Current Perspectives and State of the Art Techniques. Utility of acellular dermis-assisted breast reconstruction in the setting of radiation: a comparative analysis // Plast Reconstr Surg. – 2012. – Vol. 130(4). – P. 750–758.
22. Colwell A.S., Damjanovic B., Zahedi B., Medford-Davis L., Hertl C., Austen W.G.Jr. Retrospective review of 331 consecutive immediate single-stage implant reconstructions with acellular dermal matrix:

23. Nahabedian M.Y. AlloDerm performance in the setting of prosthetic breast surgery, infection, and irradiation, *Plast Reconstr Surg*, 2009, Vol. 124(6), pp. 1743–1753.
24. Weichman K.E., Wilson S.C., Weinstein A.L., Hazen A., Levine J.P., Choi M., Karp N.S. The use of acellular dermal matrix in immediate two-stage tissue expander breast reconstruction, *Plast Reconstr Surg*, 2012, Vol. 129(5), pp. 1049–1058.
25. Weichman K., Disa J. *Prosthetic Breast Reconstruction with Acellular Dermal Matrix* in Breast Reconstruction – Current Perspectives and State of the Art Techniques, chapter 4. pp. 67–80. doi: 10.5772/56331
26. Breuing K.H., Colwell A.S. Inferolateral AlloDerm hammock for implant coverage in breast reconstruction, *Ann Plast Surg*, 2007, Vol. 59(3), pp. 250–255.
27. Breuing K.H., Warren S.M. Immediate bilateral breast reconstruction with implants and inferolateral AlloDerm slings, *Ann Plast Surg*, 2005, Vol. 55(3), pp. 232–239.
28. Parks J.R., Hammond S.E., Walsh W.A., Adams R.L., Chandler R.G., Luce E.A. Human acellular dermis versus no acellular dermis in tissue expansion breast reconstruction, *Plast Reconstr Surg*, 2012, Vol. 130(4), pp. 736–740.
29. Vardanian A.J., Clayton J.L., Roostaeian J., Shirvanian V., Da Lio A., Lipa J.E., Crisera C., Festekjian J.H. Comparison of implant-based immediate breast reconstruction with and without acellular dermal matrix, *Plast Reconstr Surg*, 2011, Vol. 128(5), pp. 403–410.
30. Baxter R.A. Intracapsular allogenic dermal grafts for breast implant-related problems, *Plast Reconstr Surg*, 2003, Vol. 112(6), pp. 1692–1696.
31. Becker S., Saint-Cyr M., Wong C., Dauwe P., Nagarkar P., Thornton J.F., Peng Y. AlloDerm versus DermaMatrix in immediate expander-based breast reconstruction: a preliminary comparison of complication profiles and material compliance, *Plast Reconstr Surg*, 2009, Vol. 123(1), pp. 1–6.
32. Bindingnavele V., Gaon M., Ota K.S., Kulber D.A., Lee D.J. Use of acellular cadaveric dermis and tissue expansion in postmastectomy breast reconstruction, *J Plast Reconstr Aesthet Surg*, 2007, Vol. 60(11), pp. 1214–1218.
33. Surgeons ASoP, *American Society of Plastic Surgeons 2011 Statistics*, 2011. Available at: http:// www.plasticsurgery.org/News-and-Resources/2011-Statistics.html
34. Spear S.L., Parikh P.M., Reisin E., Menon N.G. Acellular dermis-assisted breast reconstruction, *Aesthetic Plast Surg*, 2008, Vol. 32(3), pp. 418–425.
35. Liu A.S., Kao H.K., Reish R.G., Hergrueter C.A., May J.W.Jr., Guo L. Postoperative complications in prosthesis-based breast reconstruction using acellular dermal matrix, *Plast Reconstr Surg*, 2011, Vol. 127(5), pp. 1755–1762.
36. Antony A.K., McCarthy C.M., Cordeiro P.G., Mehrara B.J., Pusic A.L., Teo E.H., Arriaga A.F., Disa J.J. Acellular human dermis implantation in 153 immediate two-stage tissue expander breast reconstructions: determining the incidence and significant predictors of complications, *Plast Reconstr Surg*, 2010, Vol. 125(6), pp. 1606–1614.
37. Gamboa-Bobadilla G.M. Implant breast reconstruction using acellular dermal matrix, *Ann Plast Surg*, 2006, Vol. 56(1), pp. 22–25.
38. Topol B.M., Dalton E.F., Ponn T., Campbell C.J. Immediate single-stage breast reconstruction using implants and human acellular dermal tissue matrix with adjustment of the lower pole of the breast to reduce unwanted lift, *Ann Plast Surg*, 2008, Vol. 61(5), pp. 494–499.

indications, complications, trends, and costs // Plast Reconstr Surg. – 2011. – Vol. 128(6). – P. 1170–1178.
23. Nahabedian M.Y. AlloDerm performance in the setting of prosthetic breast surgery, infection, and irradiation // Plast Reconstr Surg. – 2009. – Vol. 124(6). – P. 1743–1753.
24. Weichman K.E., Wilson S.C., Weinstein A.L., Hazen A., Levine J.P., Choi M., Karp N.S. The use of acellular dermal matrix in immediate two-stage tissue expander breast reconstruction // Plast Reconstr Surg. – 2012. – Vol. 129(5). – P. 1049–1058.
25. Weichman K., Disa J. Prosthetic Breast Reconstruction with Acellular Dermal Matrix // Breast Reconstruction – Current Perspectives and State of the Art Techniques. – chapter 4. – p. 67–80. doi: 10.5772/56331
26. Breuing K.H., Colwell A.S. Inferolateral AlloDerm hammock for implant coverage in breast reconstruction // Ann Plast Surg. – 2007. – Vol. 59(3). – P. 250–255.
27. Breuing K.H., Warren S.M. Immediate bilateral breast reconstruction with implants and inferolateral AlloDerm slings // Ann Plast Surg. – 2005. – Vol. 55(3). – P. 232–239.
28. Parks J.R., Hammond S.E., Walsh W.A., Adams R.L., Chandler R.G., Luce E.A. Human acellular dermis versus no acellular dermis in tissue expansion breast reconstruction // Plast Reconstr Surg. – 2012. – Vol. 130(4). – P. 736–740.
29. Vardanian A.J., Clayton J.L., Roostaeian J., Shirvanian V., Da Lio A., Lipa J.E., Crisera C., Festekjian J.H. Comparison of implant-based immediate breast reconstruction with and without acellular dermal matrix // Plast Reconstr Surg. – 2011. – Vol. 128(5). – P. 403–410.
30. Baxter R.A. Intracapsular allogenic dermal grafts for breast implant-related problems // Plast Reconstr Surg. – 2003. – Vol. 112(6). – P. 1692–1696.
31. Becker S., Saint-Cyr M., Wong C., Dauwe P., Nagarkar P., Thornton J.F., Peng Y. AlloDerm versus DermaMatrix in immediate expander-based breast reconstruction: a preliminary comparison of complication profiles and material compliance // Plast Reconstr Surg. – 2009. – Vol. 123(1). – P. 1–6.
32. Bindingnavele V., Gaon M., Ota K.S., Kulber D.A., Lee D.J. Use of acellular cadaveric dermis and tissue expansion in postmastectomy breast reconstruction // J Plast Reconstr Aesthet Surg. – 2007. – Vol. 60(11). – P. 1214–1218.
33. Surgeons ASoP. American Society of Plastic Surgeons 2011 Statistics, 2011. Available at: http:// www.plasticsurgery.org/News-and-Resources/2011-Statistics.html
34. Spear S.L., Parikh P.M., Reisin E., Menon N.G. Acellular dermis-assisted breast reconstruction // Aesthetic Plast Surg. – 2008. – Vol. 32(3). – P. 418–425.
35. Liu A.S., Kao H.K., Reish R.G., Hergrueter C.A., May J.W.Jr., Guo L. Postoperative complications in prosthesis-based breast reconstruction using acellular dermal matrix // Plast Reconstr Surg. – 2011. – Vol. 127(5). – P. 1755–1762.
36. Antony A.K., McCarthy C.M., Cordeiro P.G., Mehrara B.J., Pusic A.L., Teo E.H., Arriaga A.F., Disa J.J. Acellular human dermis implantation in 153 immediate two-stage tissue expander breast reconstructions: determining the incidence and significant predictors of complications // Plast Reconstr Surg. – 2010. – Vol. 125(6). – P. 1606–1614.
37. Gamboa-Bobadilla G.M. Implant breast reconstruction using acellular dermal matrix // Ann Plast Surg. – 2006. – Vol. 56(1). – P. 22–25.
38. Topol B.M., Dalton E.F., Ponn T., Campbell C.J. Immediate single-stage breast reconstruction using implants and human acellular dermal tissue matrix with adjustment of the lower pole of the breast to reduce unwanted lift // Ann Plast Surg. – 2008. – Vol. 61(5). – P. 494–499.

ORIGINAL ARTICLES

MATHEMATICAL MODEL OF DETECTION OF INTRA-ERYTHROCYTE PATHOLOGIES USING OPTOACOUSTIC METHOD

Kravchuk D.A.
Southern Federal University, Taganrog, Russiaa

Abstract

Malaria causes a serious health problem in the tropical and subtropical regions of the globe. In many cases, the consequences of this disease are fatal. Therefore, a simple, fast, accurate and affordable diagnostic system for the early detection of this disease is necessary for the timely administration of antimalarial drugs.
The malarial parasite, during its intra-erythrocyte development, processes a significant amount of hemoglobin, which in this case turns into a hem form called hemozoin. Hemozoin and hemoglobin have different molar extinction coefficients at certain optical wavelengths, hence, light absorption and an optoacoustic signal (OAS) from the infected cell will be different from that of a healthy cell. The paper describes the developed theoretical model intended for studying the influence of intra-erythrocyte malarial parasite development on optoacoustic signals. The OAS were calculated based on the models of healthy and infected blood modeled on the basis of a 3D model.
The simulated OAS were analyzed in the temporal and frequency domains to obtain signs of infection at various stages. The calculated OAS spectra have different amplitude levels, which indicates that the optoacoustic method can be useful for differentiating various intra-erythrocyte stages of the malarial parasite. The carried out modeling and the results obtained allow us to continue working on the creation of an optoacoustic flow cytometer.

Keywords: optoacoustic signal, aggregation, erythrocytes, spectral power density, laser.

For citations: Kravchuk D.A. Mathematical model of detection of intra-erythrocyte pathologies with the help of an optoacoustic method, *Biomedical Photonics,* 2018, T. 7, No. 3. – P. 36–42. (in Russian). doi: 10.24931/2413–9432–2018–7–3–36–42..

Contacts: Kravchuk D.A., e-mail: Kravchukda@sfedu.ru

МАТЕМАТИЧЕСКАЯ МОДЕЛЬ ОБНАРУЖЕНИЯ ВНУТРИЭРИТРОЦИТАРНЫХ ИНФЕКЦИЙ С ПОМОЩЬЮ ОПТОАКУСТИЧЕСКОГО МЕТОДА

Д.А. Кравчук
Южный федеральный университет, Таганрог, Россия

Резюме

Малярия вызывает серьезную проблему со здоровьем в тропических и субтропических регионах земного шара. Во многих случаях последствия этого заболевания являются фатальными. Поэтому необходима простая, быстрая, точная и доступная диагностическая система раннего выявления этого заболевания для своевременного назначения противомалярийных препаратов.
Малярийный паразит во время его внутриэритроцитарного развития перерабатывает значительное количество гемоглобина, который при этом превращается в форму гема, называемую гемозоином. Гемозоин и гемоглобин имеют разные молярные коэффициенты экстинкции при определенных длинах волн оптического излучения, следовательно, поглощение света и оптоакустический сигнал (ОАС) от зараженной клетки будут отличаться от аналогичных параметров здоровой клетки. В работе описана теоретическая модель, предназначенная для изучения влияния внутриэритроцитарного развития малярийного паразита на оптоакустические сигналы. ОАС были рассчитаны на основе смоделированных на основе 3D-модели образцов здоровой и инфицированной крови.
Моделируемые ОАС анализировались во временной и частотной областях для получения признаков наличия инфекции разных стадий. Рассчитанные спектры ОАС имеют различные уровни амплитуды, что указывает на то, что оптоакустический метод может быть полезен для дифференциации различных внутриэритроцитарных стадий малярийного паразита. Проведенное моделирование и полученные результаты позволяют продолжить работы по созданию оптоакустического проточного цитометра.

Ключевые слова: оптоакустический сигнал, агрегация, эритроциты, спектральная плотность мощности, лазер.

Для цитирования: Кравчук Д.А. Математическая модель обнаружения внутриэритроцитарных патологий с помощью оптоакустического метода // Biomedical Photonics. – 2018 – Т. 7, № 3 – С. 36–42. doi: 10.24931/2413–9432–2018–7–3–36–42.

Контакты: Кравчук Д.А., e-mail: Kravchukda@sfedu.ru

Introduction

It is known that optoacoustic effect leads to the generation of an ultrasonic wave when optical energy is absorbed in a liquid. The absorption of near-infrared laser radiation in the blood depends on the concentration of hemoglobin, which is its most common chromophore. When a blood vessel is irradiated with a short laser pulse, an ultrasonic wave is generated in the blood during absorption and the subsequent thermoelastic expansion; then the wave is detected by an ultrasonic transducer. The amplitude and time profile of the converter signal depend on the attenuation coefficient of the blood and, therefore, on the total concentration of hemoglobin [1-3]. In addition to the problem addressed in this article, this property underlies the study of the possibilities for the use of optoacoustic methods for tissue visualization tissues [4–6].

Many researchers study the structural and biochemical properties of the malaria pigment known as hemozoin, but, unfortunately, the microscopic examination of smears remains the best diagnostic method for detecting malaria. During its development in the red blood cell, the malaria parasite affects the hemoglobin necessary for its metabolism and produces hemozoin. D. Balasubramanian et al. [7, 8] used the optoacoustic effect to detect the malaria pigment. The conclusions of this study are that changes are detected in the spectra of the optoacoustic signal (OAS) for chloroatomic parasites in the presence of erythrocytic forms of plasmodia and ferriprotoporphyrin (heme). Plasmodia receive amino acids from erythrocyte hemoglobin, breaking it down with proteases, as a result of which, in addition to amino acids, ferriprotoporphyrin toxic to plasmodium is released, which polymerizes and loses its toxicity, turning into non-toxic hemozoin. It was noted that parasites resistant to chloroquine are easily detectable by this method due to a partial decrease in hemoglobin.

Theoretical information

If the illuminated region contains two types of absorbing spheres with different optical absorption coefficients, then the generated optoacoustic field can be expressed through a linear superposition of waves emitted by individual cells. The initial equation is an inhomogeneous wave equation [9]:

$$\Delta p' - \frac{1}{c^2}\frac{\partial^2 p'}{\partial t^2} + \frac{b}{c_0^2 \rho_0}\frac{\partial}{\partial t}\Delta p' = -Q,$$

where the sources are the following: $Q = \rho_0 \beta \frac{\partial^2 T'}{\partial t^2}$,

β – is the coefficient of volume expansion, ρ_0 – is the equilibrium density value, c_0 – is the speed of sound in a liquid,

$$b = \varsigma + \frac{4}{3}\eta + k\left(\frac{1}{C_V} - \frac{1}{C_{Ps}}\right),$$

η and ς – are shear and bulk viscosities, k – is the thermal conductivity coefficient, C_{Ps} and C_v – are specific heat capacities at constant pressure and volume, respectively.

The OAS field generated by a spherical absorber of radius is obtained by solving the wave equation, which is obtained under the condition of thermal limitation in the frequency domain with the corresponding boundary conditions [10]:

$$p(r_n, f) = \frac{i\mu_s \beta_s I_0 c_S a_s^2}{C_{Ps} r_n} \times \frac{j_1(q) e^{jkf(r_n - a_s)}}{[(1-\rho)(\sin q/q) - \cos q + i\rho c \sin q]}$$

where I_0 – is the intensity of the incident light propagating along the x axis and modulated by ω frequency. The wave numbers of the acoustic wave inside the liquid and the absorbing medium are denoted, respectively, as $k_f = \omega/c_f$ and $k_s = \omega/c_s$. Here c_f and c_s – are the speed of sound for these carriers, respectively. Similarly, ρ_f and ρ_s indicate density for such cases. Non-dimensional values are defined as $\rho = \rho_s/\rho_f$, $c = c_s/c_f$ и $q = k_{s*}a_s$. In addition, β_s, C_{Ps} and μ_s are the isobaric coefficient of thermal expansion, isobaric specific heat, and light absorption coefficient for the medium inside the spherical absorber, respectively. j_1 – is the spherical first-order Bessel function.

If the illuminated area contains more than one absorber (Fig. 1), the resulting sound pressure of the

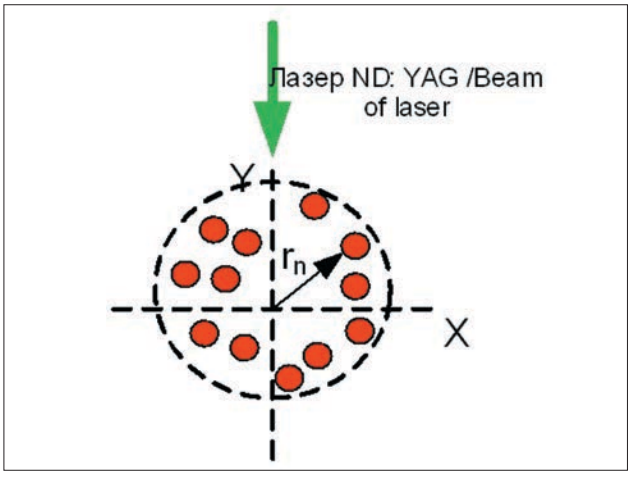

Рис. 1. Схема геометрии формирования оптоакустического сигнала (где r_n –радиус-вектор до n эритроцита)
Fig. 1. The geometry of the optoacoustic signal formation (where r_n is the radius vector to the n^{th} erythrocyte)

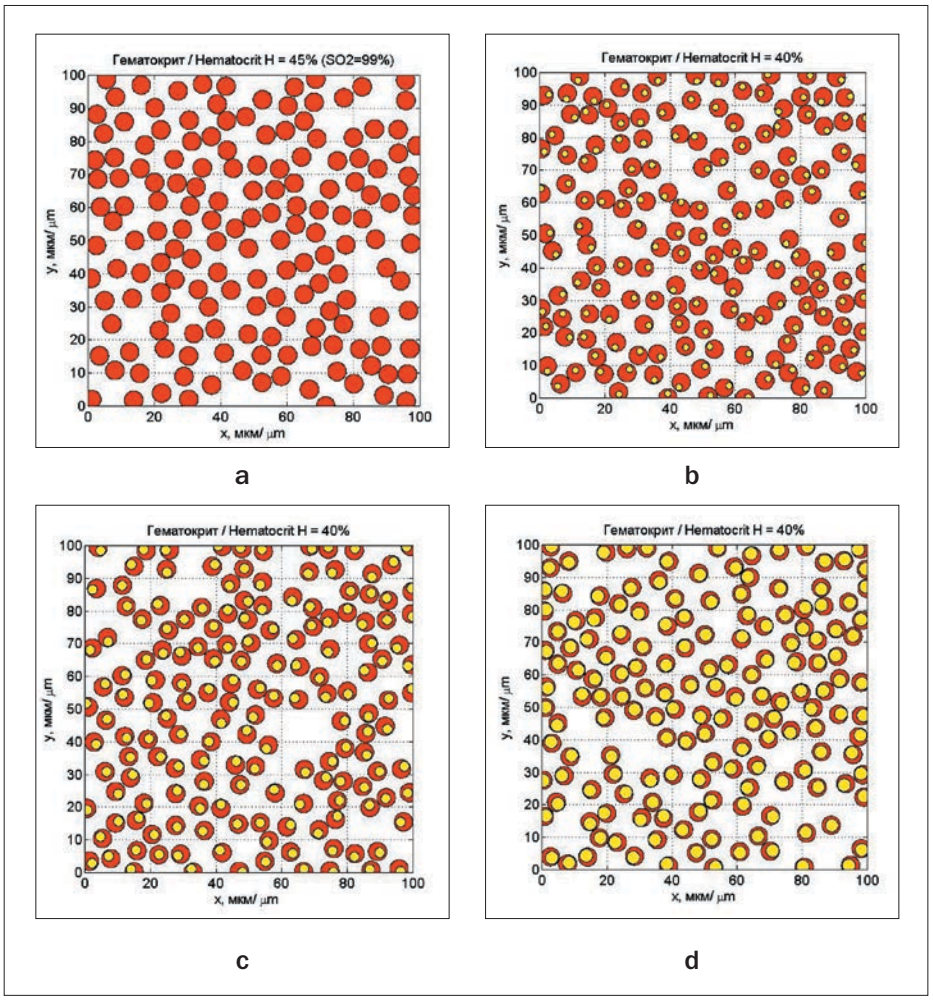

Рис. 2. Случайно помещенные неперекрывающиеся эритроциты, моделирующие реализацию 2D-ткани:
а – здоровый эритроцит;
б – кольцо;
в – трофозоит;
г – шизонт

Fig. 2. Randomly placed non-overlapping erythrocytes modeling the 2D tissue:
a – healthy erythrocyte;
b – ring;
c – trophozoite;
d – schizont

OAS can be obtained by linear superposition of waves emitted by individual sources, as in [11]:

$$p_f^{\Sigma}(r_n,k_f) \approx \frac{i\mu_s\beta_s I_0 c_S a_s^2}{C_{P_S} r_n} \times \frac{j_1(q)e^{ik_f(r_n-a_s)}}{[(1-\rho)(\sin q/q)-\cos q+i\rho c\sin q} \times \sum_{n=1}^{N} e^{-ik_f r_n}.$$

Materials and methods

The method of mathematical modeling is as follows: first, a three-dimensional realization of tissues is generated with the condition of absence of overlapping of the spheres which represent red blood cells. Modeling is done with MathLab software environment. The simulation volume size was assumed as 100 * 100 * 100 μm^3. This volume is filled with red blood cells approximated in the form of liquid spheres with a hematocrit level of 40% [12–14]. The calculation of tissue configurations in 3D at such a high concentration of cells is rather difficult, and, therefore, for the purpose of effectively creating tissue realizations, the simulated volume was divided into several subunits.

One of the conditions for modeling was the absence of overlapping of the spheres. Spheres close to the borders also met the condition of the absence of overlap with neighboring subunits. Figure 2 shows the simulated tissue configurations corresponding to the normal, annular, trophozoite and schizot stages. Here, the solid filled circles represent red blood cells, and the inner circles indicate parasitic vacuoles.

Inner circles were also placed inside the cells at random. There are two nuclei in each infected cell. The hemoglobin and hemozoin molecules are present in the outer and inner nuclei, respectively.

Fig. 2 shows four different stages of infection. Each large circle is an erythrocyte, and the inner circles indicate parasitic vacuoles at different stages. A 2D realization was chosen to better visualize tissue configurations.

To calculate expression (1), numerical values of various physical parameters for the red blood cells are required. The estimated values of the mechanical and thermal parameters were taken from literary sources [15–17]. Quantitative values for the physical parameters of a human erythrocyte a_s = 2.7 μm, c_s = 1639 m/s, s_f = 1498 m/s, other parameters for calculation were taken from the works by Y.K. Park, K.K. Shung, M. Toubal et al. [15–17]. The optical absorption coefficients for a fully oxygenated red blood cell at different stages of infection are taken from the study by A. U. Orjih and C.D. Fitch [18].

The malaria pigment (hemozoin) is contained in the cytoplasm of the erythrocyte stages of plasmodium and is a decay product of hemoglobin; in this case, there is hemozoin in vacuoles. (fig. 2). Both of these substances act as chromophores and contribute to the absorption coefficient [18].

For each stage, 200 different configurations of three-dimensional tissue were modeled. The averaged simulation results for 200 measurements are presented in Fig. 4*a-d*.

Fig. 4*a* shows the OAS for a sample with healthy cells when illuminated with a 532 nm laser beam. Similarly, fig. 4*d* shows OAS from a plurality of infected cells (at the schizont stage) under incident light with the same wavelength.

It can be seen from these figures that the signal level from each boundary is much higher than that of the central region. This is because OSA from individual sources close to each border are found simultaneously due to their proximity. However, for the central region, signals from different sources interfere with the increase in amplitude, which leads to a large suppression of the signal in this region. In addition, the signal level in Fig. 4*a* is much higher than the signal level shown in fig. 4*d*. It is expected that the coefficient of cellular absorption for healthy cells is higher than that of infected cells with given optical radiation parameters [15–17].

Conclusion

The signal power spectral density averaged over 200 simulation results for normal and infected cells is shown in Fig. 5 and 6. The spectral curves for healthy red blood cells and erythrocytes with a ring degree of damage are very little separated. However, the spectra obtained in the analysis of samples with red blood cells at other stages of the lesion are clearly separable. It is also noted that the intensity of the ultrasonic signal decreases with the development of a malaria infection at a laser wavelength of 532 nm.

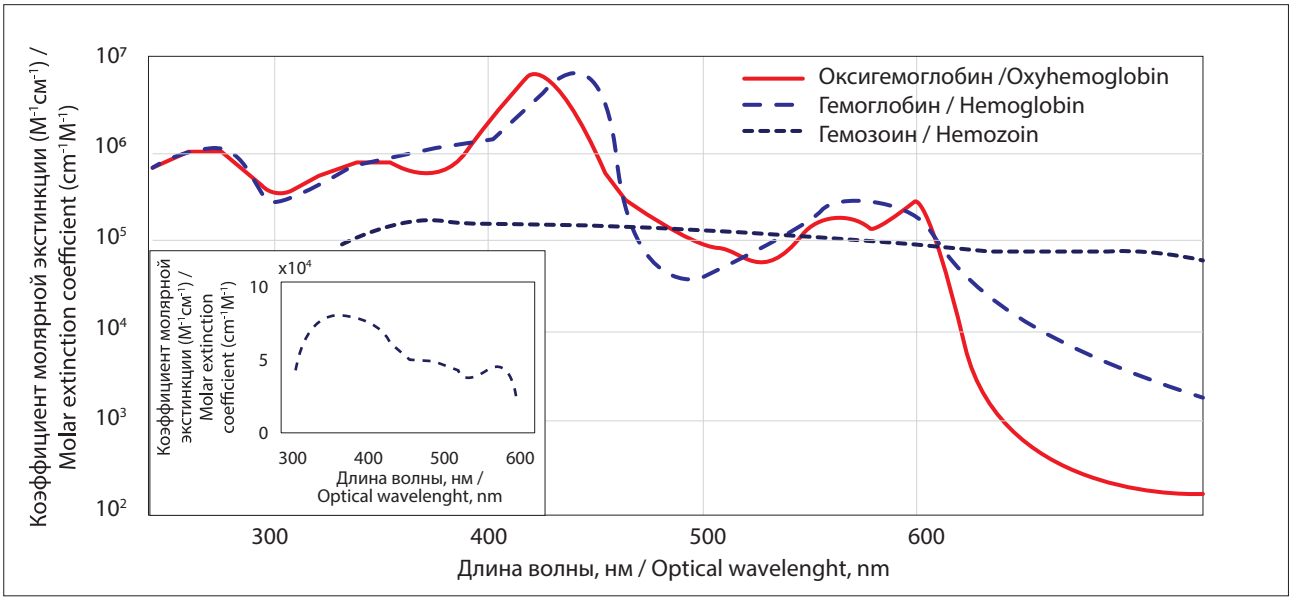

Рис. 3. Спектральная зависимость молярного коэффициента экстинкции оксигемоглобина и гемозойных молекул [18]
Fig. 3. Spectral dependence of the molar extinction coefficient of oxyhemoglobin and hemozoic molecules [18]

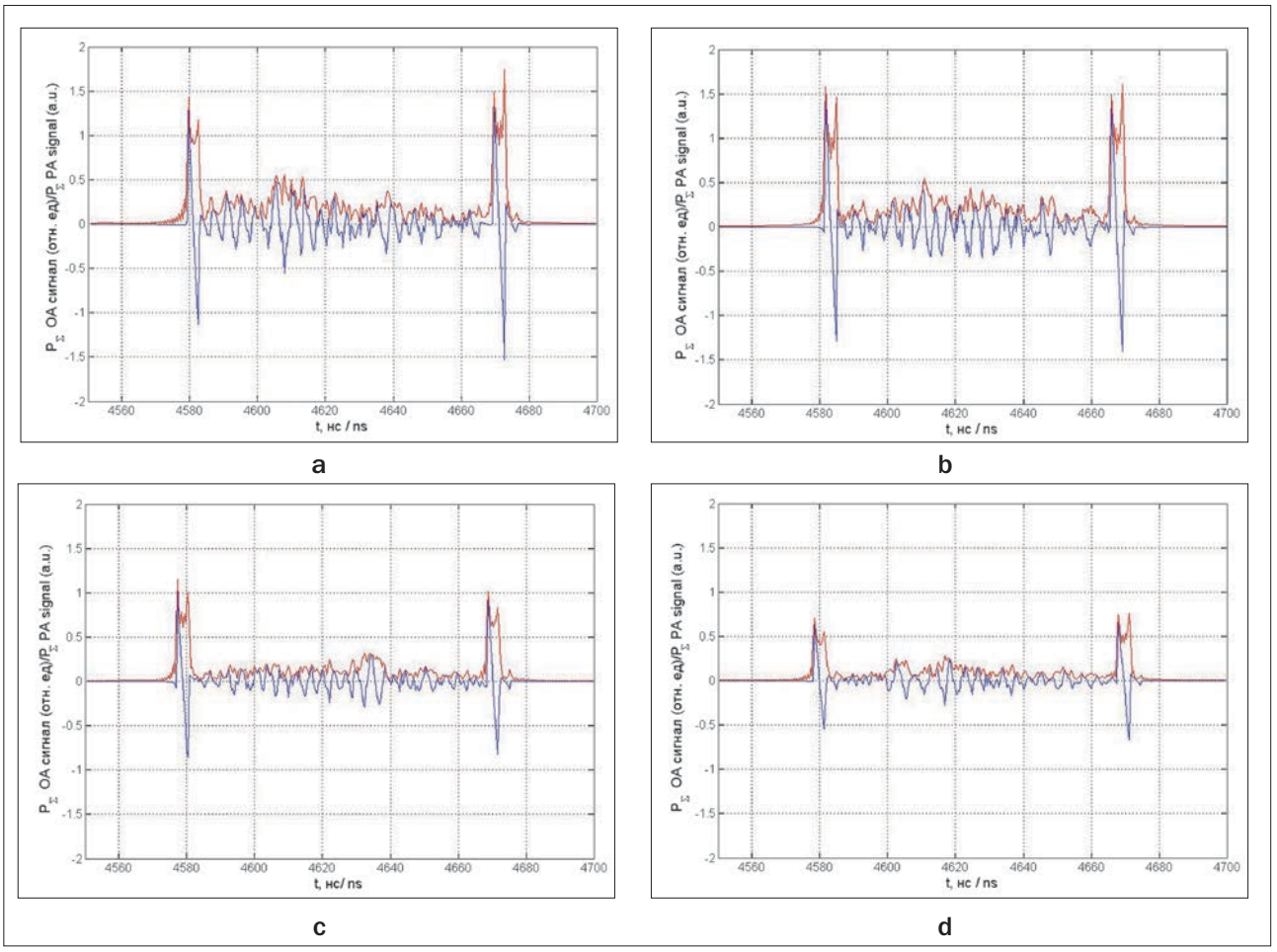

Рис. 4. Моделируемый при 532 нм оптоакустический сигнал падающего оптического излучения для образца:
а – состоящего из нормальных клеток;
б – для клеток со стадией кольца;
в – для клеток со стадией трофозоита;
г – для клеток со стадией шизонта
Fig. 4. Simulated optoacoustic signal for 532 nm incident optical radiation for a sample:
a – consisting of normal cells;
b – for cells at the ring stage;
c – for cells at the trophozoite stage;
d – for cells at the schizont stage

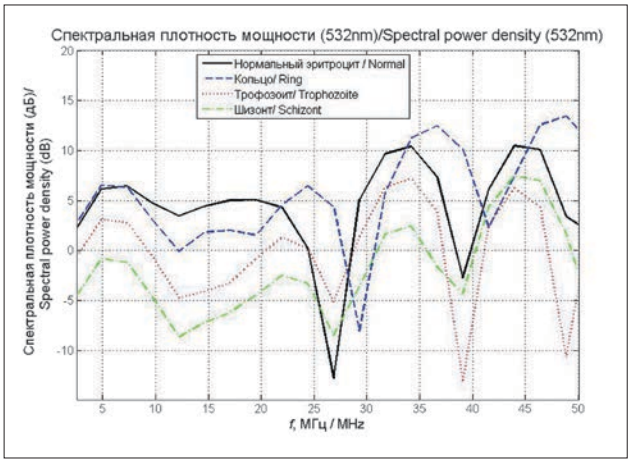

Рис. 5. Спектральная плотность мощности оптоакустического сигнала при длине волны оптического излучения 532 нм
Fig. 5. The spectral power density of the optoacoustic signal under optical irradiation at 532 nm

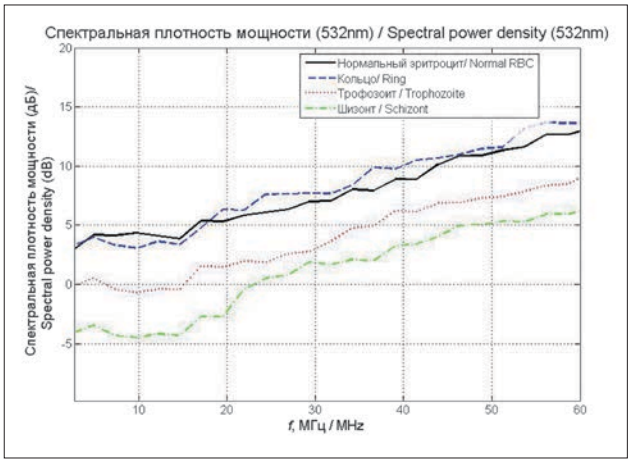

Рис. 6. Спектральная плотность мощности ОАС (скользящие средние) при облучении оптическим излучением с длинной волны 532 нм
Fig. 6. Spectral power density of the optoacoustic signal (moving averages) under optical radiation irradiation at 532 nm

The spectra have different levels of amplitude, which indicates that the optoacoustic method may be useful for differentiating the various intra-erythrocytic stages of the malaria parasite in practice. The simulation and the results obtained make it possible to continue the work on the development of an optoacoustic flow cytometer [19–20]. It is also necessary to perform simulations for other laser wavelengths, for example, for 1064 nm (working laser wavelength ND: YAG) and verify the consistency of the applied mathematical model with the experimental data obtained on the existing LIMO 100-532/1064-U unit [19].

REFERENCES

1. Deán-Ben X.L, Razansky D. Functional optoacoustic human angiography with handheld video rate three dimensional scanner, *Photoacoustics*, Vol. 1(3), pp. 68–73.
2. Kirillin M., Perekatova V., Turchin I., Subochev P. Fluence compensation in raster-scan optoacoustic angiography, 2017, *Photoacoustics*, Vol. 8, pp. 59–67.
3. Held K.G., Jaeger M., Rička J., Frenz M., Akarçay H.G. Multiple irradiation sensing of the optical effective attenuation coefficient for spectral correction in handheld OA imaging, *Photoacoustics*, 2016, Vol. 4(2), pp. 70–80.
4. Petrov I., Petrov Y., Prough D., Cicenaite I., Deyo D., Esenaliev R. Optoacoustic monitoring of cerebral venous blood oxygenation though intact scalp in large animals, *Optics express*, 2012, Vol. 20(4), pp. 4159–4167.
5. Perekatova V., Subochev P., Kleshnin M., Turchin I. Optimal wavelengths for optoacoustic measurements of blood oxygen saturation in biological tissues, *Biomedical Optics Express*, 2016, Vol. 7(10), pp. 3979–3995.
6. Bosschaart N., Edelman G.J., Aalders M.C., van Leeuwen T.G., Faber D.J. A literature review and novel theoretical approach on the optical properties of whole blood, *Lasers in medical science*, 2014, Vol. 29(2), pp. 453–479.
7. Balasubramanian D. Photoacoustic spectroscopy and its use in biology, *Bioscience Reports*, 1983, Vol. 3, pp. 981–995.
8. Balasubramanian D., Rao C.M., Panijpan B. The malaria parasite monitored by photoacoustic spectroscopy, *Science*, 1984, Vol. 223, pp. 828–830.
9. Novikov B.K., Rudenko O.V., Timoshenko V.I. *Nelinejnaya gidroakustika*. Leningrad, Sudostroenie Publ., 1981. 264 p.
10. Diebold G.J. Photoacoustic monopole radiation: Waves from objects with symmetry in one, two and three dimensions in *Photoacoustic imaging and spectroscopy*, Edt. L.V. Wang. Taylor and Francis Group, LLC. pp. 3–17.
11. Saha R.K., Kolios M.C. A simulation study on photoacoustic signals from red blood cells, *J. Acoust. Soc. Am.*, 2011, Vol. 129(5), pp. 2935–2943.
12. Kravchuk D.A., Starchenko I.B. Mathematical modeling of the optoacoustic signal from aggregated erythrocytes to assess the level of aggregation, *Nauchnoe priborostroenie*, 2018, Vol. 28, No. 1, pp. 30–36. (in Russian)
13. Kravchuk D.A., Starchenko I.B. Modeling the process of oxygen saturation of biological tissues using the optoacoustic method, *Nauchnoe priborostroenie,* 2018, Vol. 28, No. 2, pp. 20–25. (in Russian)
14. Kravchuk D.A., Starchenko I.B. Mathematical modeling of the optoacoustic signal from erythrocytes, *Vestnik novykh meditsins-kikh tekhnologii*. 2018, No. 1, pp. 96–101. (in Russian)
15. Park Y., Diez-Silva M., Popescu G., Lykotrafitis G., Choi W., Feld M.S., Suresh S. Refractive index maps and membrane dynamics of human red blood cells parasitized by Plasmodium falciparum, *Proceedings of National Academy of Sciences*, 2008, Vol. 105(37), pp. 13730–13735.

ЛИТЕРАТУРА

1. Deán-Ben X.L, Razansky D. Functional optoacoustic human angiography with handheld video rate three-dimensional scanner // Photoacoustics. – 2013. – Vol. 1(3). – P. 68–73.
2. Kirillin M., Perekatova V., Turchin I., Subochev P. Fluence compensation in raster-scan optoacoustic angiography // Photoacoustics. – 2017. – Vol. 8. – P. 59–67.
3. Held K.G., Jaeger M., Rička J., Frenz M., Akarçay H.G. Multiple irradiation sensing of the optical effective attenuation coefficient for spectral correction in handheld OA imaging // Photoacoustics. – 2016. – Vol. 4(2). – P. 70–80.
4. Petrov I., Petrov Y., Prough D., et al. Optoacoustic monitoring of cerebral venous blood oxygenation though intact scalp in large animals // Optics express. – 2012. – Vol. 20(4). – P. 4159–4167.
5. Perekatova V., Subochev P., Kleshnin M., Turchin I. Optimal wavelengths for optoacoustic measurements of blood oxygen saturation in biological tissues // Biomedical Optics Express. – 2016. – Vol. 7(10). – P. 3979–3995.
6. Bosschaart N., Edelman G.J., Aalders M.C., et al. A literature review and novel theoretical approach on the optical properties of whole blood // Lasers in medical science. – 2014. – Vol. 29(2). – P. 453–479.
7. Balasubramanian D. Photoacoustic spectroscopy and its use in biology // Bioscience Reports. – 1983. – Vol. 3. – P. 981–995.
8. Balasubramanian D., Rao C.M., Panijpan B. The malaria parasite monitored by photoacoustic spectroscopy // Science. – 1984. – Vol. 223. – P. 828–830.
9. Новиков Б.К., Руденко О.В., Тимошенко В.И. Нелинейная гидроакустика. – Ленинград: Судостроение, 1981. – 264 с.
10. Diebold G.J. Photoacoustic monopole radiation: Waves from objects with symmetry in one, two and three dimensions in Photoacoustic imaging and spectroscopy / Edt. L.V. Wang. – Taylor and Francis Group, LLC, 2009. – P. 3–17.
11. Saha R.K., Kolios M.C. A simulation study on photoacoustic signals from red blood cells // J. Acoust. Soc. Am. – 2011. – Vol. 129(5). – P. 2935–2943.
12. Кравчук Д.А., Старченко И.Б. Математическое моделирование оптоакустического сигнала от агрегированных эритроцитов для оценки уровня агрегации // Научное приборостроение. – 2018. – Т. 28, № 1. – С. 30–36.
13. Кравчук Д.А, Старченко И.Б. Моделирование процесса насыщения кислородом биологических тканей с помощью оптоакустического метода // Научное приборостроение. – 2018. – Т. 28, № 2. – С. 20–25.
14. Кравчук Д.А., Старченко И.Б. Математическое моделирование оптикоакустического сигнала от эритроцитов // Вестник новых медицинских технологий. – 2018. – № 1. – С. 96–101.
15. Park Y., Diez-Silva M., Popescu G., et al. Refractive index maps and membrane dynamics of human red blood cells parasitized by Plasmodium falciparum // Proceedings of National Academy of Sciences. – 2008. – Vol. 105(37). – P. 13730–13735.
16. Shung K.K., Yuan Y.W., Fei D.Y., Tarbell J.M. Effect of flow disturbance on ultrasonic backscatter from blood // J. Acoust. Soc. Am. – 1984. – Vol. 75. – P. 1265–1272.

16. Shung K.K., Yuan Y.W., Fei D.Y., Tarbell J.M. Effect of flow disturbance on ultrasonic backscatter from blood, *J. Acoust. Soc. Am.*, 1984, Vol. 75, pp. 1265–1272.
17. Toubal M., Asmani M., Radziszewski E., Nongaillard B. Acoustic measurement of compressibility and thermal expansion coefficient of erythrocytes, *Phys. Med. Biol.,* 1999, Vol. 44, pp. 1277–1287.
18. Orjih A.U., Fitch C.D. Hemozoin production by Plasmodium falciparum: variation with strain and exposure to chloroquine, *Biochimica et Biophysica Acta*, 1993, Vol. 1157, pp. 270–274.
19. Starchenko I.B., Kravchuk D.A., Kirichenko I.A. An Optoacoustic Laser Cytometer Prototype, *Meditsinskaya tekhnika*, 2017, No. 5, pp. 4–7. (in Russian)
20. Starchenko I. B., Kravchuk D.A., Kirichenko I.A. An Optoacoustic Laser Cytometer Prototype, *Biomedical Engineering*, 2018, Vol. 51, No. 5, pp. 308–312.
17. Toubal M., Asmani M., Radziszewski E., Nongaillard B. Acoustic measurement of compressibility and thermal expansion coefficient of erythrocytes // Phys. Med. Biol. – 1999. – Vol. 44. – P. 1277–1287.
18. Orjih A.U., Fitch C.D. Hemozoin production by Plasmodium falciparum: variation with strain and exposure to chloroquine // Biochimica et Biophysica Acta. – 1993. – Vol. 1157. – P. 270–274.
19. Старченко И.Б., Кравчук Д.А., Кириченко И.А. Прототип оптоакустического лазерного цитометра // Медицинская техника. – 2017. – № 5. – С. 4–7.
20. Starchenko I.B., Kravchuk D.A., Kirichenko I.A. An Optoacoustic Laser Cytometer Prototype // Biomedical Engineering. – 2018. – Vol. 51, No. 5. – P. 308–312.

COMPARATIVE EXPERIMENTAL STUDY OF 5-ALA AND 5-ALA HEXYL ESTER SPECIFIC ACTIVITY

Yakubovskaya R.I.[1], Pankratov A.A.[1], Filonenko E.V.[1, 2], Lukyanets E.A.[3], Ivanova-Radkevich V.I.[3, 4], Trushin A.A.[2], Kaprin A.D.[1]
[1]P. Herzen Moscow Oncology Research Institute – branch of the National Medical Research Radiological Center of the Ministry of Health of the Russian Federation, Moscow, Russia
[2]I.M. Sechenov First Moscow State Medical University, Moscow, Russia
[3]State Scientific Center Scientific Research Institute Organic Intermediates and Dyes, Moscow, Russia
[4]Peoples' Friendship University of Russia (RUDN University), Moscow, Russia

Abstract

A comparative experimental study of the specific activity of drugs based on 5-aminolevulinic acid (5-ALA) and its hexyl ester (5-ALA HE) was carried out. Their ability to induce the synthesis of photoactive protoporphyrin IX in the healthy tissues of the rabbit bladder when instilling the drug solutions at various concentrations has been estimated. It was shown that 5-ALA HE results in the induction and accumulation of PPIX in the rabbit bladder epithelium at much lower concentrations than 5-ALA. Thus, a significant increase in the fluorescence intensity in comparison with the control was achieved by instillation of 5-ALA HE solution in the rabbit' bladder at a concentration of only 0.0001% (fluorescence intensity 2.20±0.60 a.u.), and for 5-ALA - only when using a solution at a concentration of 0.3% (fluorescence intensity 2.60±1.02 a.u.).

Keywords: fluorescence diagnosis, protoporphyrin IX, 5-aminolevulinic acid, hexyl ester of 5-aminolevulinic acid, bladder cancer.

For citations: Yakubovskaya R.I., Pankratov A.A., Filonenko E.V., Lukyanets E.A., Ivanova-Radkevich V.I., Trushin A.A., Kaprin A.D. Comparative experimental study of 5-ALA and 5-ALA hexyl ester specific activity, *Biomedical Photonics,* 2018, T. 7, No. 3, pp. 43-46 (in Russian). doi: 10.24931/2413–9432–2018–7–3–43–46.

Contacts: Filonenko E.V., e-mail: derkul23@mail.ru

СРАВНИТЕЛЬНОЕ ЭКСПЕРИМЕНТАЛЬНОЕ ИССЛЕДОВАНИЕ СПЕЦИФИЧЕСКОЙ АКТИВНОСТИ 5-АЛК И ГЕКСИЛОВОГО ЭФИРА 5-АЛК

Р.И. Якубовская[1], А.А. Панкратов[1], Е.В. Филоненко[1, 2], Е.А. Лукьянец[3], В.И. Иванова-Радкевич[3, 4], А.А. Трушин[2], А.Д. Каприн[1, 4]
[1]МНИОИ им П.А.Герцена – филиал ФГБУ «НМИЦ радиологии» Минздрава России, Москва, Россия
[2]Первый Московский государственный медицинский университет им. И.М. Сеченова, Москва, Россия
[3]Научно-исследовательский институт органических полупродуктов и красителей, Москва, Россия
[4]Российский Университет дружбы народов, Москва, Россия

Резюме

Проведено сравнительное экспериментальное исследование специфической активности препаратов на основе 5-аминолевулиновой кислоты (5-АЛК) и ее гексилового эфира (ГЭ 5-АЛК). Оценена их способность индуцировать синтез фотоактивного протопорфирина IX в здоровых тканях мочевого пузыря кролика при инстилляции растворов препаратов в различных концентрациях. Исследования показали, что ГЭ 5-АЛК вызывает индукцию и накопление ППIX в эпителии мочевого пузыря кролика в значительно меньших концентрациях, чем 5-АЛК. Так, достоверное увеличение интенсивности флуоресценции по сравнению с контролем удалось достичь при инстилляции в мочевой пузырь кролика раствора ГЭ 5-АЛК в концентрации всего 0,0001% (интенсивность флуоресценции 2,20±0,60 усл.ед.), а для 5-АЛК – только при использовании раствора в концентрации 0,3% (интенсивность флуоресценции 2,60±1,02 усл.ед.).

Ключевые слова: флуоресцентная диагностика, протопорфирин IX, 5-аминолевулиновая кислота, гексиловый эфир 5-аминолевулиновой кислоты, мочевой пузырь.

Для цитирования: Якубовская Р.И., Панкратов А.А., Филоненко Е.В., Лукьянец Е.А., Иванова-Радкевич В.И., Трушин А.А., Каприн А.Д. Сравнительное экспериментальное исследование специфической активности 5-АЛК и гексилового эфира 5-АЛК // Biomedical Photonics. – 2018. – Т. 7, № 3. – С. 43-46. doi: 10.24931/2413–9432–2018–7–3–43–46.

Контакты: Филоненко Е.В., e-mail: derkul23@mail.ru

Introduction

Among modern methods for early cancer diagnosis, fluorescence methods are currently considered the most promising, as they are based on the possibility of recognizing malignant tissue by the characteristic fluorescence induced by light radiation of exogenous or endogenous fluorochromes [1,2].

Fluorescence diagnostics (PD) of tumors is based on the selectivity of accumulation in tumor node tissues and the possibility of its detection by the spectra of exogenous fluorescence from the area illuminated by laser radiation. This method allows the detection of tumors, as well as determines their topography when scanning spots of exciting laser radiation on the surface of the tissue [3].

Fluorescence cancer diagnosis is the most promising for the detection of small tumors (up to 1 mm) localized in the surface layers (epidermis, mucosal epithelium), since the sensitivity of this method is significantly higher than of other modern early diagnosis methods. The effectiveness of the method depends on the level of accumulation and localization of the dye in individual structures of the tumor focus and surrounding tissue [4].

Photosensitizers of the first generation, which belong to hematoporphyrin derivatives group, have a number of disadvantages that reduce their diagnostic potential: low fluorescence intensity and fluorescence contrast (tumor vs. normal tissue). For this reason, the laboratories of many countries continue the search and synthesis of new photosensitizers with improved diagnostic properties.

One of the ways to create effective concentrations of the photosensitizer in the tumor tissue is to stimulate the body to produce porphyrins, which are endogenous photoactive compounds, in particular, the metabolite of heme protoporphyrin (PPIX) synthesis. One of the compounds that effectively induces the synthesis of endogenous PPIX is 5-aminolevulinic acid (5-ALA), an endogenous compound, one of the intermediate products of heme synthesis. Excessive administration of 5-ALA leads to an increased formation of PPIX, which is quickly utilized in healthy tissues, turning into heme under the action of the enzyme ferrochelatase [5,6]. In tumor cells, a deficiency of ferrochelase is observed, resulting in a temporary but significant increase in the level of PPIX, which remains in the tumor cells for several hours. The result is a high fluorescence contrast between the tumor and surrounding tissue, which in some tumors reaches 10-15 times [7]. The accumulation of 5-ALA-induced PPIX, which intensively fluoresces in the red region of the spectrum with a maximum at 635 nm, provides an opportunity to detect tumors and determine the precise boundaries of their spread [8].

Both in Russia and abroad, PD of bladder cancer is effected with 5-ALA-based preparations. Clinical studies have shown that the sensitivity of the PD method with 5-ALA-based preparations with fluorescence cystoscopy reaches more than 90%, which by far exceeds the maximum sensitivity of routine endoscopic examination of the bladder (up to 50%). At the same time, the high sensitivity of the method is accompanied by lower specificity (50–65%), which reduces its diagnostic accuracy [9].

Continuation of studies to improve fluorescence diagnostics led to the development of diagnostic tools based on 5-ALA methyl and hexyl esters, which undergo metabolic transformation in the body to 5-ALA [10]. Being more lipophilic compounds than 5-ALA itself, esters are better at penetrating biological membranes, so they accumulate in cells faster and to a greater extent, and become included in biosynthesis as PPIX precursors.

In this work, *in vivo* experiments were used to compare the ability of 5-ALA preparations and its hexyl ester (HE 5-ALA) at various concentrations to induce the synthesis and accumulation of photoactive PPIX in the tissues of the bladder.

Materials and methods

The study examined the specific activity of two drugs: 5-ALA and HE 5-ALA.

In experiments aimed at evaluation of the intensity of 5-ALA-induced fluorescence of protoporphyrin IX in the mucous membrane of the bladder with intravesical administration of 5-ALA, its solutions were used in concentrations of 3.0%, 0.3%, 0.03%, and 0.01%.

For preparation of solutions of the required concentration, 5-ALA powder is taken in an amount of 300 mg (to obtain a 3.0% solution), 30 mg (0.3% solution), 3 mg (0.03% solution) or 1 mg (0.01% solution) and dissolved in 10 ml of 5% sodium bicarbonate solution. The resulting solutions were clear, colorless. 10 ml of the solutions

was injected into the rabbit bladder immediately after preparation.

Another product used for the research was HE 5-ALA, a lyophilisate for the preparation of the solution used for instillations.

In the experiments, the specific activity of 0.2%, 0.01%, 0.002%, 0.001%, 0.0001% and 0.00005% solutions of HE 5-ALA preparation was investigated.

For preparation of solutions of the required concentration, HE 5-ALA powder is taken in an amount of 20 mg (to obtain a 0.2% solution), 1 mg (0.01% solution) and 0.2 mg (0.002% solution) and dissolved in 10 ml of 0.9% sodium chloride solution. To prepare 0.001%, 0.0001% and 0.00005% solutions, the 0.01% solution produved as described above was diluted with a 0.9% sodium chloride solution to 0.001%, 0.0001% and 0.00005% concentrations, respectively. The resulting solutions were clear, colorless. Solutions were injected, at a dose of 10 ml, into the rabbit bladder immediately after preparation.

Studies were performed on intact chinchilla rabbits, females weighing 2.5–3.5 kg. After preliminary sedation by intravenous administration of relanium (10–30 mg) or droperidol (5 mg), bladder immobilization was performed. Then, HE 5-ALA or 5-ALA solutions at concentrations listed above were injected into the bladder. The exposure time was 2 h, then the animal was killed by an overdose of anesthesia drugs, the bladder was removed and the specific fluorescence of PPIX was recorded.

Induced fluorescence in the bladder mucosa was evaluated by local fluorescence spectroscopy with excitation of radiation from a solid-state laser with a wavelength of 532 nm. During mathematical processing, the integrated fluorescence intensity in the range of 620–650 nm was normalized to the integrated tissue autofluorescence intensity in the range of 555–585 nm, the obtained value was designated as a diagnostic parameter (DP). Fluorescence was recorded by the contact method with the use of «Spektr-Claster» diagnostic unit (manufacturer: OOO «Klaster», Russia). The power density at the end of the fiber is 7 mW. In each tissue sample, from 5 to 10 spectra were measured to obtain a reliable result. The differences were considered significant at $p \leq 0.05$.

The control was the measured fluorescence spectra from the mucous membrane of the bladder of rabbits which were not administered the preparation.

Results and discussion

The dependence of 5-ALA induced PPIX fluorescence on the concentration of 5-ALA solution used for instillation is shown in Fig. 1. It can be seen that a 2-hour exposure to 3% and 0.3% solutions of 5-ALA preparation led to a significant induction of PPIX synthesis in rabbit bladder epithelium (DP – 2.69 ± 1.37 conventional units and 2.60 ± 1.02 conventional units, respectively). With a decrease in the concentration of the drug solution to 0.03%, a 2-fold decrease in the intensity of specific fluorescence of PPIX was observed (DP – 1.35 ± 0.32 conventional units) compared with the fluorescence observed with the use of 5-ALA in the form of 3% solution, and its uneven synthesis. The use of 5-ALA in the form of a 0.01% solution did not induce synthesis of endogenous PPIX in normal rabbit bladder epithelium (DP – 0.90 ± 0.03 conventional units), which was comparable with the control group.

Bladder exposure of an aqueous solution of HE 5-ALA for 2 hours at concentrations of 0.2%, 0.01%, 0.002% and 0.001% led to a significant induction of

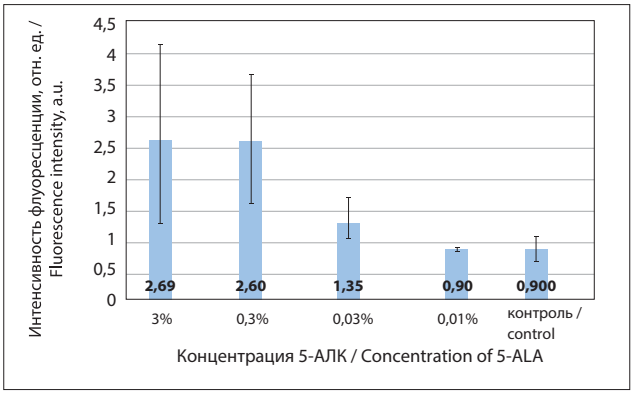

Рис. 1. Интенсивность нормированной флуоресценция ППIX в здоровом эпителии мочевого пузыря кролика после 2-часовой экспозиции растворов 5-АЛК
Fig. 1. PPIX normalized fluorescence intensity in the healthy epithelium of the rabbit bladder after a 2-hour exposure to 5-ALA solutions

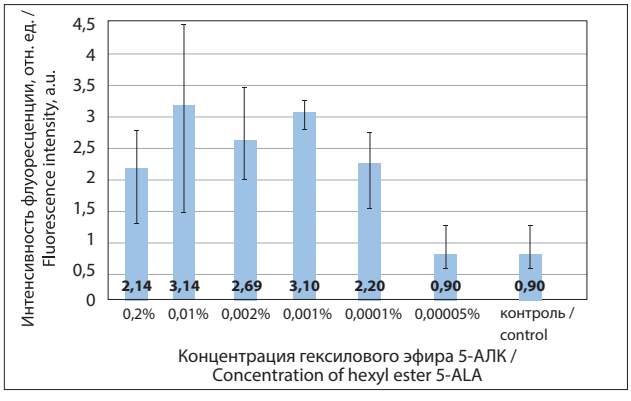

Рис. 2. Интенсивность нормированной флуоресценция ППIX в здоровом эпителии мочевого пузыря кролика после 2-часовой экспозиции растворов ГЭ 5-АЛК
Fig. 2. PPIX normalized fluorescence intensity in the healthy epithelium of the rabbit bladder after a 2-hour exposure to 5-ALA HE solutions

PPIX synthesis (DP – 2.14±0.59 conv. units, 3.14±1.64 conventional units, 2.69±0.78 conventional units and 3.10±0.16 conventional units, respectively). It should be noted that the fluorescence intensity of PPIX when HE 5-ALA solutions were used at concentrations of up to 0.001% was the same as when using a 0.3% 5-ALA solution. When the concentration of HE 5-ALA solution of the preparation was reduced to 0.0001%, a slight decrease (in the form of a trend, statistically unreliable) of the intensity of the specific fluorescence of fluorochrome to 2.20 ± 0.60 conventional units was observed. The introduction of a 0.00005% solution of HE 5-ALA did not induce endogenous PPIX synthesis in normal rabbit bladder epithelium (DP – 0.90 ± 0.03 conventional units), which was comparable with the control group.

Conclusion

A comparative analysis of the fluorescence level of PPIX after the introduction of 5-ALA and its hexyl ether, depending on the concentration of the injected solutions, showed a significantly higher efficiency of HE 5-ALA solutions. Upon instillation of a 0.0001% solution of HE 5-ALA solutions in a rabbit bladder, the fluorescence intensity (DP – 2.20 ± 0.60 conventional units) was comparable with the same indicator upon instillation of a 0.3% 5-ALA solution (DP – 2.60±1.02 conventional units) in a bladder. Thus, a comparison of the average fluorescence intensity data indicates that HE 5-ALA better induces and promotes the accumulation of PPIX in rabbit bladder epithelium at lower concentrations than 5-ALA.

REFERENCES

1. Sokolov V.V., Chissov V.I., Filonenko E.V., Yakubovskaya R.I., Lukyanets E.A., Vorozhtsov G.N., Kuzmin S.G. Fluorescent diagnostics and photodynamic therapy with photosens and alasens: the experience of 11-year clinical use, *Rossiiskii bioterapevticheskii zhurnal*, 2006, Vol. 5, No. 1, pp. 32–33. (in Russian)
2. Fotinos N., Campo M.A., Popowycz F., Gurny R., Lange N. 5-Aminolevulinic acid derivatives in photomedicine: Characteristics, application and perspectives, *Photochem Photobiol*, 2006, Vol. 82, No. 4, pp. 994–1015.
3. Sokolov V.V., Filonenko E.V., Telegina L.V., Bulgakova N.N., Smirnov V.V. Combination of fluorescence imaging and local spectrophotometry in fluorescence diagnostics of early larynx and bronchial cancer, *Kvantovaya elektronika*, 2002, Vol. 32, No. 11, pp. 963–969. (in Russian)
4. Kelly J.F., Snell M.E. Hematoporphyrin derivate: a possible aid in diagosis and therapy of carcinoma of the bladder, *J. Urol.*, 1976, Vol. 115, pp. 150–151.
5. Geavlete B., Mulţescu R., Georgescu D., Geavlete P. Hexvix induced fluorescence blue light cystoscopy – a new perspective in superficial bladder tumors diagnosis, *Chirurgia (Bucur)*, 2008, Vol. 103(5), pp. 559–564.
6. Stepp H., Baumgartner R., Beyer W., et al. Fluorescence imaging and spectroscopy of ALA-induced protoporphyrin IX preferentially accumulated in tumor tissue, *Proc. SPIE,* 1995, Vol. 2627, pp. 13–24.
7. Kennedy J.C., Pottier R.H. Endogenous protoporhyrin IX, a clinically useful photosensitizer for photodynamic therapy (review), *Photohem. Photobiol.*, 1994, No. 4, pp. 275–292.
8. Filonenko E.V., Grishaeva A.B. Methodological aspects of malignant tumors fluorescent diagnostics with alasens, *Ros. onkol. zhurn.*, 2011, No. 5, pp. 30–33. (in Russian)
9. Schmidbauer J., Witjes F., Schmeller N., et al. Improved detection of urothelial carcinoma in situ with hexaminolevulinate fluorescence cystoscopy, *J. Urol.*, 2004, Vol. 171, pp. 135–138.
10. Pankratov A.A., Venediktova Yu.B., Andreeva T.A., Yakubovskaya R.I., Rayhlin N.T. Experimental estimation of the hexasens general toxic properties, *Ros. onkol. zhurn.*, 2010, No. 3, pp. 19–21. (in Russian)

ЛИТЕРАТУРА

1. Соколов В.В., Чиссов В.И., Филоненко Е.В. и др. Флюоресцентная диагностика и фотодинамическая терапия с препаратами фотосенс и аласенс: опыт 11-летнего клинического применения // Российский биотерапевтический журнал. – 2006. – Т. 5, № 1. – С. 32–33.
2. Fotinos N., Campo M.A., Popowycz F., et al. 5-Aminolevulinic acid derivatives in photomedicine: Characteristics, application and perspectives // Photochem Photobiol. – 2006. – Vol. 82, No. 4. – P. 994–1015.
3. Соколов В.В., Филоненко Е.В., Телегина Л.В. и др. Комбинация флуоресцентного изображения и локальной спектрофотометрии при флуоресцентной диагностике раннего рака гортани и бронхов // Квантовая электроника. – 2002. – Т. 32, № 11. – С. 963–969.
4. Kelly J.F., Snell M.E. Hematoporphyrin derivate: a possible aid in diagosis and therapy of carcinoma of the bladder // J. Urol. – 1976. – Vol. 115. – P. 150–151.
5. Geavlete B., Mulţescu R., Georgescu D., Geavlete P. Hexvix induced fluorescence blue light cystoscopy – a new perspective in superficial bladder tumors diagnosis // Chirurgia (Bucur). – 2008 – Vol. 103(5). – P. 559–564.
6. Stepp H., Baumgartner R., Beyer W., et al. Fluorescence imaging and spectroscopy of ALA-induced protoporphyrin IX preferentially accumulated in tumor tissue // Proc. SPIE. – 1995. – Vol. 2627. – P. 13–24.
7. Kennedy J.C., Pottier R.H. Endogenous protoporhyrin IX, a clinically useful photosensitizer for photodynamic therapy (review) // Photohem. Photobiol. – 1994. – No. 4. – P. 275–292.
8. Филоненко Е.В., Гришаева А.Б. Методологические аспекты флюоресцентной диагностики злокачественных опухолей с препаратом аласенс // Рос. онкол. журн. – 2011. – № 5. – С. 30–33.
9. Schmidbauer J., Witjes F., Schmeller N., et al. Improved detection of urothelial carcinoma in situ with hexaminolevulinate fluorescence cystoscopy // J. Urol. – 2004. – Vol. 171. – P. 135–138.
10. Панкратов А.А., Венедиктова Ю.Б., Андреева Т.А. и др. Оценка общетоксических свойств препарата гексасенс в эксперименте // Российский онкологический журнал. – 2010. – № 3. – С. 19–21.

NEW APPROACHES TO SELECTIVE LASER TRABECULOPLASTY

Petrov S.Yu., Poleva R.P.
Scientific Research Institute of Eye Diseases, Moscow, Russia

Abstract

Selective laser trabeculoplasty (SLT) is the "golden standard" of laser glaucoma surgery. Its efficacy can be compared to pharmacological therapy, while in some cases its advantages may even lead to a more stable hypotensive effect. SLT may be used as a primary treatment for primary open-angle glaucoma patients and patients with ocular hypertension, while also considered safe and effective in cases when a repeat procedure is required. SLT may potentially decrease the demand for antiglaucoma drugs, improve patient's response to treatment, make the treatment more comfortable and overall increase the patient's quality of life. New modifications of standard laser treatment procedures have been emerging lately. This article summarizes scientific data on the efficacy and safety of the new generation of laser trabeculoplasty. It specifies the charateristics of micropulse laser trabeculoplasty (MLT), pattern-scanning laser trabeculoplasty (PLT) and titanium-sapphire laser trabeculoplasty (TSLT) and recounts the latest research dedicated to them.

Keywords: glaucoma, selective laser trabeculoplasty, micropulse laser trabeculoplasty, pattern-scanning trabeculoplasty, titanium-sapphire laser trabeculoplasty.

For citations: Petrov S.Yu., Poleva R.P. New approaches to selective laser trabeculoplasty, *Biomedical photonics,* 2018, T. 7, No. 3, pp. 47-56 (in Russian). doi: 10.24931/2413–9432–2018–7–3–47–56.

Contacts: Petrov S.Yu., e-mail: glaucomatosis@gmail.com

НОВЫЕ ПОДХОДЫ К СЕЛЕКТИВНОЙ ЛАЗЕРНОЙ ТРАБЕКУЛОПЛАСТИКЕ

С.Ю. Петров, Р.П. Полева
Научно-исследовательский институт глазных болезней, Москва, Россия

Резюме

Селективная лазерная трабекулопластика (СЛТ) является «золотым стандартом» лазерной хирургии глаукомы. Её эффективность сопоставима с медикаментозной терапией; в отдельных случаях она обладает рядом преимуществ, способствующих созданию более стойкого гипотензивного эффекта, и может рассматриваться в качестве стартовой терапии первичной открытоугольной глаукомы и офтальмогипертензии. СЛТ безопасна и эффективна при повторном проведении процедуры. Потенциально СЛТ способна снизить потребность в антиглаукомных препаратах, повысить приверженность лечению и сделать его более комфортным, что в конечном итоге может улучшить качество жизни. В последние годы завоевывают популярность новые модификации стандартных лазерных технологий. В приводимом ниже обзоре суммированы данные научной литературы о безопасности и эффективности лазерной трабекулопластики нового поколения. Приведены характеристики микроимпульсной лазерной трабекулопластики, паттерн-сканирующей лазерной трабекулопластики и титан-сапфировой лазерной трабекулопластики и описаны посвященные им исследования последних лет.

Ключевые слова: глаукома, селективная лазерная трабекулопластика, микроимпульсная лазерная трабекулопластика, паттерн-сканирующая лазерная трабекулопластика, титан-сапфировая лазерная трабекулопластика.

Для цитирования: Петров С.Ю., Полева Р.П. Новые подходы к селективной лазерной трабекулопластике // Biomedical photonics. – 2018. – Т. 7, № 3. – С. 47-56. doi: 10.24931/2413–9432–2018–7–3–47–56.

Контакты: Петров С.Ю., e-mail: glaucomatosis@gmail.com

Introduction

The widespread use of laser technology in the surgical treatment of glaucoma to reduce intraocular pressure began in the 1970s, with argon laser trabeculoplasty (ALT). The efficacy and safety of ALT was demonstrated during a large multicenter prospective clinical study on the use of lasers for the treatment of glaucoma (Glau-

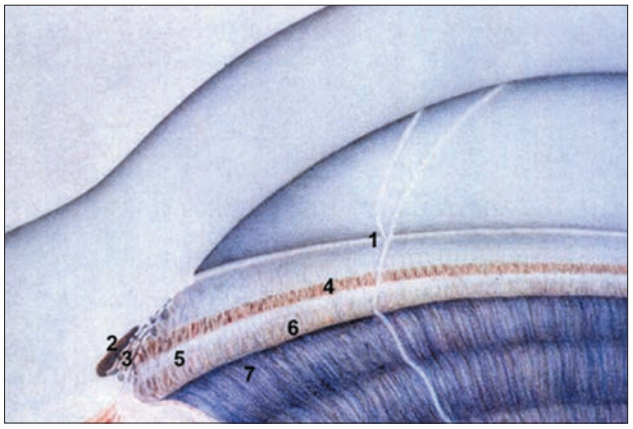

Рис. 1. Строение угла передней камеры глаза:
1 – переднее пограничное кольцо Швальбе, 2 – вырезка, 3 – трабекула, 4 – Шлеммов канал, 5 – склеральная шпора, 6 – цилиарное тело, 7 – периферия корня радужки
Fig. 1. Anterior chamber angle anatomy:
1 – anterior Schwalbe's annular line, 2 – incisura, 3 – trabecular meshwork, 4 – Schlemm's canal, 5 – scleral spur, 6 – ciliary body, 7 – peripheral part of the iris root

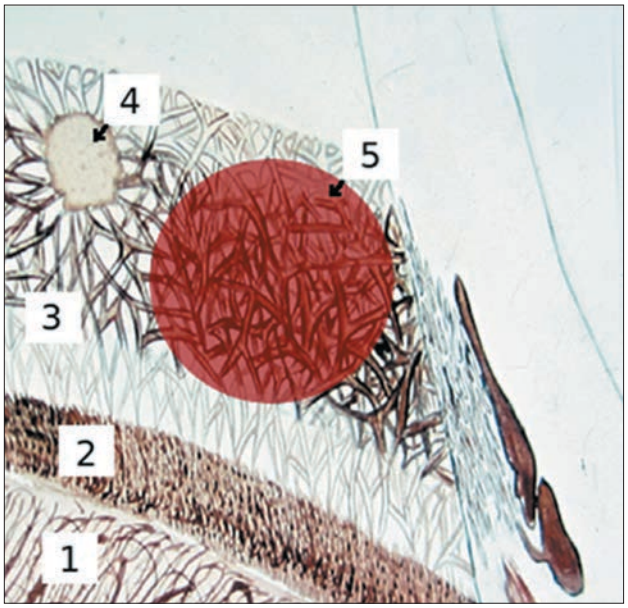

Рис. 2. Схема нанесения лазерных коагулятов при трабекулопластике:
1 – радужка, 2 – цилиарное тело, 3 – трабекулярная сеть, 4 – лазеркоагулят после аргон-лазерной трабекулопластики (коагулирующее поражение трабекулы после термического ожога), 5 – воздействие при СЛТ (селективное воздействие на пигментированные меланинсодержащие клетки без последующих дефектов трабекулы)
Fig. 2. Scheme of applying laser coagulation in trabeculoplasty:
1 – iris, 2 – ciliary body, 3 – trabecular meshwork, 4 – laser burn after ALT (trabecular coagulation defect after the thermic burn), 5 – SLT laser exposure zone (selective action on the melaniferous cells without any subsequent visual or structural damage)

coma Laser Trial) [1], and ALT remained the method of choice for open-angle glaucoma for a long time [2, 3].

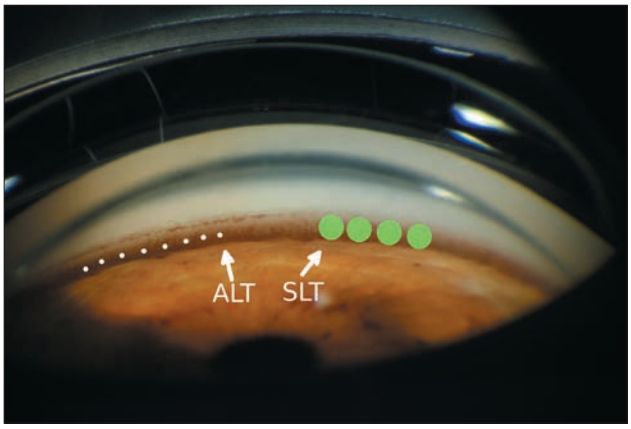

Рис. 3. Сравнение размеров светового пятна при АЛТ и СЛТ
Fig. 3. Comparison of the ALT and SLT light spot sizes

However, despite the positive results of studies, this technique has not replaced the instillation of antihypertensive drugs as a starting treatment for primary open-angle glaucoma (POAG), which was associated with the emergence of more modern and effective means of drug therapy and with a number of shortcomings of ALT itself. Interest in laser treatment has increased again in recent years with the advent of new techniques that do not have the disadvantages of ALT, such as selective laser trabeculoplasty (SLT) [4]. With the same hypotensive effect of SLT at 360° and ALT at 180°, SLT only minimally injures endothelial cells and leaves the trabecular meshwork intact, which, in turn, leads to less severe inflammation in the anterior chamber after the procedure, while ALT in some cases can lead to the formation of peripheral anterior synechia and scarring of the trabecular meshwork [5–7]. The schemes showing the location of the eye angle structures, the application of laser coagulates during trabeculoplasty and a comparison of the sizes of the light spot are provided in Fig. 1, 2 and 3, respectively.

With efficacy similar to that of drug therapy and SLT [8–11], laser intervention has several advantages, such as the absence of problems associated with adherence to treatment or being unable to purchase drugs in a timely manner, and thus contributes to a more stable hypotensive effect. Moreover, in recent years, SLT is often considered as the first line of treatment for POAG and ophthalmic hypertension [12-14]. The comparability of the results of the use of drug and laser techniques has been repeatedly proven in studies such as the Glaucoma Laser Trial and Ocular Hypertension Treatment Study, as well as in numerous research papers by a number of foreign and

Russian scientists. Moreover, in the studies of J. Tsai and R. Lee, laser trabeculoplasty made it possible to achieve a more stable decrease in intraocular pressure (IOP) [10, 15].

Despite somewhat limited data regarding repeated SLT with a decrease in the antihypertensive effect in the long term, it is believed that the procedure can be repeated annually, being a safe and effective option for maintenance therapy [16–18]. Potentially, SLT can reduce the need for anti-glaucoma drugs, increase treatment adherence and make it more comfortable, which can ultimately improve the quality of life. In recent years, a wide variety of studies have been conducted on the safety and efficacy of SLT in various types of glaucoma in order to study the possible ways of using the treatment with the most beneficial effect by optimizing the level of laser energy, identifying prognostic factors for a successful outcome, determining the nature of the correlation of IOP if the procedure is performed in both eyes and assessment of the impact on other glaucoma progress risk factors (for example, IOP fluctuations) [19–28].

The introduction of minimally invasive glaucoma surgery into clinical practice has not led to a gradual decrease in the frequency of trabeculoplasty. Although the indications for these procedures are partially the same, laser trabeculoplasty has several advantages: it is less invasive, being an extraocular manipulation, is not combined with cataract extraction and is a cheaper treatment option. Trabeculoplasty still plays an important role in various glaucoma treatment strategies, and thanks to the achievements of modern science, its efficacy and safety continue to grow.

New generation laser trabeculoplasty procedures that help reduce IOP and drug demand include micropulse laser trabeculoplasty (MLT), pattern-scanning laser trabeculoplasty (PLT), and titanium-sapphire laser trabeculoplasty (TSLT). The review below summarizes the scientific literature data on the safety and efficacy of new generation laser trabeculoplasty.

Micropulse laser trabeculoplasty

The technology of micropulse laser trabeculoplasty (MLT) involves the supply of energy in the form of repeating subthreshold micropulses with interruptions between them. Such a scheme can reduce the accumulation of thermal energy, control the temperature increase and avoid cicatricial damage to eye tissue [29, 30]. The effect from the use of a new generation of laser trabeculoplasty is generated due to stimulation of the cell biochemical cascade mediated by cytokines, which ultimately helps to increase the aqueous outflow with less tissue damage [31]. According to scanning electron microscopy, MLT does not cause coagulation damage to the trabecular meshwork [32], which is the advantage of MLT compared to continuous-wave laser technologies such as ALT, which lead to mechanical damage and scarring of trabecular structures [33]. Moreover, despite the fact that SLT also does not lead to scarring, it is still inferior to MLT in terms of safety, since the latter does not damage pigment cells of the trabecular meshwork [34].

For MLT, there is no mandatory endpoint for treatment in the form of tissue blanching at the site of exposure or the formation of a gas-vapor bubble in the trabecula structure. Since the inflammatory process is minimal or absent, anti-inflammatory drugs after MLT are not necessary [35].

The advantages of MLT over SLT are especially pronounced in patients with an increased risk of IOP elevation after the laser procedure, in particular, those with pronounced pigmentation of the trabecular meshwork. In the first studies, MLT showed promising results for open-angle glaucoma. It is rightfully suggested that, based on the results of large-scale multicenter studies currently being conducted, MLT will prove to be just as effective as SLT, but safer [35–36].

MLT is normally performed with the following laser settings: spot diameter: 300 μm (with SLT, spot diameter is 400 μm), exposure: 300 ms, power: 1000 mW, fill factor: 15%. The fill factor is a value that characterizes the degree of laser use in the treatment process. N.M. Radcliffe recommends application of 100 individual coagulates around the circumference (360°), while I.K. Ahmed suggests making them confluent [37, 38]. Like other types of laser trabeculoplasty, MLT requires only local anesthesia. If the patient experiences pain during the procedure, the laser energy is gradually reduced.

The efficacy of MLT is confirmed by the results of various studies. In a study by A. M. Fea et al. with the involvement of 20 patients, the application of confluent coagulates was carried out with a subthreshold micropulse laser exposure (laser wavelength: 810 nm) in the lower segment of the trabecular meshwork anterior section at 180°. The laser characteristics were the following: spot diameter 200 μm, power 2000 mW, exposure 200 ms, fill factor: 15%, number of cauterizations: 70–84. In 15 patients (75%), MLT was successful, as within 12 months the IOP level decreased by about 20%. In 5 cases (25%),

MLT was found to be unsuccessful, in 4 patients during the first week and in 1 patient within 6 months [39].

D. Gossage et al. presented biennial results of MLT (wavelength 532 nm) performed on 18 eyes with POAG. The laser power was 300 mW, 700 mW and 1000 mW. In the group which had MLT, conducted with laser power of 1000 mW, the results were statistically significantly better: after 24 months, the IOP decreased by 24% [40].

According to preliminary data obtained by P. Coombs in his comparison of MLT and SLT, the efficacy of the techniques is similar. In 12 eyes, MLT was performed, and SLT in 14 eyes. In both groups, a significant decrease in IOP was observed, by an average of 3.9 mm Hg and 2.6 mm Hg, respectively. After MLT, the need for medications decreased slightly more than after SLT (by 0.6 and 0.1, respectively) [41].

In Abuja, a study of E. Olufemi was held, which involved 34 cycles of laser therapy performed on 30 eyes of 16 patients. The main selection criterion was failure to compensate IOP with maximum antihypertensive therapy. One hour after the completion of the procedure, the IOP decreased by an average of 3.2 mm Hg. and subsequently remained at a steady level reliably decreased by 17.2% compared to the base level of IOP [42].

There are also reports in the literature about the efficacy of MLT performed after SLT [43].

During a short-term prospective controlled pilot study D. Ingvoldstad compared the efficacy and safety of MLT and ALT performed after randomization in 21 eyes. MLT was performed with the following laser settings: spot diameter 300 μm, power 2000 mW, fill factor; 15%, number of cauterizations: 66 (applied at 180° from the nasal side). After 3 months, the IOP in both groups decreased by 20%, there were no statistically significant differences between the groups. Pain during the procedure and the inflammatory process in the postoperative period (cell suspension or opalescence of the anterior chamber moisture) are expressed insignificantly, and it was noted that after MLT these phenomena were much less common [44].

A study by E. Rantala suggests that 180° MLT may not be effective in open-angle glaucoma. According to the data obtained in this retrospective study, a decrease in IOP by ≥20% was observed only in 1 out of 40 cases (2.5%), and over the 19 months of observation IOP decreased by ≥ 3 mm Hg only in 3 people (7.5%). The final conclusion about the lack of effect from MLT was made after approximately 3 months. In the sample described, the initial mean IOP level was relatively low (21.8 ± 4.9 mm Hg, with the range of 14–34 mm Hg), with patients using an average of 2.0 ± 1.3 drugs. MLT was performed with the following laser settings: spot diameter 300 μm, power 2000 mW, exposure 200 ms, fill factor: 15%, number of cauterizations: 60–66 (applied at 180°) [45].

In general, researchers agree on the safety of MLT in patients with open-angle glaucoma. A. M. Fea et al. report an increase in IOP and opalescence of moisture in the anterior chamber after MLT for pigmented glaucoma; IOP levels returned to normal after 3 days with the use of systemic drugs. MLT is well tolerated, with the exception of a burning or heating sensation during the procedure, which was experienced by 4 patients (20% of cases) [39]. No data is found in the scientific literature in respect of late postoperative complications of MLT.

Pattern-scanning laser trabeculoplasty

The process of pattern-scanning laser trabeculoplasty (PLT) involves applying laser coagulates to the trabecular meshwork according to a predefined pattern under computer control. Today, PLT is most commonly used for massive laser fundus interventions, such as pan-retinal laser coagulation (PRLC). In recent years, its use in the treatment of patients with POAG has also become popular, since the complete treatment of the trabecular meshwork with the calculated alignment of each pattern and automated rotation makes it possible to avoid both overlapping of coagulates and the formation of excessively wide gaps between them [46]. It is suggested that the cellular response to PLT is accompanied by less severe scarring and coagulation damage. With PLT, the pulse duration is much shorter compared to ALT, which reduces the degree of thermal damage. The efficacy of the procedure is due to the fact that approximately 10 times more laser coagulates are applied to the area of the trabecular meshwork [47].

PASCAL semi-automated pattern-scanning system (Optimedica Corp, USA) is based on a doubled frequency Nd-YAG laser (continuous exposure to a green beam with a wavelength of 532 nm or a yellow beam with a wavelength of 577 nm). The spot diameter is 100 μm, the exposure is 5–10 ms, and the power is calibrated until at 10 ms trabecular meshwork blanching occurs in the lower segment of the eye, where the laser permeability is the highest. Tissue blanching occurs within 10 ms at a power level of less than 1 W. The exposure time is then reduced

to 5ms, so sub-visible treatment spots are produced. Next, a computer-controlled pattern scanning algorithm is used. Each pattern includes two or three rows (24–66 coagulates) of arcuate coagulates and has a length of 22.5°. After the pattern is completed, the beam automatically rotates by 22.5°. 8 adjacent coagulation segments correspond to 180° of the trabecular meshwork, and 16 segments correspond to 360° [48].

In a prospective pilot study conducted by M. Turati, 360° PLT (16 segments, wavelength 532 nm) was performed in 47 eyes of 25 patients. During the 6 months of observation, the mean IOP decreased from 21.9±4.1 to 15.5±2.7 mm Hg. However, 17 eyes were excluded from the study due to the development of viral conjunctivitis or the need for additional anti-glaucoma therapy in connection with an increase in IOP after the treatment. In 20 of 30 eyes (67%), the average IOP level decreased by 24% [49].

The results of several studies have been published, in which the efficacy of ALT and PLT is compared. According to a retrospective study by C. Barbu, after a PLT performed in 20 eyes of 20 patients, over 8 weeks, the average IOP decreased from 20.2±1.1 to 15.6±0.8 mm Hg ($p < 0.001$). There was no statistically significant difference between the results of PLT and ALT ($p = 0.26$) [46]. According to the study by J. Kim, after 6 months, PLT reduces the mean IOP by 27.1%, from 24.1 ± 4.2 to 17.6 ± 2.6 mm Hg. ($p = 0.03$). There was no statistically significant difference found between the results of PLT and ALT [50]. A study by K. Mansouri and T. Shaarawy, performed on 58 eyes with primary and secondary glaucoma, showed similar efficacy and safety profiles of PLT and SLT with a slightly more pronounced antihypertensive effect of PLT 1 month and 3 months after the treatment, as well as with better tolerability of the PLT procedure by patients [51].

T. Turati et al., it was been demonstrated that PLT did not lead to IOP increase or inflammation [49]. The results of a retrospective study of a series of clinical cases (9 patients, 11 eyes) show that IOP decreased by 31% within 6 months after PMT (wavelength 577 nm). There was no statistically significant difference between the number of drugs used before and after the procedure (2.6 and 2.8, respectively). In one case, there was a transient rise in IOP after the performance of PLT. No cases of the formation of peripheral anterior synechia or damage to the corneal endothelium have been reported [47].

Thus, PLT is an effective method of reducing IOP. The positive results of the first studies will give rise to larger-scale controlled studies of its safety, efficacy and the long-term stability of the antihypertensive effect.

Titanium-sapphire laser trabeculoplasty

The advantage of TSLT is a deeper (about 200 μm) penetration of laser radiation due to the wavelength used (790 nm, i. e., a spectrum close to infrared radiation), while the energy comes in the form of pulses with a duration of 5 to 10 ms . Such characteristics make it possible to reach the juxtacanalicular meshwork and the inner wall of the Schlemm's canal. Then, the laser is selectively absorbed by pigmented phagocytic cells, which protects the trabecular meshwork from damage [52].

The laser beam is focused on the pigmented trabecular meshwork and produces 50 separate (not overlapping) coagulates at 180° on the meshwork. The diameter of the spot at a depth of 200 μm is smaller than in the case of SLT or MLT. The laser energy is 50 mJ, but, if necessary, it can be reduced to 30 mJ. The treatment endpoint of treatment is the formation of mini-bubbles or a visible burn of the pigment of the trabecular meshwork [52, 53].

In 2009, M. Goldenfeld et al. published the data obtained during the pilot study lasting 15 months, which was aimed at comparing the efficacy of TSLT and ALT. It was shown that after TSLT, the IOP level decreases on average by 8 mm Hg. (32%), and after ALT, by 6.5 mm Hg (25%). No statistically significant difference between the groups wqas found. The number of drugs used after trabeculoplasty decreased, albeit not significantly (from 1.4 ± 1.0 to 1.3 ± 1.0 in the TSLT group and from 2.1 ± 0.8 to 2.0 ± 0.8 in the ALT group) [52].

An increase in IOP after TSLT was observed in one patient. No cases of the formation of peripheral anterior synechia in the postoperative period are reported. No long-term complications (within 2 years after TSLT) were recorded [53, 54].

The results of histological studies of G. Simon on donor eyes indicate insignificant anatomical changes in the trabecular meshwork due to laser exposure when thermal damage is excluded, which suggests the possibility of multiple repeated TSLT procedures if the hypotensive effect decreases [55].

Since TSLT is a relatively new technology, only limited amount of information can be found in its respect

Таблица
Сравнение характеристик модификаций лазерной трабекулопластики
Table
Comparison of the characteristics of laser trabeculoplasty modifications

	АЛТ ALT	СЛТ SLT	МЛТ MLT	ПЛТ PLT	ТСЛТ TSLT
Длина волны **Wavelength**	488–512 нм 488–512 nm	532 нм 532 nm	532, 577 или 810 нм 532, 577 or 810 nm	532 или 577 нм 532 or 577 nm	790 нм 790 nm
Продолжительность импульса **Pulse duration**	0,1 с 0.1 s	$3x10^{-9}$ с $3x10^{-9}$ s	$200–300x10^{-3}$ с $200–300x10^{-3}$ s	$5–10x10^{-3}$ с $5–10x10^{-3}$ s	$5–10x10^{-3}$ с $5–10x10^{-3}$ s
Мощность импульса (мВт) или количество энергии на 1 импульс (мДж) **Pulse power (mW) or pulse energy (mJ)**	400–1200 мВт 400–1200 mW	0,1–2,0 мДж 0.1–2.0 mJ	1000–2000 мВт 1000–2000 mW	500–1000 мВт 500–1000 mW	30–50 мДж 30–50 mJ
Размер лазеркоагулята **Laser coagulant size**	50 мкм 50 μm	400 мкм 400 μm	200–300 мкм 200–300 μm	100 мкм 100 μm	200 мкм 200 μm
Рекомендуемое количество лазеркоагулятов **Recommended number of laser coagulants**	50–100 равномерно рассредоточенных коагулятов 50–100 uniformly spread coagulants	50 или 100 сливных лазеркоагулятов 50 or 100 merging laser coagulants	60–100 одиночных или сливных коагулятов 60–100 independent or merged coagulants	8 или 16 сегментов 8 or 16 segments	50 граничащих, но не сливающихся коагулятов 50 bordering but not merging coagulants
Величина угла воздействия на трабекулярную сеть **Angle of effect on the trabecular network**	180–360°	180° или 360° 180° or 360°	180° или 360° 180° or 360°	180° или 360° 180° or 360°	180°
Реакция тканей **Tissue reaction**	Очаговая депигментация, возможно образование пузырьков газа («эффект попкорна») Focal depigmentation, possible formation of gas bubbles ("popcorn effect")	Небольшие пузырьки. Мощность воздействия калибруется до появления пузырьков в точке воздействия, затем мощность поступательно снижается с шагом 0,1 мДж до порога отсутствия реакции Small bubbles. The affecting power is calibrated until the appearance of bubbles at the affected point, then the energy is gradually decreased in steps of 0.1 mJ until a threshold of no reaction	Видимая реакция тканей отсутствует No visible tissue reaction	После калибровки мощности видимая реакция тканей отсутствует No visible tissue reaction after power calibration	Образование мини-пузырьков или видимого ожога пигмента трабекулярной сети Formation of mini-bubbles or visible burn of the trabecular network pigment

Реакция/ Осложнения Reaction / Complications	Офтальмогипертензия, воспаление в передней камере, в отдельных случаях возможно повреждение эндотелия, образование периферических передних синехий и рубцевание трабекулярной сети Ocular hypertension, inflammation in the anterior chamber, in some cases, damage to the endothelium, the formation of peripheral anterior synechiae and scarring of the trabecular network	Офтальмогипертензия, воспаление в передней камере Ocular hypertension, inflammation in the anterior chamber	Жжение. Редко – офтальмогипертензия, воспаление в передней камере Burning sensation. Rarely – ocular hypertension, inflammation in the anterior chamber	Возможна транзиторная реактивная офтальмогипертензия Possible transient reactive ocular hypertension	Возможна реактивная офтальмогипертензия Possible reactive ocular hypertension

in the scientific literature, and, therefore, large-scale randomized trials are necessary to make meaningful conclusions about its efficacy and safety, including in the long term.

Conclusion

Selective laser trabeculoplasty once revived the interest in laser methods of treating open-angle glaucoma and today is the gold standard of laser surgery. According to the first studies, the developing new technologies such as MLT, PLT and TSLT reduce the IOP level with comparable efficacy, often have better tolerance and are less likely to provoke complications including postoperative inflammation and IOP increase. A comparison of the characteristics of the listed laser trabeculoplasty modifications is privided in table.

REFERENCES

1. The Glaucoma Laser Trial (GLT) and glaucoma laser trial follow-up study: 7. Results. Glaucoma Laser Trial Research Group, *Am J Ophthalmol*, 1995, Vol. 120, pp. 718–731.
2. Wise J.B., Witter S.L. Argon laser therapy for open-angle glaucoma. A pilot study, *Arch Ophthalmol*, 1979, Vol. 97, pp. 319–322.
3. Ticho U., Zauberman H. Argon laser application to the angle structures in the glaucomas, *Arch Ophthalmol*, 1976, Vol. 94, No 1, pp. 61–64.
4. Latina M.A., Sibayan S.A., Shin D.H., Noecker R.J., Marcellino G. Q-switched 532-nm Nd: YAG laser trabeculoplasty (selective laser trabeculoplasty), a multicenter, pilot, clinical study, *Ophthalmology*, 1998, Vol. 105, No 11, pp. 2082–2090.
5. Odberg T., Sandvik L. The medium and long-term efficacy of primary argon laser trabeculoplasty in avoiding topical medication in open angle glaucoma, *Acta Ophthalmol Scand*, 1999, Vol. 77, No 2, pp. 176–181.
6. Wong M.O., Lee J.W., Choy B.N., Chan J.C., Lai J.S. Systematic review and meta-analysis on the efficacy of selective laser trabeculoplasty in open-angle glaucoma, *Surv Ophthalmol*, 2015, Vol. 60, pp. 36–50.
7. Kramer T.R., Noecker R.J. Comparison of the morphologic changes after selectivelaser trabeculoplasty and argon laser trabeculo-

ЛИТЕРАТУРА

1. The Glaucoma Laser Trial (GLT) and glaucoma laser trial follow-up study: 7. Results. Glaucoma Laser Trial Research Group // Am J Ophthalmol. – 1995. – Vol. 120. – P. 718–731.
2. Wise J.B., Witter S.L. Argon laser therapy for open-angle glaucoma. A pilot study // Arch Ophthalmol. – 1979. – Vol. 97. – P. 319–322.
3. Ticho U., Zauberman H. Argon laser application to the angle structures in the glaucomas // Arch Ophthalmol. – 1976. – Vol. 94, No 1. – P. 61–64.
4. Latina M.A., Sibayan S.A., Shin D.H., et al. Q-switched 532-nm Nd: YAG laser trabeculoplasty (selective laser trabeculoplasty), a multicenter, pilot, clinical study // Ophthalmology. – 1998. – Vol. 105, No 11. – P. 2082–2090.
5. Odberg T., Sandvik L. The medium and long-term efficacy of primary argon laser trabeculoplasty in avoiding topical medication in open angle glaucoma // Acta Ophthalmol Scand. – 1999. – Vol. 77, No 2. – P. 176–181.
6. Wong M.O., Lee J.W., Choy B.N., et al. Systematic review and meta-analysis on the efficacy of selective laser trabeculoplasty in open-angle glaucoma // Surv Ophthalmol. – 2015. – Vol. 60. – P. 36–50.
7. Kramer T.R., Noecker R.J. Comparison of the morphologic changes after selectivelaser trabeculoplasty and argon laser

plasty in human eye bank eyes.*Ophthalmology*, 2001, Vol. 108, pp. 773–779.
8. Katz L.J., Steinmann W.C., Kabir A., Molineaux J., Wizov S.S., Marcellino G. Selective laser trabeculoplasty versus medicaltherapy as initial treatment of glaucoma: a prospective, randomized trial, *J Glaucoma*, 2012, Vol. 21, pp. 460–468.
9. Li X., Wang W., Zhang X. Meta-analysis of selective laser trabeculoplasty versus topical medication in the treatment of open-angle glaucoma, *BMC Ophthalmol*, 2015, Vol. 19, No 15, pp. 107.
10. Lee R., Hutnik C.M. Projected cost comparison of selective laser trabeculoplasty versus glaucoma medication in the Ontario Health Insurance Plan, *Can J Ophthalmol*, 2006, Vol. 41, No 4, pp. 449–456.
11. Lee J.W., Chan C.W., Wong M.O., Chan J.Ch., Li Q., Lai J.S., A randomized control trial to evaluate the effect of adjuvant selective laser trabeculoplasty versus medication alone in primary open-angle glaucoma, preliminary results, *Clin Ophthalmol*, 2014, No 8, pp. 1987–1992.
12. Melamed S., Ben Simon G.J., Levkovitch-Verbin H. Selective laser trabeculoplasty asprimary treatment for open-angle glaucoma: a prospective, nonrandomized pilotstudy. *Arch Ophthalmol,* 2003, Vol. 121, pp. 957–960.
13. Kadasi L.M., Wagdi S., Miller K.V. Selective Laser Trabeculoplasty as Primary Treatment for Open-Angle Glaucoma, *R I Med J*, 2016, Vol. 99, No 6, pp. 22–25.
14. Waisbourd M., Katz L.J. Selective laser trabeculoplasty as a first-line therapy: a review, *Can J Ophthalmol*, 2014, Vol. 49, No 6, pp. 519–522.
15. Tsai J.C. Medication adherence in glaucoma, approaches for optimizing patient compliance, *Curr Opin Ophthalmol*, 2006, Vol. 17, pp. 190–195.
16. Francis B.A., Loewen N., Hong B., Dustin L., Kaplowitz K., Kinast R., Bacharach J., Radhakrishnan S., Iwach A., Rudavska L., Ichhpujani P., Katz L.J. Repeatability of selective laser trabeculoplasty for open-angle glaucoma, *BMC Ophthalmol*, 2016, Vol. 16, pp. 128.
17. Hong B.K., Winer J.C., Martone J.F., Wand M., Altman B., Shields B. Repeat selective laser trabeculoplasty, *J Glaucoma*, 2009, Vol. 18, pp. 180–183.
18. Durr G.M., Harasymowycz P. The effect of repeat 360-degree selective laser trabeculoplasty on intraocular pressure control in open-angle glaucoma, *J Fr Ophtalmol*, 2016, Vol. 39, No 3, pp. 261–264.
19. Mao A.J., Pan X.J., McIlraith I., Strasfeld M., Colev G., Hutnik C. Development of a prediction rule to estimate the probability of acceptable intraocular pressure reduction after selective laser trabeculoplasty in open-angle glaucoma and ocular hypertension, *J Glaucoma*, 2008, Vol. 17, pp. 449–454.
20. Lee J.W., Liu C.C., Chan J.C., Lai J.S. Predictors of success in selective laser trabeculoplasty for normal tension glaucoma, *Medicine*, 2014, Vol. 93, pp. 236.
21. Lee J.W., Wong M.O., Liu C.C., Lai J.S. Optimal selective laser trabeculoplasty energy for maximal intraocular pressure reduction in open-angle glaucoma, *J Glaucoma*, 2015, Vol. 24, pp. 128–131.
22. Abdelrahman A.M. Noninvasive Glaucoma Procedures, Current Options and Future Innovations, *Middle East Afr J Ophthalmol*, 2015, Vol. 22, No 1, pp. 2–9.
23. Hongyang Z., Yangfan Y., Jiangang X., Minbin Y. Selective laser trabeculoplasty in treating post-trabeculectomy advanced primary open-angle glaucoma, *Exp Ther Med*, 2016, Vol. 11, No 3, pp. 1090–1094.
24. Day D.G., Sharpe E.D., Atkinson M.J, Stewart J.A., Stewart W.C. The clinical validity of the treatment satisfaction survey for intraocular pressure in ocular hypertensive and glaucoma patients, *Eye (Lond)*, 2006, Vol. 20, No 5, pp. 583–590.
25. Ting N.S., Li Yim J.F., Ng J.Y. Different strategies and cost-effectiveness in the treatment of primary open angle glaucoma. *Clinicoecon Outcomes Res*. 2014, Vol. 6, pp. 523–530.

trabeculoplasty in human eye bank eyes // Ophthalmology. – 2001. – Vol. 108. – P. 773–779.
8. Katz L.J., Steinmann W.C., Kabir A., et al. Selective laser trabeculoplasty versus medicaltherapy as initial treatment of glaucoma: a prospective, randomized trial // J Glaucoma. – 2012. – Vol. 21. – P. 460–468.
9. Li X., Wang W., Zhang X. Meta-analysis of selective laser trabeculoplasty versus topical medication in the treatment of open-angle glaucoma // BMC Ophthalmol. – 2015. – Vol. 19, No 15. – P. 107.
10. Lee R., Hutnik C.M. Projected cost comparison of selective laser trabeculoplasty versus glaucoma medication in the Ontario Health Insurance Plan // Can J Ophthalmol. – 2006. – Vol. 41, No 4. – P. 449–456.
11. Lee J.W., Chan C.W., Wong M.O., et al. A randomized control trial to evaluate the effect of adjuvant selective laser trabeculoplasty versus medication alone in primary open-angle glaucoma, preliminary results // Clin Ophthalmol. – 2014. – No 8. – P. 1987–1992.
12. Melamed S., Ben Simon G.J., Levkovitch-Verbin H. Selective laser trabeculoplasty asprimary treatment for open-angle glaucoma: a prospective, nonrandomized pilotstudy // Arch Ophthalmol. – 2003. – Vol. 121. – P. 957–960.
13. Kadasi L.M., Wagdi S., Miller K.V. Selective Laser Trabeculoplasty as Primary Treatment for Open-Angle Glaucoma // R I Med J. – 2016. – Vol. 99, No 6. – P. 22–25.
14. Waisbourd M., Katz L.J. Selective laser trabeculoplasty as a first-line therapy: a review // Can J Ophthalmol. – 2014. – Vol. 49, No 6. – P. 519–522.
15. Tsai J.C. Medication adherence in glaucoma, approaches for optimizing patient compliance // Curr Opin Ophthalmol. – 2006. – Vol. 17. – P. 190–195.
16. Francis B.A., Loewen N., Hong B., et al. Repeatability of selective laser trabeculoplasty for open-angle glaucoma // BMC Ophthalmol. – 2016. – Vol. 16. – P. 128.
17. Hong B.K., Winer J.C., Martone J.F., et al. Repeat selective laser trabeculoplasty // J Glaucoma. – 2009. – Vol. 18. – P. 180–183.
18. Durr G.M., Harasymowycz P. The effect of repeat 360-degree selective laser trabeculoplasty on intraocular pressure control in open-angle glaucoma // J Fr Ophtalmol. – 2016. – Vol. 39, No 3. – P. 261–264.
19. Mao A.J., Pan X.J., McIlraith I., et al. Development of a prediction rule to estimate the probability of acceptable intraocular pressure reduction after selective laser trabeculoplasty in open-angle glaucoma and ocular hypertension // J Glaucoma. – 2008. – Vol. 17. – P. 449–454.
20. Lee J.W., Liu C.C., Chan J.C., Lai J.S. Predictors of success in selective laser trabeculoplasty for normal tension glaucoma // Medicine. – 2014. – Vol. 93. – P. 236.
21. Lee J.W., Wong M.O., Liu C.C., Lai J.S. Optimal selective laser trabeculoplasty energy for maximal intraocular pressure reduction in open-angle glaucoma // J Glaucoma. – 2015. – Vol. 24. – P. 128–131.
22. Abdelrahman A.M. Noninvasive Glaucoma Procedures, Current Options and Future Innovations // Middle East Afr J Ophthalmol. – 2015. – Vol. 22, No 1. – P. 2–9.
23. Hongyang Z., Yangfan Y., Jiangang X., Minbin Y. Selective laser trabeculoplasty in treating post-trabeculectomy advanced primary open-angle glaucoma // Exp Ther Med. – 2016. – Vol. 11, No 3. – P. 1090–1094.
24. Day D.G., Sharpe E.D., Atkinson M.J, et al. The clinical validity of the treatment satisfaction survey for intraocular pressure in ocular hypertensive and glaucoma patients // Eye (Lond). – 2006. – Vol. 20, No 5. – P. 583–590.
25. Ting N.S., Li Yim J.F., Ng J.Y. Different strategies and cost-effectiveness in the treatment of primary open angle glaucoma // Clinicoecon Outcomes Res. – 2014. – Vol. 6. – P. 523–530.

26. Hodge W.G., Damji K.F., Rock W, Buhrmann R., Bovell A.M., Pan Y. Baseline IOP predicts selective laser trabeculoplasty success at 1 year post-treatment: results from a randomised clinical trial, *Br J Ophthalmol*, 2005, Vol. 89, No 9, pp. 1157–1160.
27. Nagar M., Luhishi E., Shah N. Intraocular pressure control and fluctuation: the effect of treatment with selective laser trabeculoplasty, *Br J Ophthalmol*. 2009, Vol. 93, No 4, pp. 497–501.
28. Detorakis E.T., Tsiklis N., Pallikaris I.G., Tsilimbaris M.K. Changes in the intraocular pressure of fellow untreated eyes following uncomplicated trabeculectomy, *Ophthalmic Surg Lasers Imaging*, 2011, Vol. 42, pp. 138–143.
29. Yadav N.K., Jayadev C., Rajendran A., Nagpal M. Recent developments in retinal lasers and delivery systems, *Indian J Ophthalmol*, 2014, Vol. 62, No 1, pp. 50–54.
30. Detry-Morel M., Muschart F., Pourjavan S. Micropulse diode laser (810 nm) versus argon laser trabeculoplasty in the treatment of open-angle glaucoma: comparative short-term safety and efficacy profile, *Bull Soc Belge Ophthalmol*, 2008, Vol. 308, pp. 21–28.
31. Alvarado J.A., Alvarado R.G., Yeh R.F., Franse-Carman L., Marcellino G.R., Brownstein M.J. A new insight into the cellular regulationof aqueous outflow: how trabecular meshwork endothelial cells drive a mechanism that regulates the permeability of Schlemm's canal endothelial cells, *Br J Ophthalmol*, 2005, Vol. 89, pp. 1500–1505.
32. Fudemberg S.J., Myers J.S., Katz L.J. Trabecular meshwork tissue examination withscanning electron microscopy: a comparison of MicroPulse Diode Laser (MLT), Selective Laser (SLT), and Argon Laser (ALT) Trabeculoplasty in Human Cadaver Tissue. *Invest Ophthalmol Vis Sci*, 2008, Vol. 49, pp. 1236.
33. Lotti R., Traverso C.E., Murialdo U., Frau B., Calabria G.A., Zingirian M. Argon laser trabeculoplasty, Long-term results, *Ophthalmic Surg*, 1995, Vol. 26, pp. 127–129.
34. Lee J.W., Yau G.S., Yick D.W., Yuen C.Y. MicroPulse Laser Trabeculoplasty for the Treatment of Open-Angle Glaucoma, *Medicine (Baltimore)*, 2015, Vol. 94(49), e2075.
35. Fea A.M., Bosone A., Rolle T., Brogliatti B., Grignolo F.M. Micropulse diode laser trabeculoplasty (MDLT), A phase II clinical study with 12 months follow-up, *Clin Ophthalmol*, 2008, Vol. 2, No 2, pp. 247–252.
36. Meyer J.J., Lawrence S.D. What's new in laser treatment for glaucoma? *Curr Opin Ophthalmol*, 2012, Vol. 23, No 2, pp. 111–117.
37. Radcliffe N.M. MLT offers safe, well-tolerated approach to lower IOP, reduce need for medication, *Ophthalmology Times*, 2014.
38. Ahmed I.K. Excellent Safety Profile of MicroPulse Laser Trabeculoplasty (MLT) for Glaucoma, *Glaucoma Today*, 2014. Available at: https://iridexsupport.zendesk.com/hc/en-us/articles/203700150-Excellent-Safety-Profile-of-MicroPulse-Laser-Trabeculoplasty-MLT-for-Glaucoma-Iqbal-Ahmed-MD
39. Fea A.M., Bosone A., Rolle T., Brogliatti B., Grignolo F.M. Micropulse diode laser trabeculoplasty (MDLT): A phase II clinical study with 12 months follow-up, *Clin Ophthalmol*, 2008, Vol. 2, 247–252.
40. Gossage D. Two-year data on MicroPulse laser trabeculoplasty, *Eye World*, 2015. Available at: http://www.eyeworld.org/article-two-year-data-on-micropulse-lasertrabeculoplasty (accessed 1 Jun 2015).
41. Coombs P., Radcliffe N.M. Outcomes of Micropulse Laser Trabeculoplasty vs. Selective Laser Trabeculoplasty, *ARVO*, 2014.
42. Olufemi E.B. Micropulse diode laser trabeculoplasty in Nigerian patients, *Clin Ophthalmol*, 2015, Vol. 9, pp. 1347–1351.
43. Tai T. Micropulse Laser Trabeculoplasty After Previous Laser Trabeculoplasty, *Glaucoma Today*, 2014.
44. Ingvoldstad D.D., Krishna R., Willoughby L. Micropulse Diode Laser Trabeculoplasty versus Argon Laser Trabeculoplasty in the treatment of Open Angle Glaucoma, *ARVO*, 2005.
45. Rantala E., Valimaki J. Micropulse diode laser trabeculoplasty – 180-degree treatment, *Acta Ophthalmologica*, 2012, Vol. 90, pp. 441–444.

26. Hodge W.G., Damji K.F., Rock W, et al. Baseline IOP predicts selective laser trabeculoplasty success at 1 year post-treatment: results from a randomised clinical trial // Br J Ophthalmol. – 2005. – Vol. 89, No 9. – P. 1157–1160.
27. Nagar M., Luhishi E., Shah N. Intraocular pressure control and fluctuation: the effect of treatment with selective laser trabeculoplasty // Br J Ophthalmol. – 2009. – Vol. 93, No 4. – P. 497–501.
28. Detorakis E.T., Tsiklis N., Pallikaris I.G., Tsilimbaris M.K. Changes in the intraocular pressure of fellow untreated eyes following uncomplicated trabeculectomy // Ophthalmic Surg Lasers Imaging. – 2011. – Vol. 42. – P. 138–143.
29. Yadav N.K., Jayadev C., Rajendran A., Nagpal M. Recent developments in retinal lasers and delivery systems // Indian J Ophthalmol. – 2014. – Vol. 62, No 1. – P. 50–54.
30. Detry-Morel M., Muschart F., Pourjavan S. Micropulse diode laser (810 nm) versus argon laser trabeculoplasty in the treatment of open-angle glaucoma: comparative short-term safety and efficacy profile // Bull Soc Belge Ophthalmol. – 2008. – Vol. 308. – P. 21–28.
31. Alvarado J.A., Alvarado R.G., Yeh R.F., et al. A new insight into the cellular regulationof aqueous outflow: how trabecular meshwork endothelial cells drive a mechanism that regulates the permeability of Schlemm's canal endothelial cells // Br J Ophthalmol. – 2005. – Vol. 89. – P. 1500–1505.
32. Fudemberg S.J., Myers J.S., Katz L.J. Trabecular meshwork tissue examination withscanning electron microscopy: a comparison of MicroPulse Diode Laser (MLT), Selective Laser (SLT), and Argon Laser (ALT) Trabeculoplasty in Human Cadaver Tissue // Invest Ophthalmol Vis Sci. – 2008. – Vol. 49. – P. 1236.
33. Lotti R., Traverso C.E., Murialdo U. Argon laser trabeculoplasty, Long-term results // Ophthalmic Surg. – 1995. – Vol. 26. – P. 127–129.
34. Lee J.W., Yau G.S., Yick D.W., Yuen C.Y. MicroPulse Laser Trabeculoplasty for the Treatment of Open-Angle Glaucoma // Medicine (Baltimore). – 2015. – Vol. 94(49). – e2075. doi: 10.1097/MD.0000000000002075
35. Fea A.M., Bosone A., Rolle T. Micropulse diode laser trabeculoplasty (MDLT), A phase II clinical study with 12 months follow-up // Clin Ophthalmol. – 2008. – Vol. 2, No 2. – P. 247–252.
36. Meyer J.J., Lawrence S.D. What's new in laser treatment for glaucoma? // Curr Opin Ophthalmol. – 2012. – Vol. 23, No 2. – P. 111–117.
37. Radcliffe N.M. MLT offers safe, well-tolerated approach to lower IOP, reduce need for medication // Ophthalmology Times. – 2014.
38. Ahmed I.K. Excellent Safety Profile of MicroPulse Laser Trabeculoplasty (MLT) for Glaucoma // Glaucoma Today. – 2014. Available at: https://iridexsupport.zendesk.com/hc/en-us/articles/203700150-Excellent-Safety-Profile-of-MicroPulse-Laser-Trabeculoplasty-MLT-for-Glaucoma-Iqbal-Ahmed-MD
39. Fea A.M., Bosone A., Rolle T., et al. Micropulse diode laser trabeculoplasty (MDLT): A phase II clinical study with 12 months follow-up // Clin Ophthalmol. – 2008. – Vol. 2. – P. 247–252.
40. Gossage D. Two-year data on MicroPulse laser trabeculoplasty // Eye World. – 2015. Available at: http://www.eyeworld.org/article-two-year-data-on-micropulse-lasertrabeculoplasty
41. Coombs P., Radcliffe N.M. Outcomes of Micropulse Laser Trabeculoplasty vs. Selective Laser Trabeculoplasty // ARVO. – 2014.
42. Olufemi E.B. Micropulse diode laser trabeculoplasty in Nigerian patients // Clin Ophthalmol. – 2015. – Vol. 9. – P. 1347–1351.
43. Tai T. Micropulse Laser Trabeculoplasty After Previous Laser Trabeculoplasty // Glaucoma Today. – 2014.
44. Ingvoldstad D.D., Krishna R., Willoughby L. Micropulse Diode Laser Trabeculoplasty versus Argon Laser Trabeculoplasty in the treatment of Open Angle Glaucoma // ARVO. – 2005.
45. Rantala E., Valimaki J. Micropulse diode laser trabeculoplasty – 180-degree treatment // Acta Ophthalmologica. – 2012. – Vol. 90. – P. 441–444.

46. Barbu C.E., Rasche W., Wiedemann P., Dawczynski J., Unterlauft J.D. Pattern laser trabeculoplasty and argonlaser trabeculoplasty for treatment of glaucoma, 2014, *Ophthalmologe*, Vol. 111, pp. 948–953.
47. Nozaki M. Pattern scanning laser trabeculoplasty, *Glaucoma Today*, 2014.
48. Nozaki M., Hirahara S., Ogura Y. Patterned Laser Trabeculoplasty with PASCAL streamline 577, *ARVO*, 2013.
49. Turati M., Gil-Carrasco F., Morales A., Quiroz-Mercado H., Andersen D., Marcellino G., Schuele G., Palanker D. Patterned laser trabeculoplasty, *Ophthalmic Surg Lasers Imaging*, 2010, Vol. 41, pp. 538–545.
50. Kim J.M., Cho K.J., Kyung S.E., Chang M.H. Short-term clinical outcomes of lasertrabeculoplasty using a 577-nm wavelength laser, *J Korean Ophthalmol Soc*, 2014, Vol. 55, pp. 563–569.
51. Mansouri K., Shaarawy T. Comparing pattern scanning laser trabeculoplasty to selective laser trabeculoplasty: A randomized controlled trial, *Acta Ophthalmol*, 2017, Vol. 95, No 5, pp. 361–365.
52. Goldenfeld M., Melamed S. Titanium-Sapphire Laser Trabeculoplasty in the Treatment of Open-Angle Glaucoma, *Journal of Current Glaucoma Practice*, 2008, Vol. 2, No 2, pp. 36–40.
53. Goldenfeld M, Melamed S, Simon G, Ben Simon G.J. Titanium, sapphire laser trabeculoplasty versus argon laser trabeculoplasty in patients with open-angle glaucoma, *Ophthalmic Surg Lasers Imaging*, 2009, Vol. 40, pp. 264–269.
54. Garcia-Sanchez J., Garcia-Feijoo J., Saenz-Frances F., Fernandez-Vidal A., Mendez-Hernandez C., Martinez-de-la-Casa J. Titanium Sapphire Laser Trabeculoplasty: Hypotensive Efficacy and Anterior Chamber Inflammation, *Investigative Ophthalmology & Visual Science*, 2007, Vol. 48, pp. 3975
55. Simon G., Lowery J.A. Comparison of three types of lasers in laser trabeculoplasty inhuman donor eyes and clinical study, *ASCRS Symposium*, 2007.

46. Barbu C.E., Rasche W., Wiedemann P. Pattern laser trabeculoplasty and argonlaser trabeculoplasty for treatment of glaucoma // Ophthalmologe. – 2014. – Vol. 111. – P. 948–953.
47. Nozaki M. Pattern scanning laser trabeculoplasty // Glaucoma Today. – 2014.
48. Nozaki M., Hirahara S., Ogura Y. Patterned Laser Trabeculoplasty with PASCAL streamline 577 // ARVO. – 2013.
49. Turati M., Gil-Carrasco F., Morales A., et al. Patterned laser trabeculoplasty // Ophthalmic Surg Lasers Imaging. – 2010. – Vol. 41. – P. 538–545.
50. Kim J.M., Cho K.J., Kyung S.E., Chang M.H. Short-term clinical outcomes of lasertrabeculoplasty using a 577-nm wavelength laser // J Korean Ophthalmol Soc. – 2014. – Vol. 55. – P. 563–569.
51. Mansouri K., Shaarawy T. Comparing pattern scanning laser trabeculoplasty to selective laser trabeculoplasty: A randomized controlled trial // Acta Ophthalmol. – 2017. – Vol. 95, No 5. – P. 361–365.
52. Goldenfeld M., Melamed S. Titanium-Sapphire Laser Trabeculoplasty in the Treatment of Open-Angle Glaucoma // Journal of Current Glaucoma Practice. – 2008. – Vol. 2, No 2. – P. 36–40.
53. Goldenfeld M., Melamed S., Simon G., Ben Simon G.J. Titanium, sapphire laser trabeculoplasty versus argon laser trabeculoplasty in patients with open-angle glaucoma // Ophthalmic Surg Lasers Imaging. – 2009. – Vol. 40. – P. 264–269.
54. Garcia-Sanchez J., Garcia-Feijoo J., Saenz-Frances F., et al. Titanium Sapphire Laser Trabeculoplasty: Hypotensive Efficacy and Anterior Chamber Inflammation // Investigative Ophthalmology & Visual Science. – 2007. – Vol. 48. – P. 3975.
55. Simon G., Lowery J.A. Comparison of three types of lasers in laser trabeculoplasty inhuman donor eyes and clinical study // ASCRS Symposium. – 2007.